25

NASA TECHNICAL MEMORANDUM

NASA TM X-3376

NASA TM X-3376

EFFECT OF REYNOLDS NUMBER ON THE AERODYNAMIC STABILITY AND CONTROL CHARACTERISTICS OF A 55° CLIPPED-DELTA-WING ORBITER CONFIGURATION AT SUPERSONIC MACH NUMBERS

A. B. Blair, Jr.

Langley Research Center
Hampton, Va. 23665

NATIONAL AERONAUTICS AND SPACE ADMINISTRATION • WASHINGTON, D. C. • MAY 1976

1. Report No.	2. Government Accession No.	3. Recipient's Catalog No.
NASA TM X-3376		

4. Title and Subtitle	5. Report Date
EFFECT OF REYNOLDS NUMBER ON THE AERODYNAMIC STABILITY AND CONTROL CHARACTERISTICS OF A 55^{o} CLIPPED-DELTA-WING ORBITER CONFIGURATION AT SUPERSONIC MACH NUMBERS	May 1976
	6. Performing Organization Code

7. Author(s)	8. Performing Organization Report No.
A. B. Blair, Jr.	L-10752
	10. Work Unit No.
9. Performing Organization Name and Address	505-11-15-03
NASA Langley Research Center Hampton, Va. 23665	11. Contract or Grant No.
	13. Type of Report and Period Covered
12. Sponsoring Agency Name and Address	Technical Memorandum
National Aeronautics and Space Administration Washington, D.C. 20546	14. Sponsoring Agency Code

15. Supplementary Notes

16. Abstract

A wind-tunnel investigation has been conducted at Mach numbers from 1.60 to 4.63 for Reynolds numbers varying from approximately 0.8×10^6 to 10.0×10^6 based on body length to determine Reynolds number effect on the static longitudinal and lateral aerodynamic stability and control characteristics of two scale models of the Grumman H-33 space shuttle orbiter.

The results indicate that for the Reynolds number range investigated, there are no Reynolds number effects on the longitudinal or lateral aerodynamic characteristics of either model with zero control deflections and only negligible effects with control deflections. The roll control is constant for both models with the possible exception of a slight increase with increases in Reynolds number up to 2.0×10^6 based on body length at the lower Mach numbers. This very small Reynolds number effect is much more apparent for the smaller model and disappears with increasing Mach and Reynolds numbers.

17. Key Words (Suggested by Author(s))	18. Distribution Statement
Reynolds number effect Space entry vehicles Delta-wing orbiter Grumman H-33 space shuttle orbiter	Unclassified – Unlimited Subject Category 02

19. Security Classif. (of this report)	20. Security Classif. (of this page)	21. No. of Pages	22. Price*
Unclassified	Unclassified	95	$4.75

*For sale by the National Technical Information Service, Springfield, Virginia 22161

EFFECT OF REYNOLDS NUMBER ON THE AERODYNAMIC STABILITY AND CONTROL CHARACTERISTICS OF A 55° CLIPPED-DELTA-WING ORBITER CONFIGURATION AT SUPERSONIC MACH NUMBERS

A. B. Blair, Jr.
Langley Research Center

SUMMARY

A wind-tunnel investigation has been conducted at Mach numbers from 1.60 to 4.63 for Reynolds numbers varying from approximately 0.8×10^6 to 10.0×10^6 based on body length to determine Reynolds number effect on the static longitudinal and lateral aerodynamic stability and control characteristics of two scale models of the Grumman H-33 space shuttle orbiter.

The results indicate that for the Reynolds number range investigated, there are no Reynolds number effects on the longitudinal or lateral aerodynamic characteristics of either model with zero control deflections and only negligible effects with control deflections. The roll control is constant for both models with the possible exception of a slight increase with increases in Reynolds number up to 2.0×10^6 based on body length at the lower Mach numbers. This very small Reynolds number effect is much more apparent for the smaller model and disappears with increasing Mach and Reynolds numbers.

INTRODUCTION

The National Aeronautics and Space Administration is currently engaged in a study designed to develop a reusable space shuttle system capable of placing large payloads in near-Earth orbit economically. As part of this study, the Langley Research Center has conducted wind-tunnel investigations of various concepts. These investigations have encompassed the Mach number range from subsonic to hypersonic speeds. One of the questions generated during these investigations concerned the effect of Reynolds number on the aerodynamic characteristics of a space shuttle configuration. Since there were only limited variations in Reynolds number at supersonic speeds, it was believed that tests were needed to expand the Reynolds number range in an effort to determine a Reynolds number effect (if any). Limited Reynolds number data have been presented across the entire Mach number range in reference 1 whereas reference 2 presents data at supersonic speeds.

The objective of the present paper is to present data showing Reynolds number effect on the static longitudinal and lateral aerodynamic characteristics of a typical orbiter configuration at supersonic speeds. The configuration selected for the investigation was a Grumman H-33 space shuttle orbiter design which had a low fineness-ratio body with a large base, a 55° clipped-delta wing, and a center-line vertical tail. Two models of different sizes with appropriately sized electrical strain-gage balances were used in order to expand the range of Reynolds numbers without losing data resolution. The investigation was conducted in the Langley Unitary Plan wind tunnel at Mach numbers from 1.60 to 4.63 for Reynolds numbers that varied from approximately 0.8×10^6 to 4.0×10^6 based on body length for the small model (0.00585 scale) and from 2.0×10^6 to 10.0×10^6 based on body length for the large model (0.0148 scale). The large-scale model was tested through a nominal angle-of-attack range from -2° to 31°. The smaller scale model was tested over an angle-of-attack range of -2° to 50°. Tests included the effect of Reynolds number on pitch- and roll-control effectiveness of the elevons.

SYMBOLS

The results of this investigation are presented as force and moment coefficients with the longitudinal characteristics referred to the body- and stability-axis system and the lateral characteristics referred to the body-axis system. The coefficients were based on model wing area, wing span, and body length; the moment reference point is located at 66.3-percent body length aft of the nose.

Measurements and calculations were made in U.S. Customary Units. The results are presented in the International System of Units (SI) with the equivalent values in U.S. Customary Units given parenthetically. (See ref. 3.)

b	wing span, large model, 43.576 cm (17.156 in.); small model, 16.863 cm (6.639 in.)
C_A	axial-force coefficient, $\frac{\text{Axial force}}{qS}$
$C_{A,b}$	base axial-force coefficient
C_D	drag coefficient, $\frac{\text{Drag}}{qS}$
C_L	lift coefficient, $\frac{\text{Lift}}{qS}$
C_{L_α}	lift-curve slope, per deg

C_l rolling-moment coefficient, $\frac{\text{Rolling moment}}{qSb}$

$C_{l_{\delta_a}}$ rolling-moment coefficient due to aileron deflection, $\frac{\Delta C_l}{\Delta \delta_a}$, per deg

C_m pitching-moment coefficient, $\frac{\text{Pitching moment}}{qSl}$

C_{m_α} slope of pitching-moment curve, $\frac{\partial C_m}{\partial \alpha} = \left(\frac{\partial C_L}{\partial \alpha}\right)\left(\frac{\partial C_m}{\partial L}\right)$, at trimmed conditions

$C_{m_{\delta_e}}$ pitch-control effectiveness of elevons at $\alpha = 0^o$, per degree of deflection for elevon deflections of 0^o and -10^o

C_N normal-force coefficient, $\frac{\text{Normal force}}{qS}$

C_n yawing-moment coefficient, $\frac{\text{Yawing moment}}{qSb}$

C_Y side-force coefficient, $\frac{\text{Side force}}{qS}$

L/D lift-drag ratio

l reference body length, large model, 60.960 cm (24.00 in.); small model, 24.089 cm (9.484 in.)

l' Grumman H-33 space shuttle orbiter design body length

M Mach number

q free-stream dynamic pressure, N/m^2 (psf)

R_l Reynolds number based on body length

S wing area, large model, 0.09868 m^2 (1.06228 ft^2); small model, 0.01541 m^2 (0.16588 ft^2)

x_{ac}/l aerodynamic-center location in percent body length from model nose ($\alpha \approx 0^o$)

α angle of attack, deg

δ_a aileron deflection, $\frac{\delta_{e,L} - \delta_{e,R}}{2}$, positive for right roll command, per deg

δ_e pitch-control deflection of elevons (symmetric), $\frac{\delta_{e,L} + \delta_{e,R}}{2}$, negative with trailing edge up, deg

$\delta_{e,L}$ left-elevon surface deflection angle (negative deflection, trailing edge up), deg

$\delta_{e,R}$ right-elevon surface deflection angle (negative deflection, trailing edge up), deg

Subscripts:

0 at zero lift

ref reference

APPARATUS AND METHODS

Tunnel

The tests were conducted in both the low and high Mach number test sections of the Langley Unitary Plan wind tunnel, a variable-pressure, continuous-flow facility. The test sections are approximately 2.13 m (7 ft) long and 1.22 m (4 ft) square. The nozzles leading to the test sections are of the asymmetric sliding-block type. Use of nozzles of this type permits a continuous variation in Mach number from about 1.5 to 2.9 in the low Mach number test section and from about 2.3 to 4.7 in the high Mach number test section.

Model

Details of the Grumman H-33 space shuttle orbiter design and test models are presented in figure 1, in table I, and in references 1 and 2. Photographs of the test models are shown in figure 2. Two models of different sizes were tested: a 0.0148-scale (large) model and a 0.00585-scale (small) model. A limited comparison of the test models with the design model can be found in figures 3 and 4. This comparison indicates that the test models were accurately built and that model geometry difference should have little effect on the data. The basic configuration of the two models had a 55^o clipped-delta wing and a center-line vertical tail. Symmetric deflections of the wing-mounted elevons produced pitch control, whereas differential deflections provided roll control. Three simulated rocket nozzles protruded from the base of the large model with the inner portion removed for sting clearance. The smaller model had no nozzles. Unless otherwise indicated, all configurations in this report had zero control deflections and a full-span unflared rudder.

Test Conditions

Tests were performed at the following tunnel conditions:

Mach number	Model	Stagnation temperature		Stagnation pressure		Unit Reynolds number		R_l
		K	°F	kN/m^2	psfa	per m	per ft	
1.60	Large	339	150	27.29	570	3.28×10^6	1.00×10^6	2.0×10^6
		339	150	54.63	1 141	6.56	2.00	4.0
		339	150	81.92	1711	9.84	3.00	6.0
		339	150	109.22	2 281	13.12	4.00	8.0
	Small	339	150	27.29	570	3.28×10^6	1.00×10^6	0.8×10^6
		339	150	69.09	1443	8.30	2.53	2.0
		339	150	138.18	2 886	16.60	5.06	4.0
2.86	Large	339	150	49.22	1 028	3.28×10^6	1.00×10^6	2.0×10^6
		339	150	98.44	2 056	6.56	2.00	4.0
		339	150	147.66	3 084	9.84	3.00	6.0
		339	150	196.88	4 112	13.12	4.00	8.0
		339	150	246.10	5 140	16.40	5.00	10.0
	Small	339	150	49.22	1 028	3.28×10^6	1.00×10^6	0.8×10^6
		339	150	124.54	2 601	8.30	2.53	2.0
		339	150	249.07	5 202	16.60	5.06	4.0
4.63	Large	352	175	126.31	2638	3.28×10^6	1.00×10^6	2.0×10^6
		352	175	252.57	5 275	6.56	2.00	4.0
		352	175	378.88	7913	9.84	3.00	6.0
		352	175	505.19	10 551	13.12	4.00	8.0
		352	175	631.45	13 188	16.40	5.00	10.0
	Small	352	175	126.31	2638	3.28×10^6	1.00×10^6	0.8×10^6
		352	175	319.51	6673	8.30	2.53	2.0
		352	175	639.06	13 347	16.60	5.06	4.0

The large model was limited in angle of attack and unit Reynolds number at $M = 1.60$ to prevent balance overloads.

The dewpoint temperature measured at stagnation pressure was maintained below 239 K (-30° F) to insure negligible condensation effects. All tests were performed with boundary-layer transition strips (located by measuring streamwise) on the fuselage 3.05 cm (1.20 in.) aft of the nose and on both sides of each wing and vertical tail 1.02 cm (0.40 in.) aft of the leading edges. For $M = 1.60$ and 2.86, the transition strips were

approximately 0.157 cm wide (0.062 in.) and were composed of number 50 sand grains sprinkled in acrylic plastic. For M = 4.63, the transition strips were composed of number 40 sand grains. The grain size and location of the strips were determined according to the recommendations of reference 4.

Measurements

Aerodynamic forces and moments were measured by means of a six-component electrical strain-gage balance housed within each of the models. Each model had an appropriately sized balance which was selected to insure that good data resolution could be obtained (for example, full-balance output). The balance in each model was rigidly fastened to a sting support system. Balance-chamber pressures were measured by means of a single static-pressure orifice located in the vicinity of the balance. In addition, pressure measurements were made at the fuselage bases of both models and at the engine nozzles of the larger model.

Corrections

Angles of attack have been corrected for tunnel-flow misalinement. Angles of attack and sideslip have been corrected for deflection of the sting and balance because of aerodynamic loads. The drag results have been adjusted to correspond to free-stream static-pressure conditions at the base of the models. Typical values of base axial-force coefficients are presented in figure 5.

Presentation of Results

An outline of the data figures follows.

RESULTS AND DISCUSSION

Longitudinal Aerodynamic Characteristics

The longitudinal aerodynamic characteristics of the large and small models with elevon pitch-control deflections are presented in figures 6 to 11. Figure 12 presents a summary plot obtained from these figures. Included in figure 12 are the longitudinal aerodynamic characteristics as a function of R_l for both models at low angles of attack ($\alpha \approx 0^{o}$) and for a flight α-schedule ($\alpha = 7.0^{o}$, 12.0^{o}, and 27.0^{o} for $M = 1.60$, 2.86, and 4.63, respectively; ref. 1) of a typical space shuttle orbiter entering the atmosphere of the Earth. For the Reynolds number range investigated, there is no apparent Reynolds number effect on the longitudinal aerodynamic characteristics of the models at $\alpha \approx 0^{o}$ (fig. 12(a)). For the flight α-schedule (fig. 12(b)), there are small R_l effects on the parameters shown; these effects are more pronounced for the smaller model at $M = 1.60$, but disappear above $R_l = 2.0 \times 10^{6}$. In addition, there appears to be a small increment in data levels between the two models. The increment may be caused by the differences in the geometry of the model bases (for example, no simulated nozzles on smaller model) and by the extent of boundary-layer flow separation ahead of the elevons for each of the models. The flight α-schedule data for each of the models were obtained from figures 8 and 9 $(\delta_e = -10^{o})$. Although several other Mach numbers ($M = 2.00$, 2.40, and 3.95) were investigated, data at these Mach numbers are not included since the trends with Reynolds number change are similar to those described in the previous paragraph.

Lateral Aerodynamic Characteristics

The lateral aerodynamic characteristics of the large and small models with asymmetric elevon roll-control deflections are presented in figures 13 to 18. For $\delta_e = 0^{o}$ (figs. 13 and 14), there is no Reynolds number effect on the lateral aerodynamic characteristics. In figures 15 and 16 $(\delta_{e,L} = 10^{o}$ and $\delta_{e,R} = -10^{o}$ for the large and small models, respectively), the rolling-moment coefficient produced by either model is constant with the possible exception of a very small Reynolds number effect at $M = 1.60$; the effect is more apparent for the smaller model. For example, in figure 16, a small

Reynolds number effect exists at the lower angles of attack but disappears with increasing Mach number and Reynolds number. Similar results can also be seen in figure 18 for the small model. The accompanying yawing moments from the elevon roll-control deflections of both models are not affected by the Reynolds number variations. A summary of the roll-control characteristics $\left(C_{l_{\delta_a}}\right)$ as a function of R_l for both models at $\alpha \approx 0^o$ and for the flight α-schedule is presented in figure 19. For the small model at $\alpha \approx 0^o$, there is a slight increase in roll control with increases in R_l up to 2.0×10^6 at the lower Mach numbers. A similar roll-control increase can be seen for the flight α-schedule with the small model at maximum roll deflection.

Figure 19 also shows a small variation in roll-control levels between the two models at $M = 1.60$ for their maximum roll-control deflections $\left(\delta_{e,L} = 0^o \text{ and } \delta_{e,R} = -30^o\right)$; this variation disappears with increasing Mach number. It is believed that this variation is primarily the result of two factors: first, there were differences in the base geometries of the models (as discussed earlier); the second factor could be a difference in the extent of boundary-layer flow separation ahead of the elevons for the two models.

CONCLUDING REMARKS

A wind-tunnel investigation has been conducted at Mach numbers from 1.60 to 4.63 for Reynolds numbers varying from approximately 0.8×10^6 to 10.0×10^6 based on body length to determine Reynolds number effect on the static longitudinal and lateral aerodynamic stability and control characteristics of two scale models of the Grumman H-33 space shuttle orbiter.

The results indicate that for the Reynolds number range investigated, there are no Reynolds number effects on the longitudinal or lateral aerodynamic characteristics of either model with zero control deflections and only negligible effects with control deflections. The roll control is constant for both models with the possible exception of a slight increase with increases in Reynolds number up to 2.0×10^6 based on body length at the lower Mach numbers. This very small Reynolds number effect is much more apparent for the smaller model and disappears with increasing Mach and Reynolds numbers.

Langley Research Center
National Aeronautics and Space Administration
Hampton, Va. 23665
March 29, 1976

REFERENCES

1. Rainey, Robert W.; Ware, George M.; Powell, Richard W.; Brown, Lawrence W.; and Stone, David R.: Grumman H-33 Space Shuttle Orbiter Aerodynamic and Handling-Qualities Study. NASA TN D-6948, 1972.

2. Blair, A. B., Jr.; and Grow, Josephine: Aerodynamic Characteristics of a 55^{o} Clipped-Delta-Wing Orbiter Model at Mach Numbers From 1.60 to 4.63. NASA TM X-2748, 1973.

3. Mechtly, E. A.: The International System of Units – Physical Constants and Conversion Factors (Second Revision). NASA SP-7012, 1973.

4. Braslow, Albert L.; and Knox, Eugene C.: Simplified Method for Determination of Critical Height of Distributed Roughness Particles for Boundary-Layer Transition at Mach Numbers From 0 to 5. NACA TN 4363, 1958.

TABLE I. - GRUMMAN H-33 SPACE SHUTTLE ORBITER AERODYNAMIC COEFFICIENT REFERENCE DIMENSIONS (DESIGN)

Reference theoretical wing area, S_{ref}, m^2 (ft^2)	449.6	(4840)
Reference body length, $l_{ref} = l'$, m (ft)	41.15	(135)
Reference theoretical wing span, $b_{ref} = b$, m (ft)	28.8	(94.5)

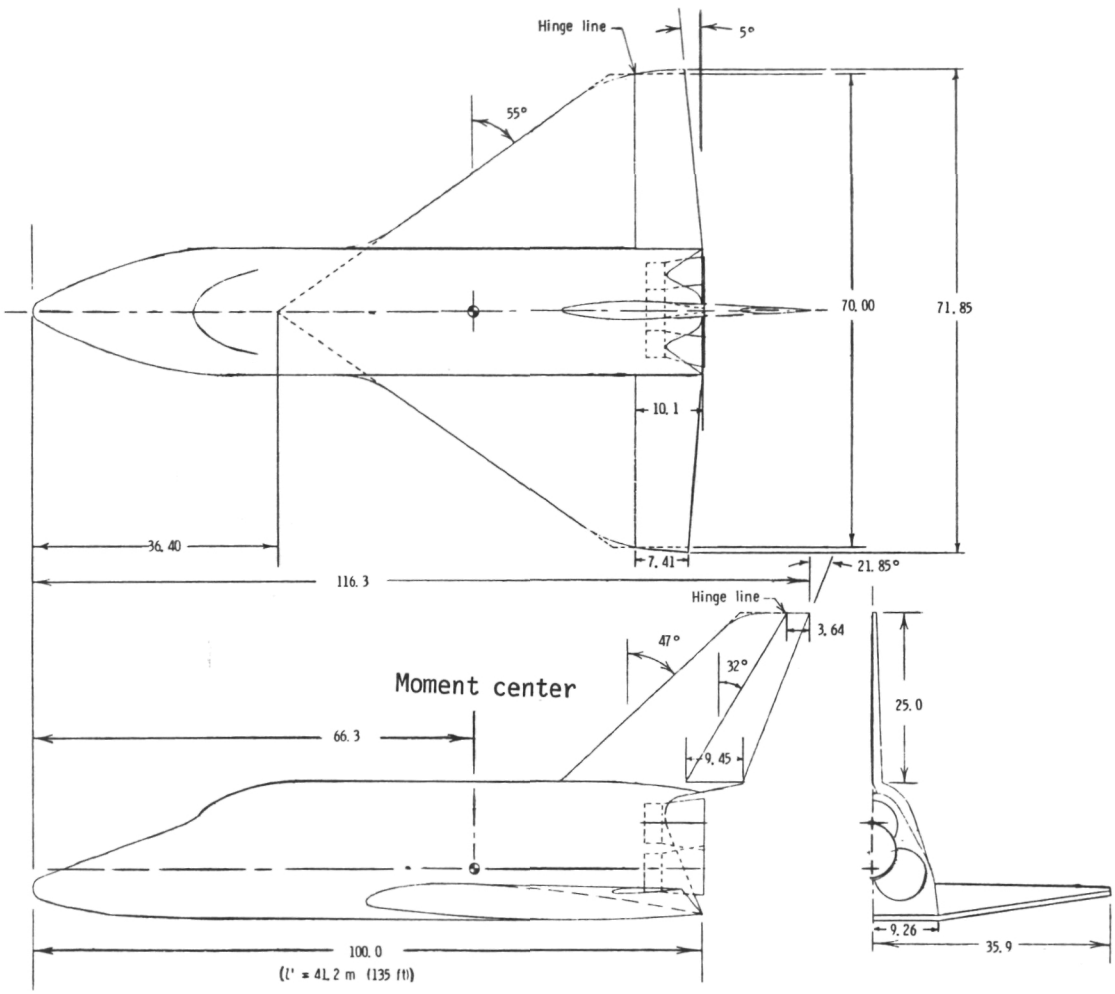

Figure 1.- Grumman H-33 space shuttle orbiter design model.
All dimensions are in percent body length.

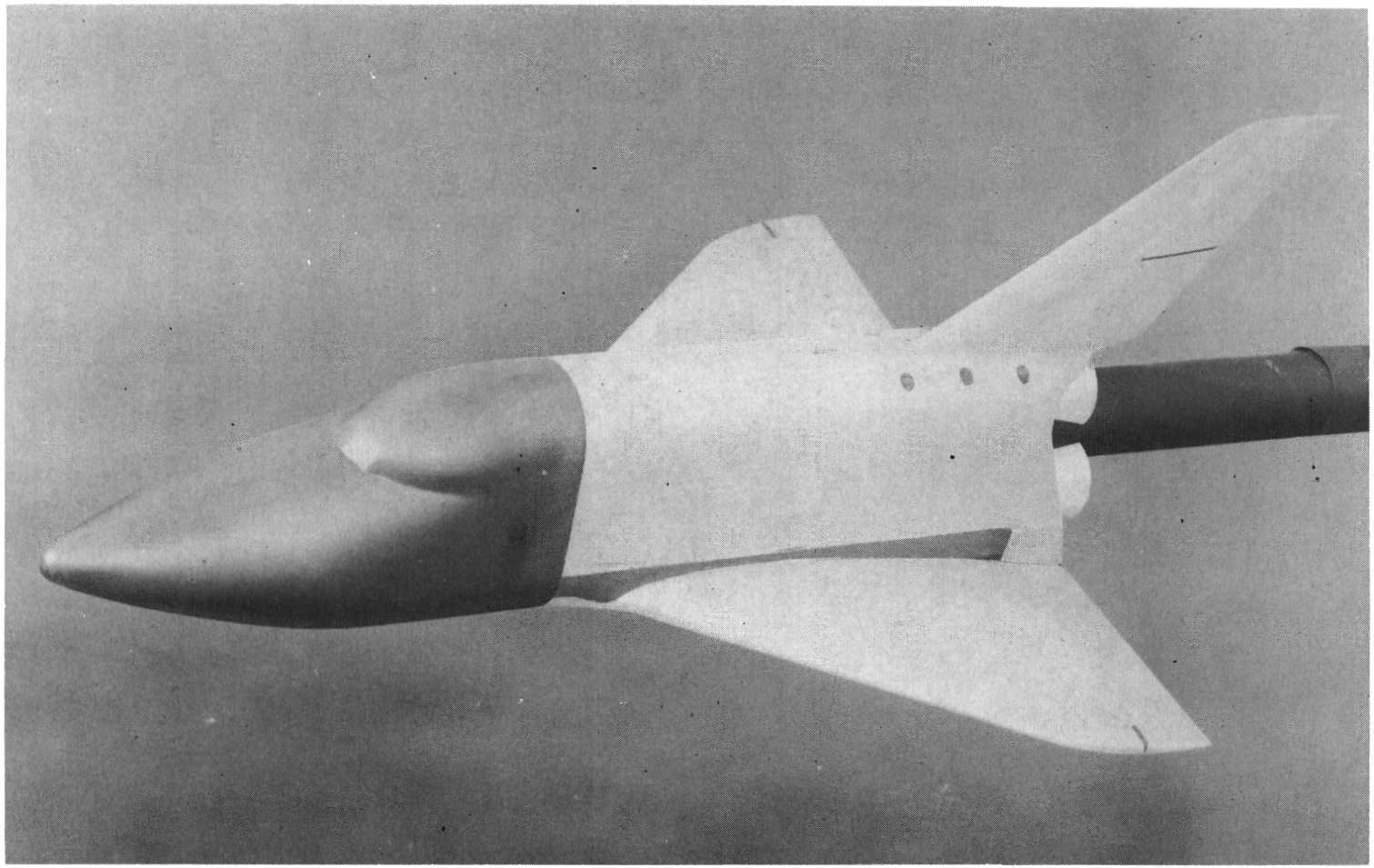

L-71-8978

(a) Large model.

Figure 2.- Model photographs.

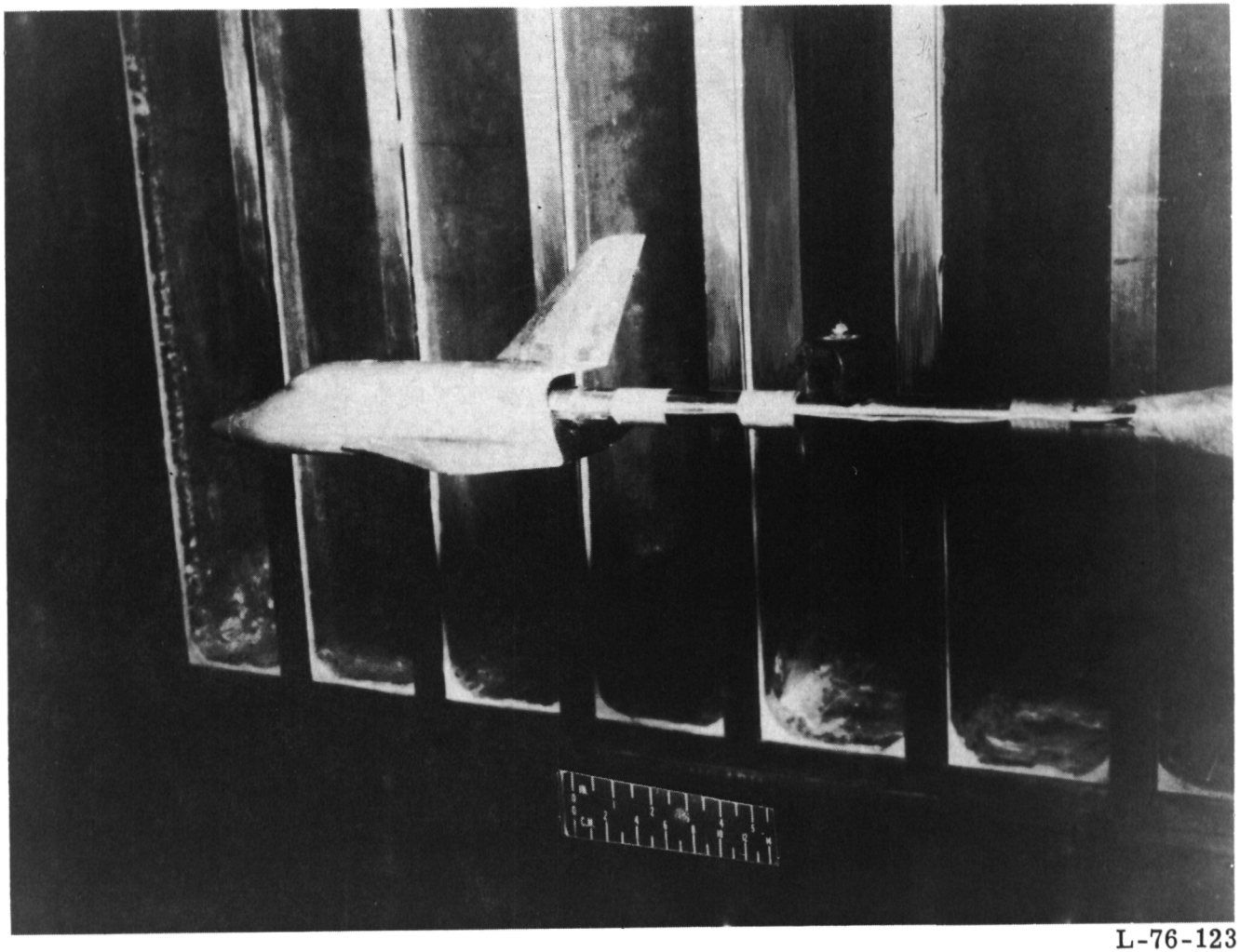

L-76-123

(b) Small model.

Figure 2.- Concluded.

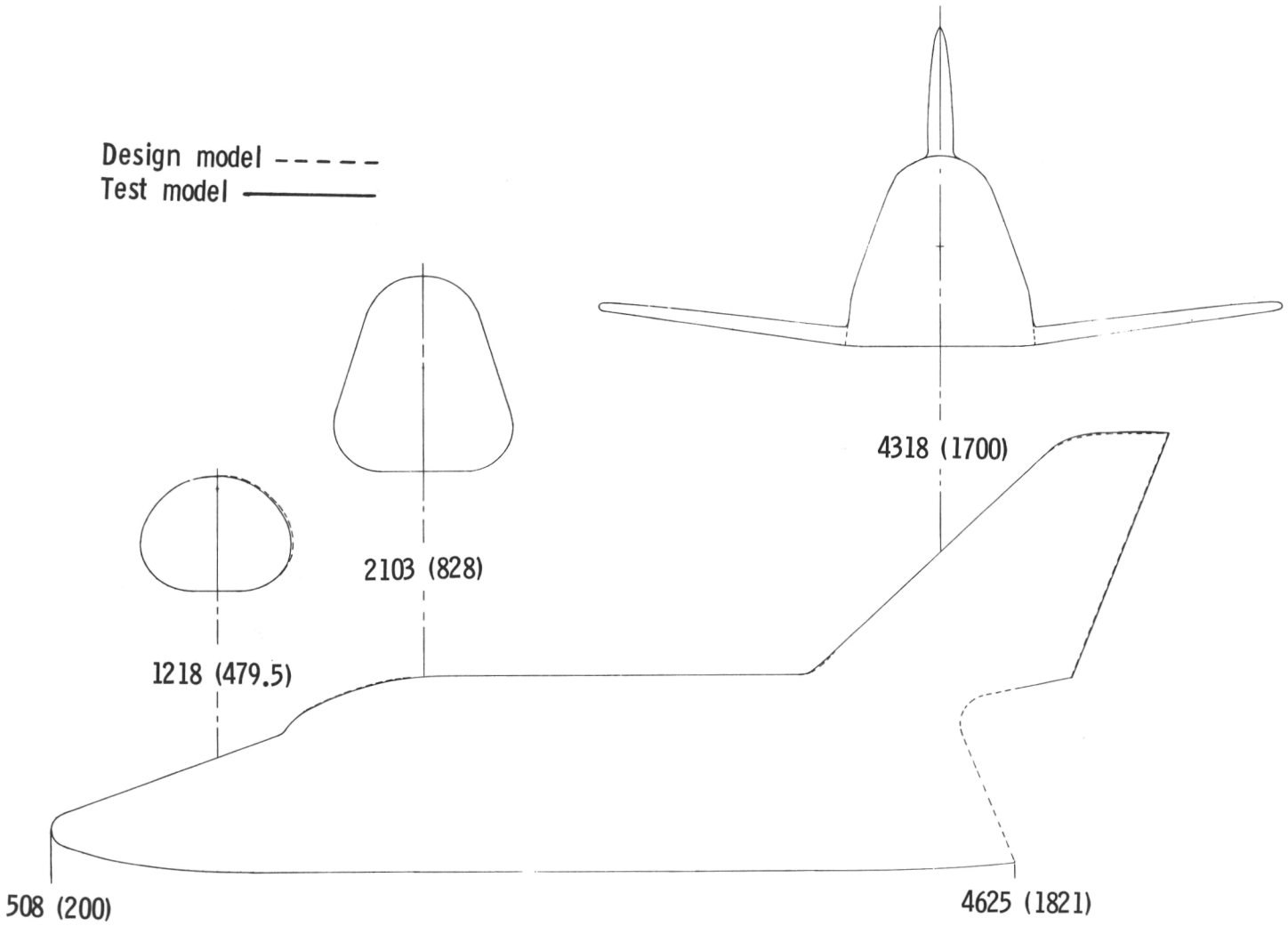

Figure 3.- Comparison of 61-cm (24-in.) test model built by Grumman Aerospace Corporation with Grumman H-33 space shuttle orbiter, 0.0148 scale.

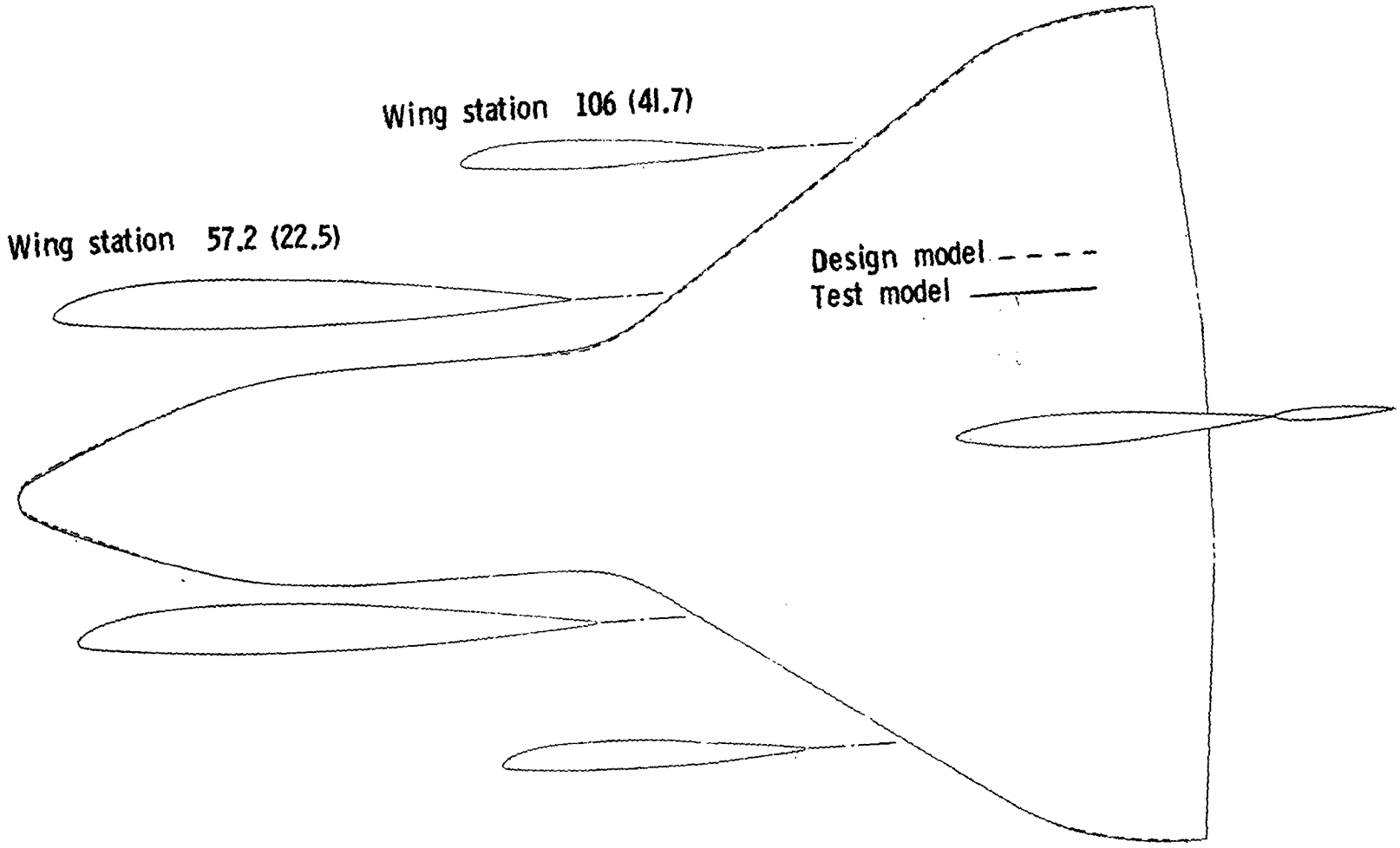

Figure 3.- Concluded.

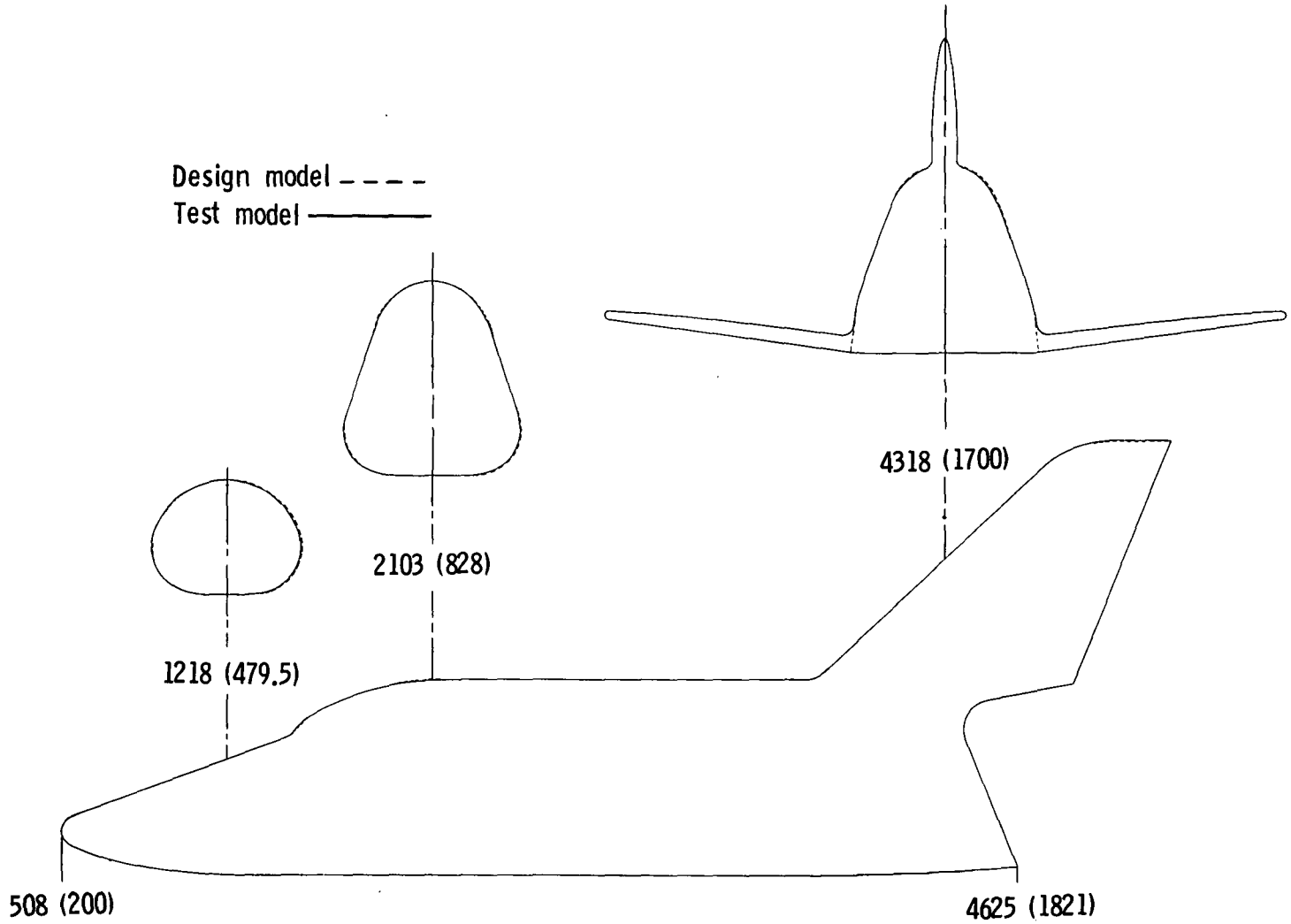

Figure 4.- Comparison of 24.1-cm (9.5-in.) model built by Langley Research Center with Grumman H-33 space shuttle orbiter, 0.00585 scale.

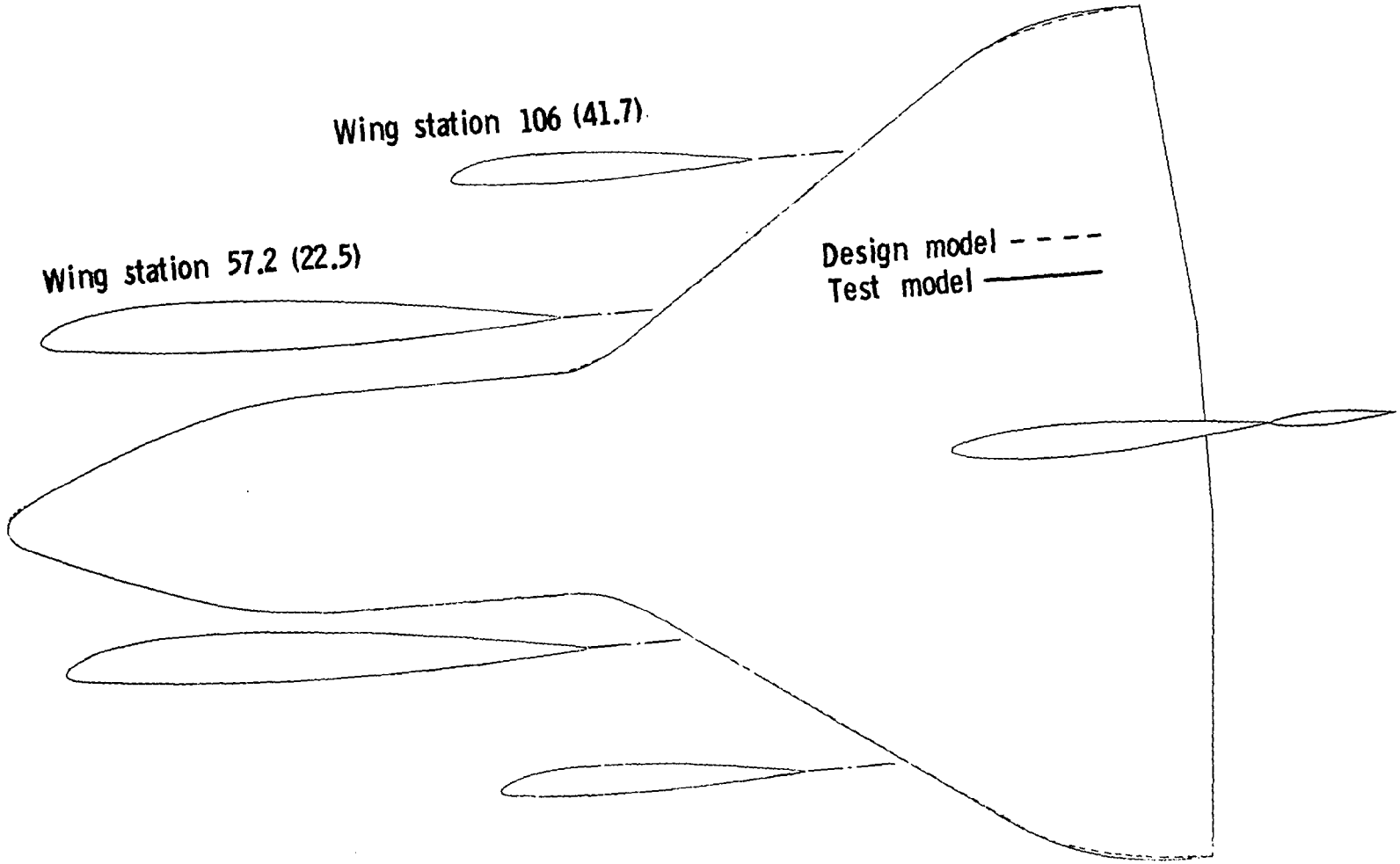

Figure 4.- Concluded.

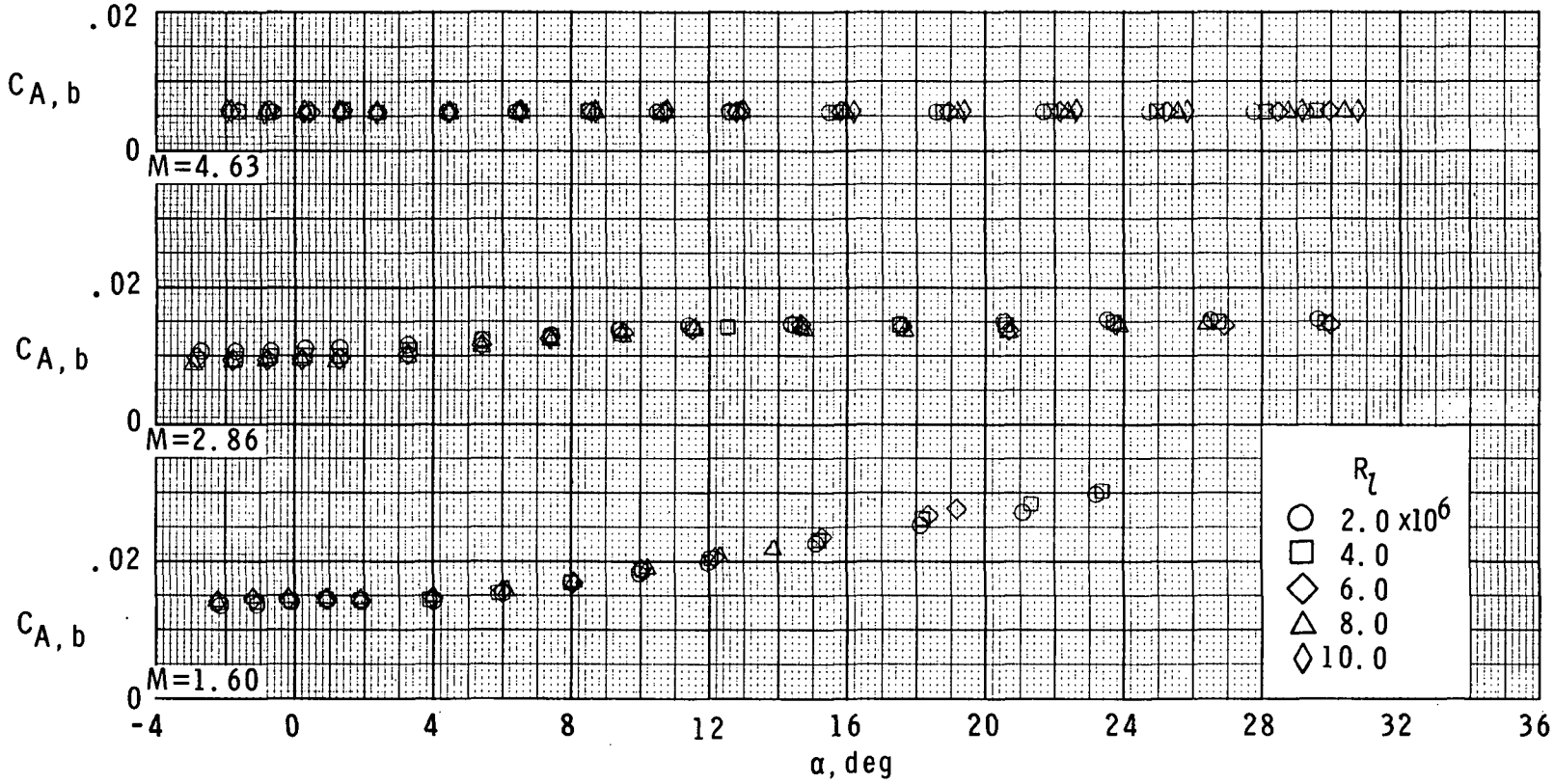

(a) Large model.

Figure 5.- Typical variation of base axial-force coefficients with angle of attack. $\delta_e = 0^o$.

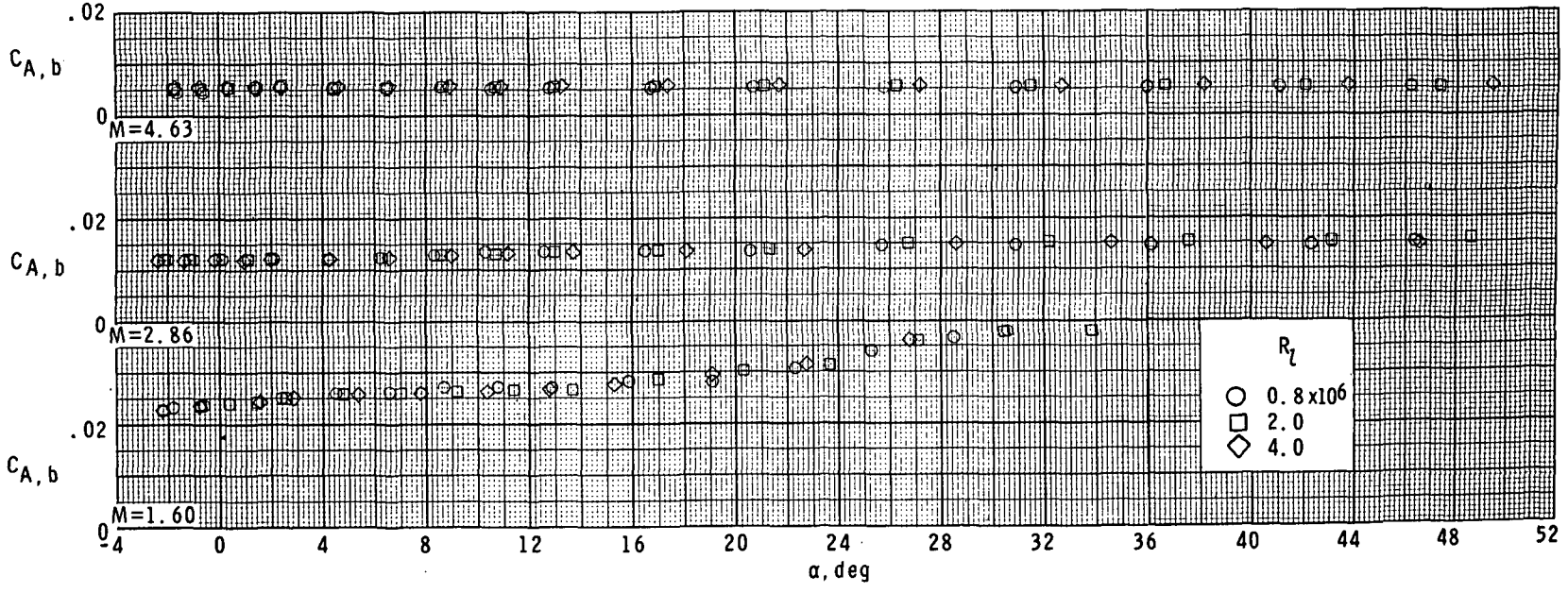

(b) Small model.

Figure 5.- Concluded.

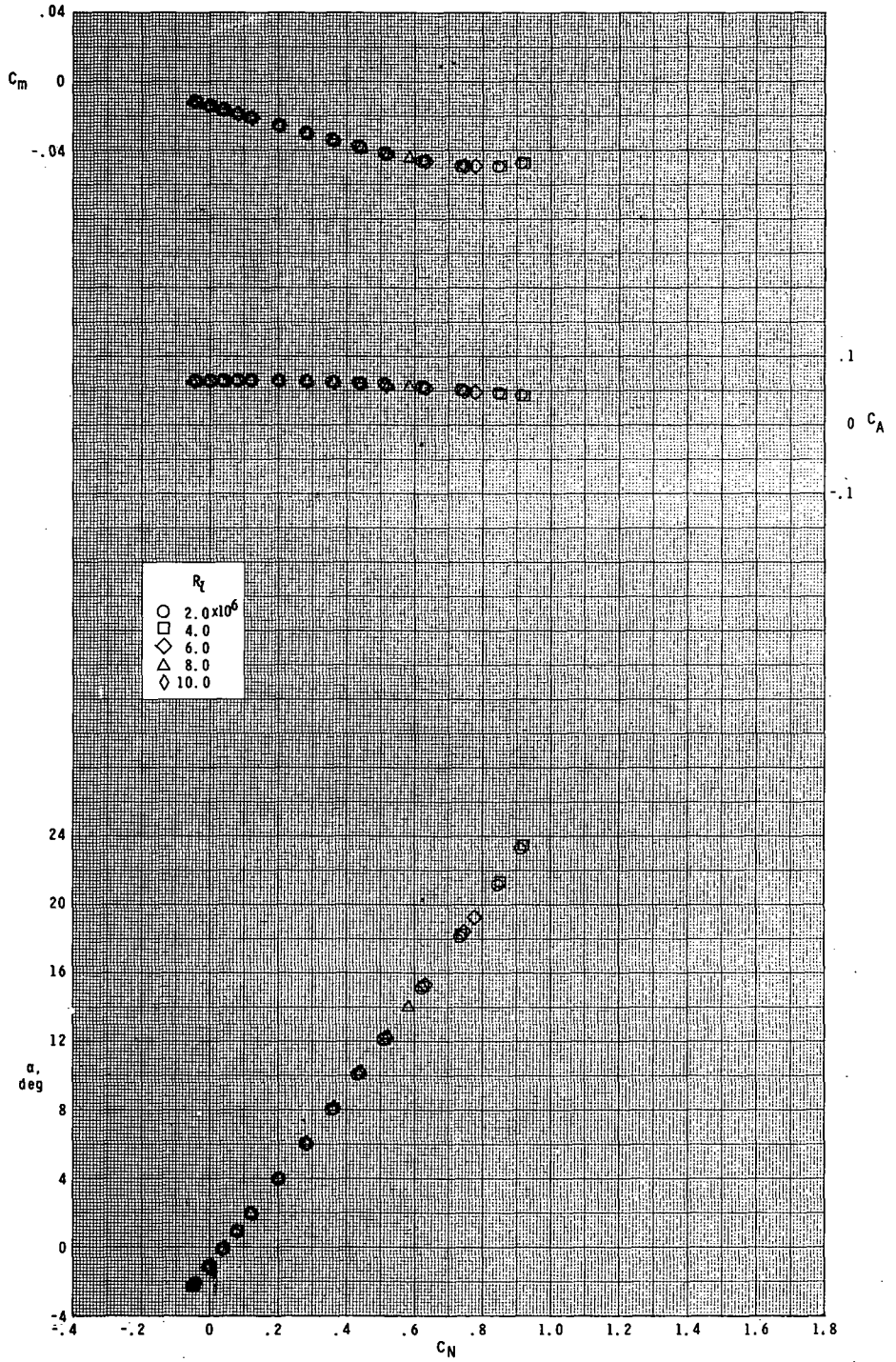

(a) M = 1.60.

Figure 6.- Effect of Reynolds number on longitudinal aerodynamic characteristics. Large model; $\delta_e = 0^o$.

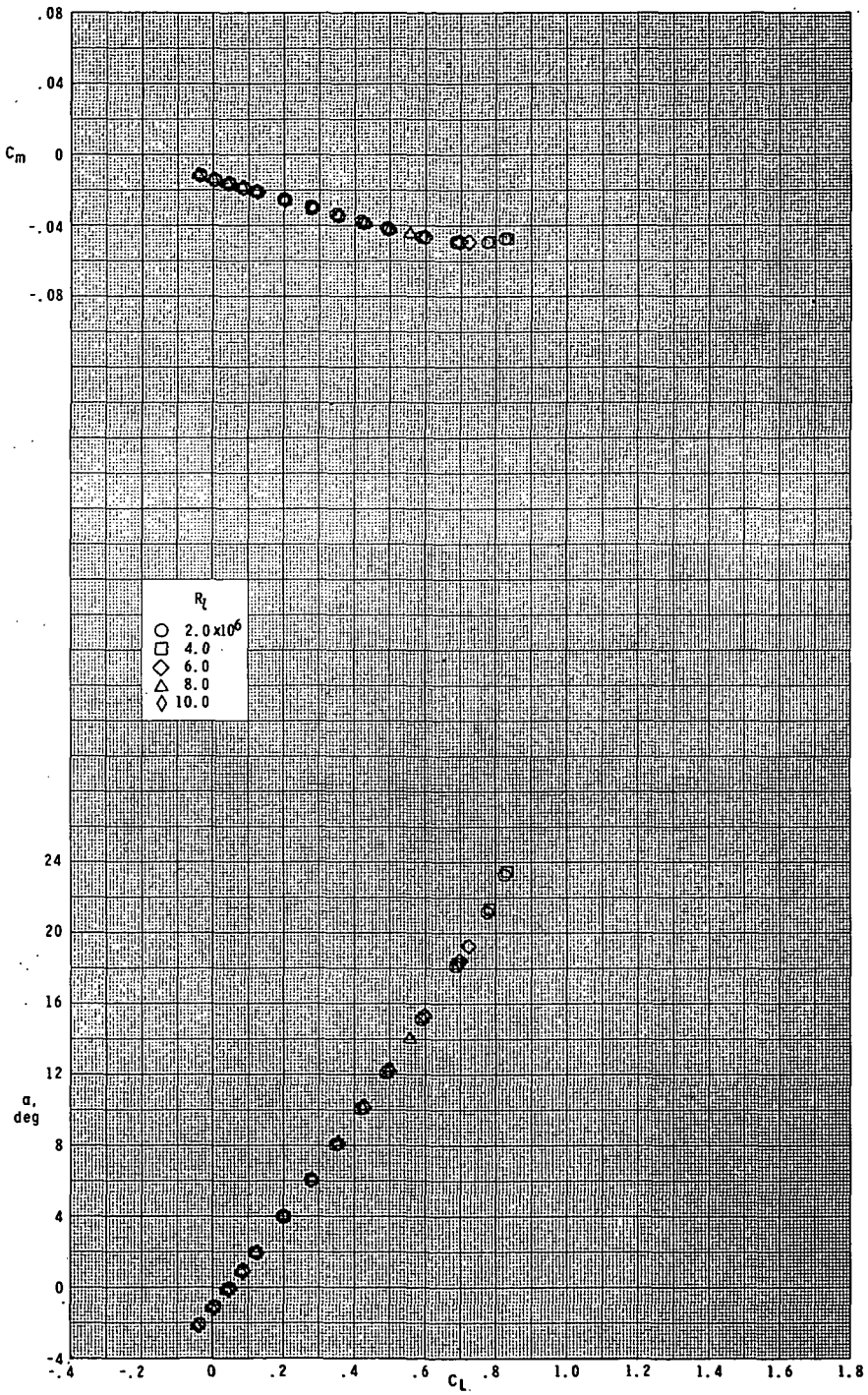

(a) Continued.

Figure 6.- Continued.

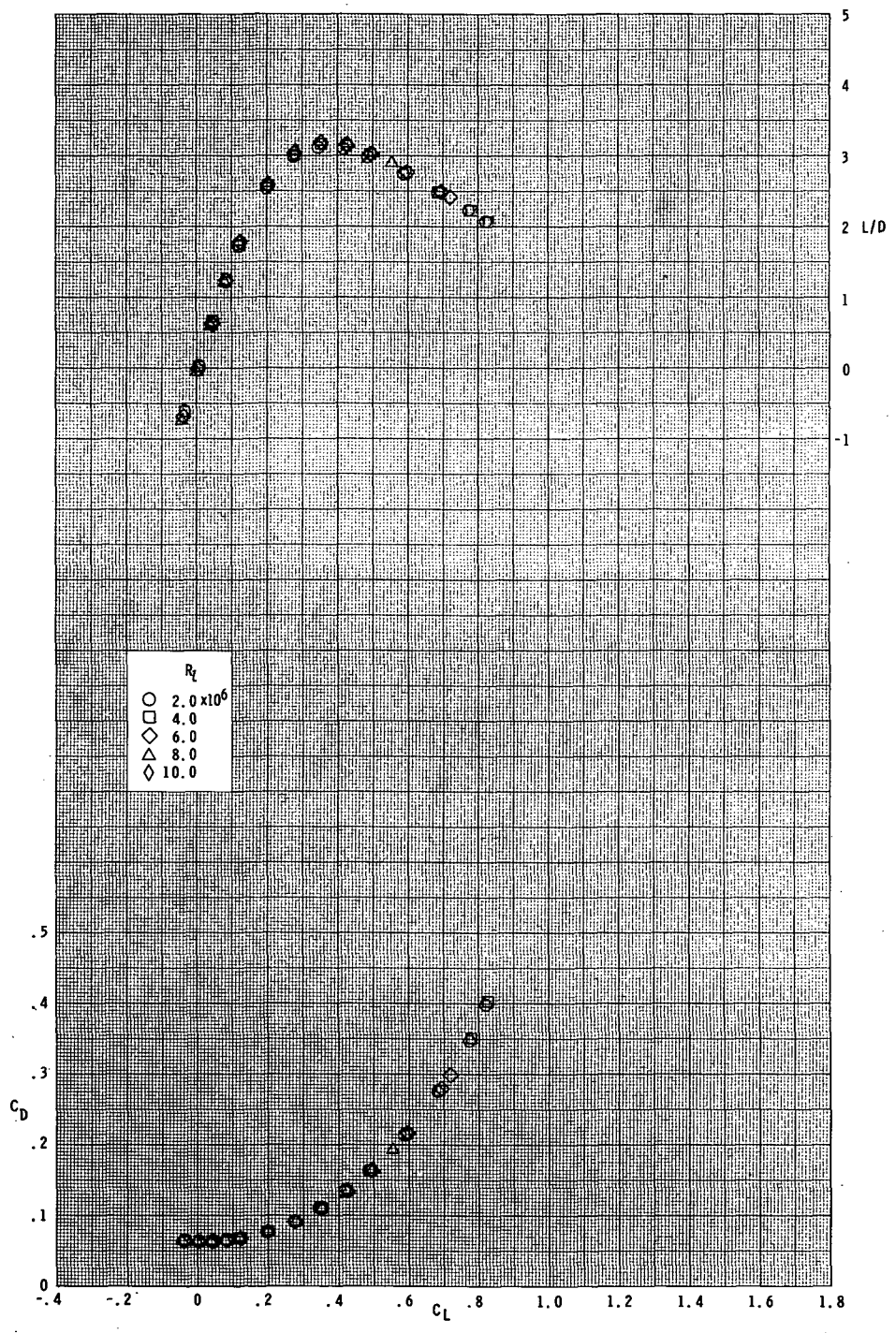

(a) Concluded.

Figure 6.- Continued.

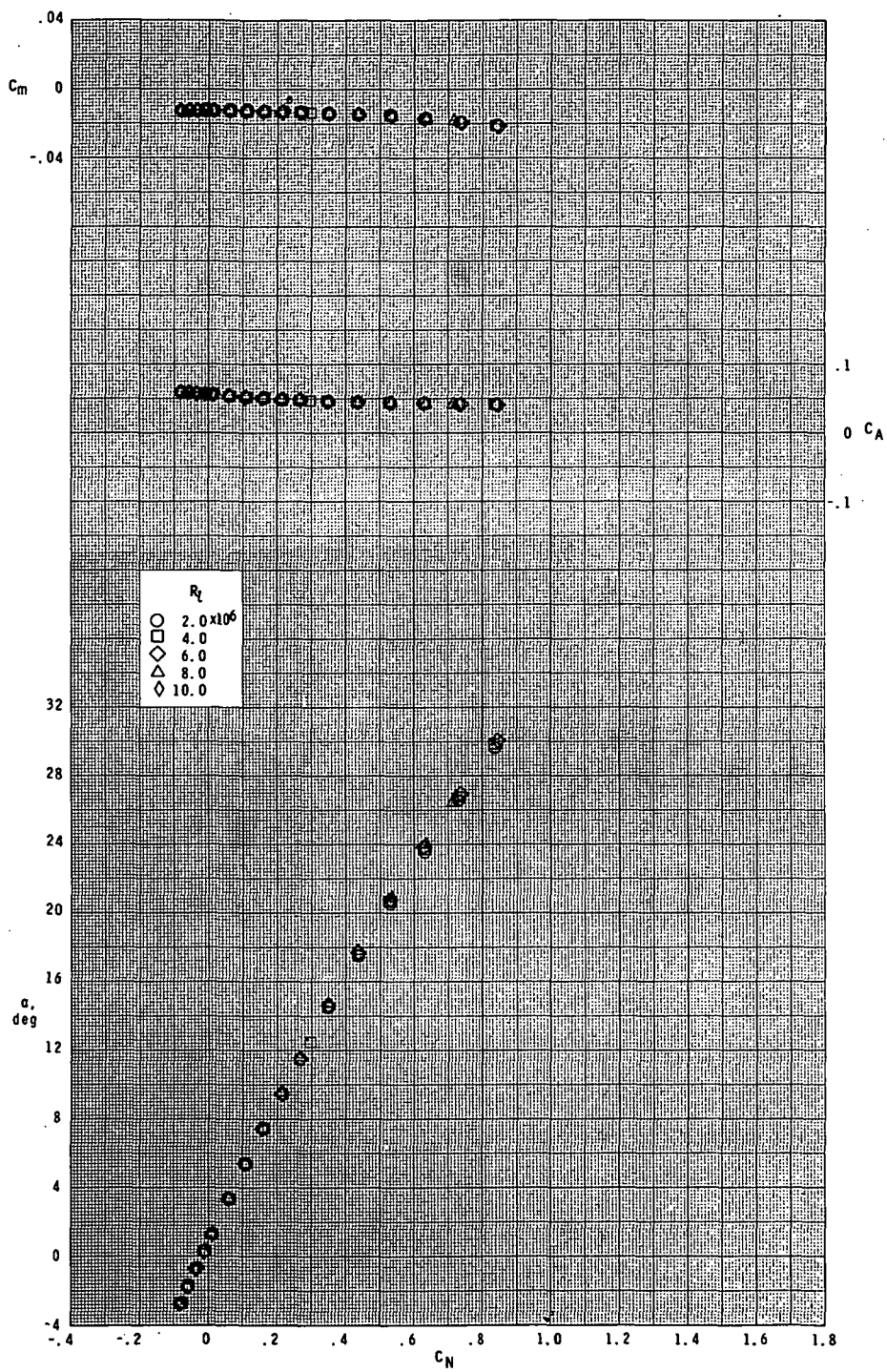

(b) M = 2.86.

Figure 6.- Continued.

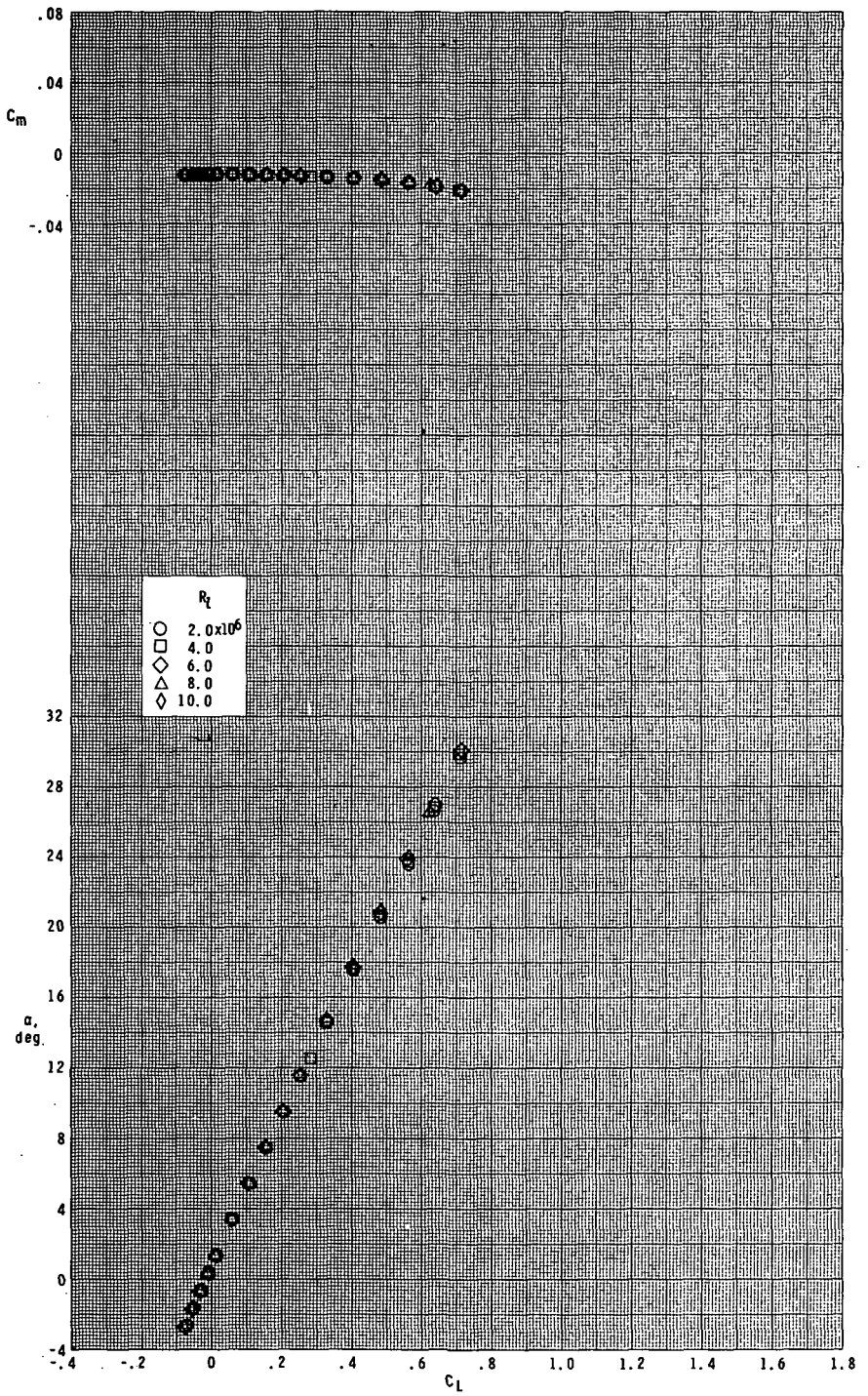

(b) Continued.

Figure 6.- Continued.

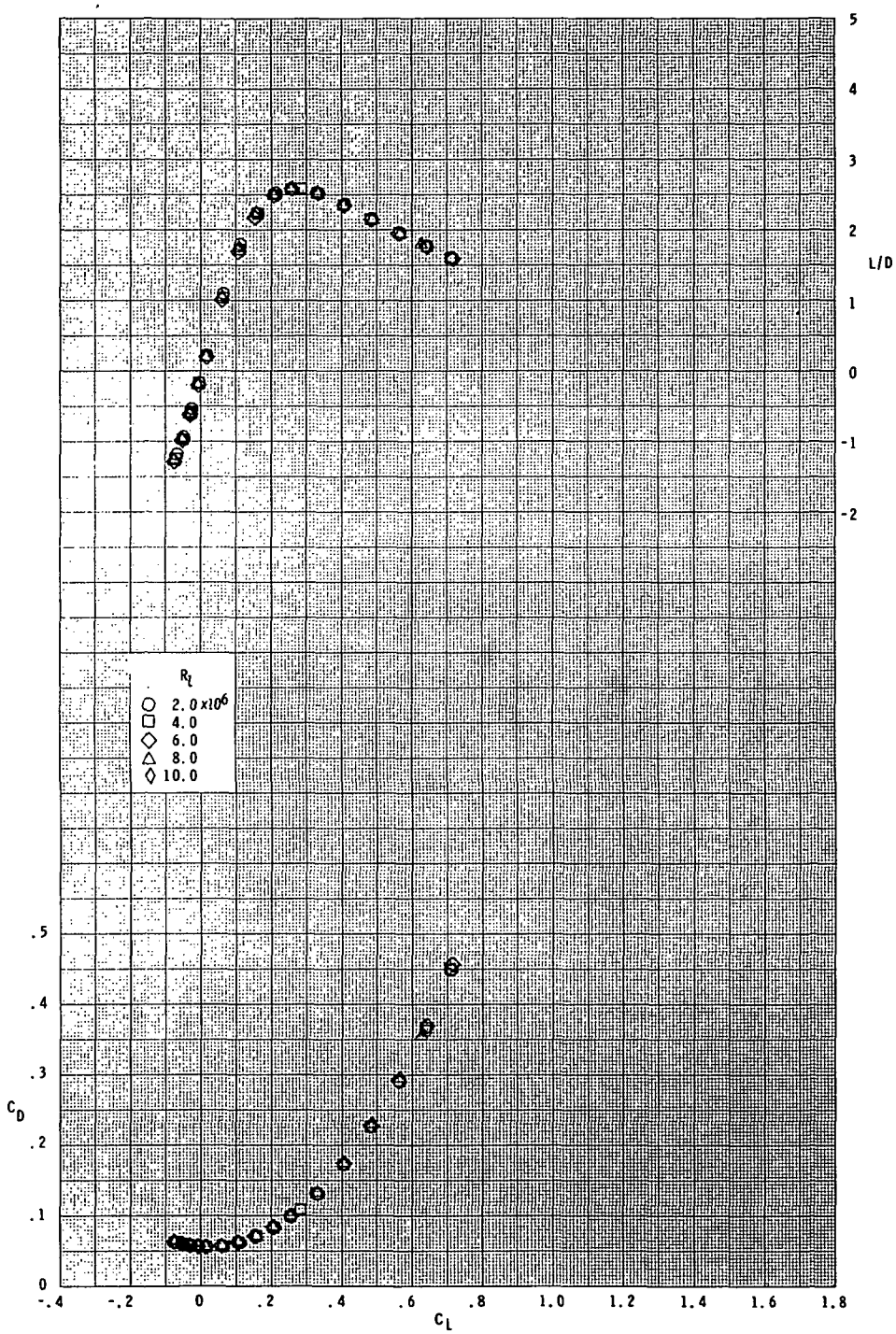

(b) Concluded.

Figure 6.- Continued.

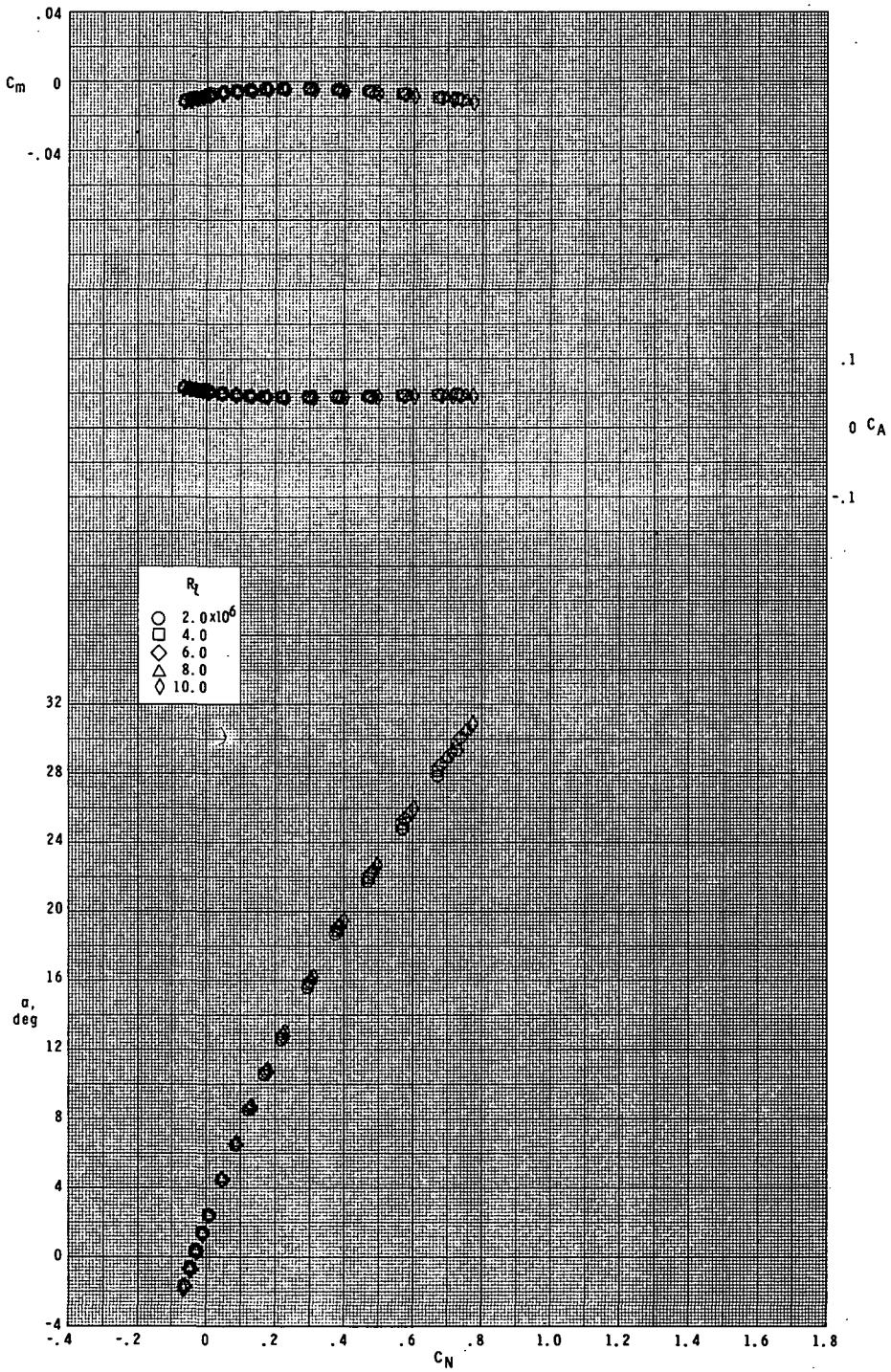

(c) M = 4.63.

Figure 6.- Continued.

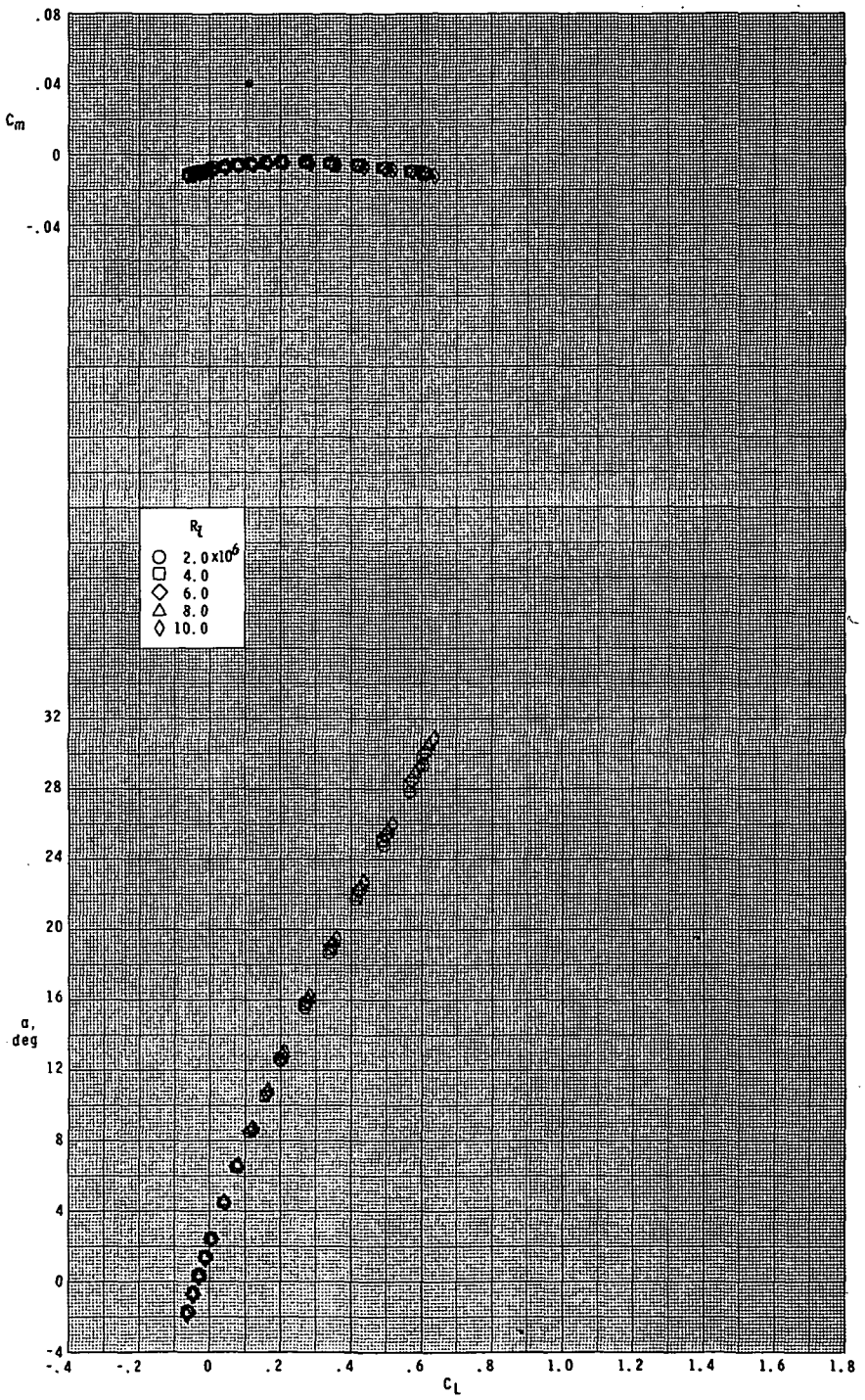

(c) Continued.

Figure 6.- Continued.

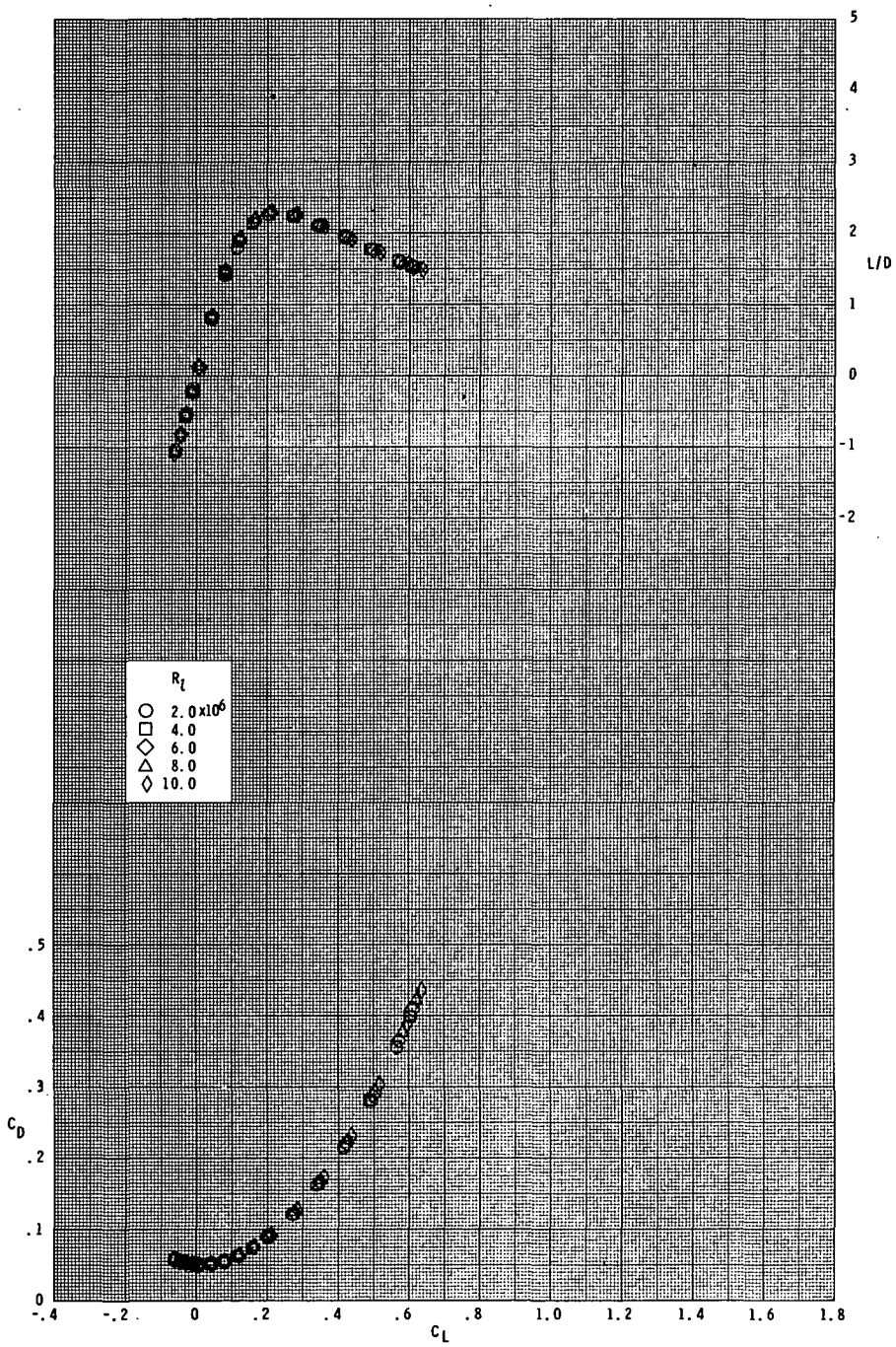

(c) Concluded.

Figure 6.- Concluded.

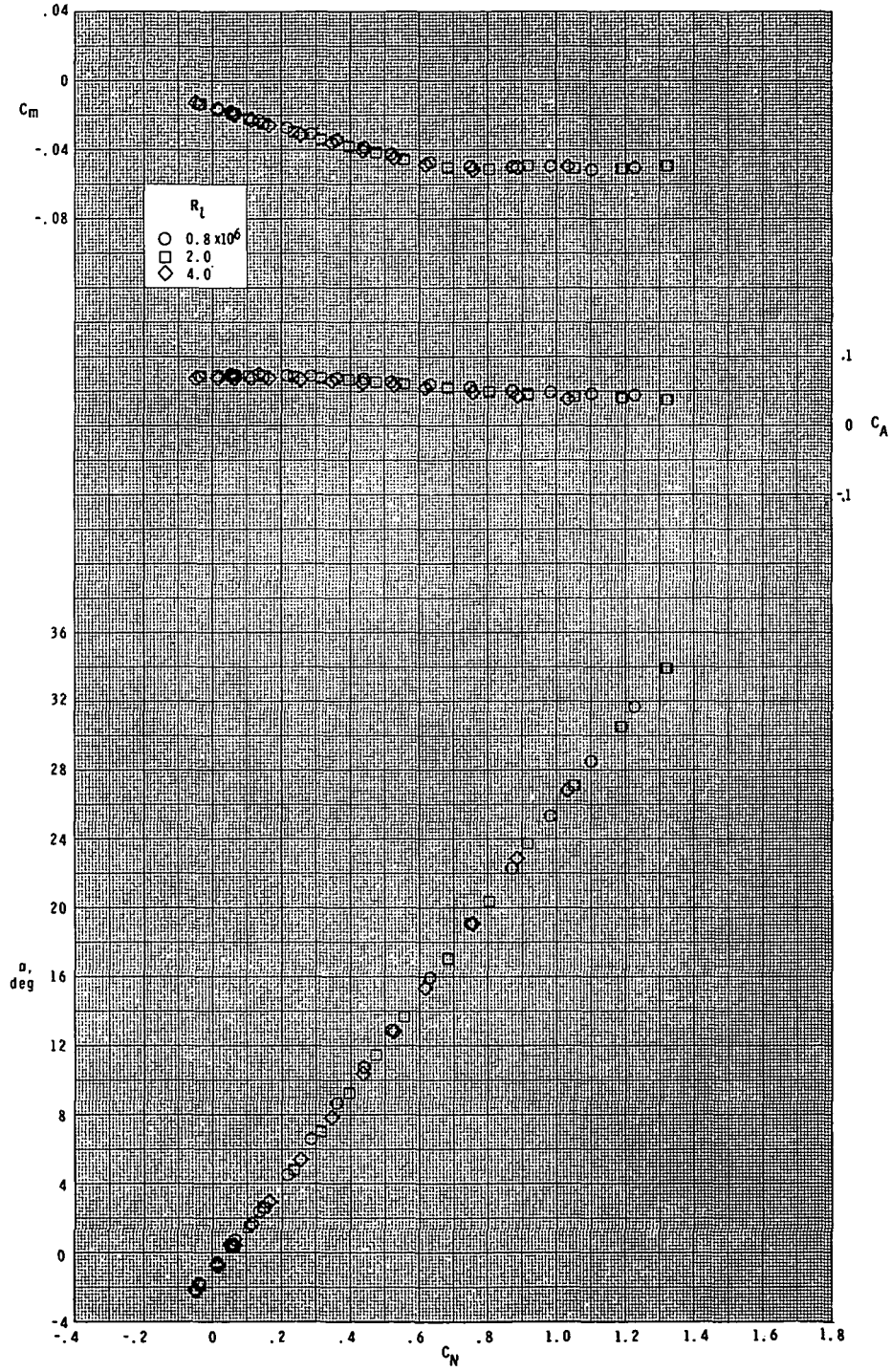

(a) M = 1.60.

Figure 7.- Effect of Reynolds number on longitudinal aerodynamic characteristics. Small model; $\delta_e = 0^o$.

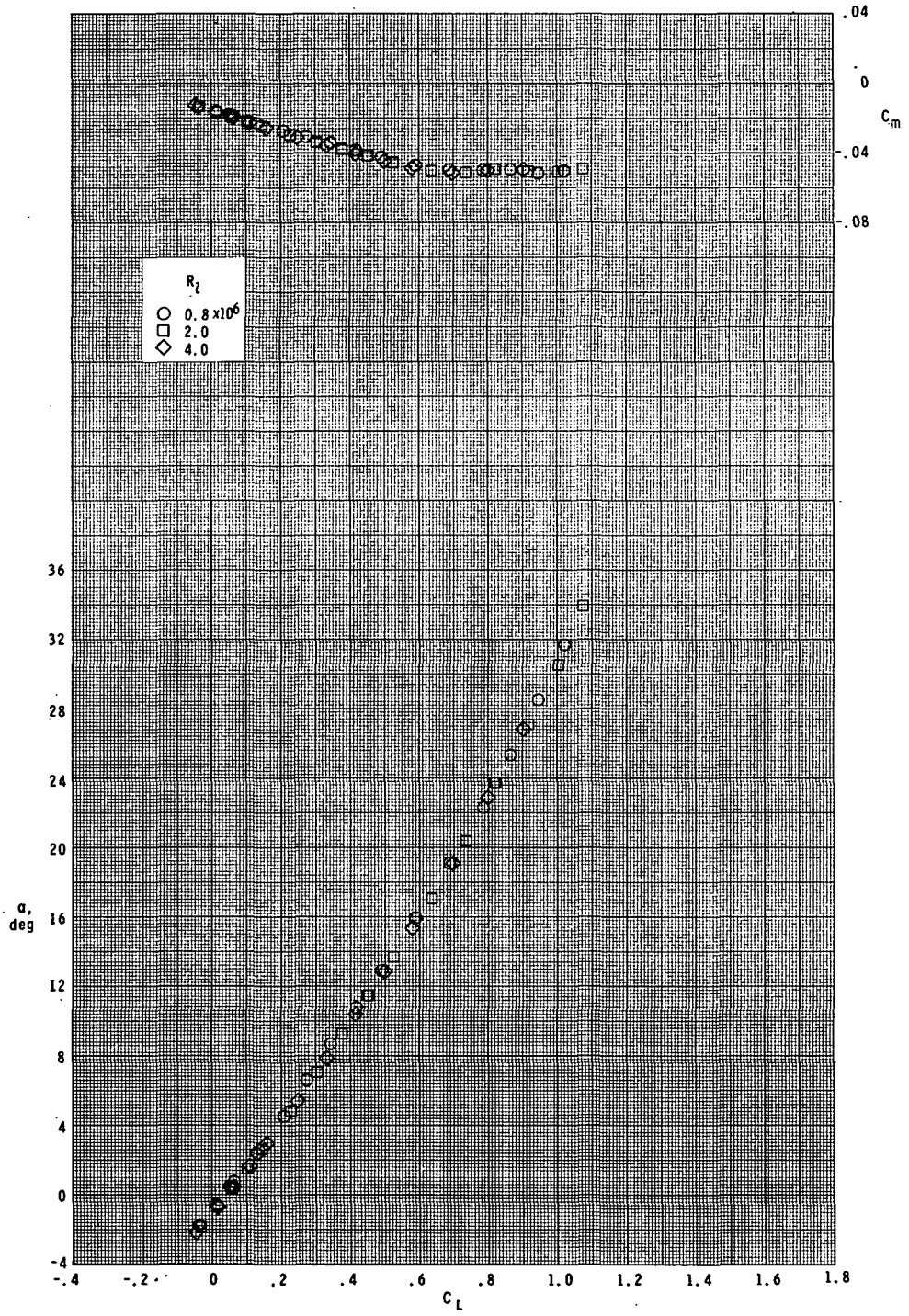

(a) Continued.

Figure 7.- Continued.

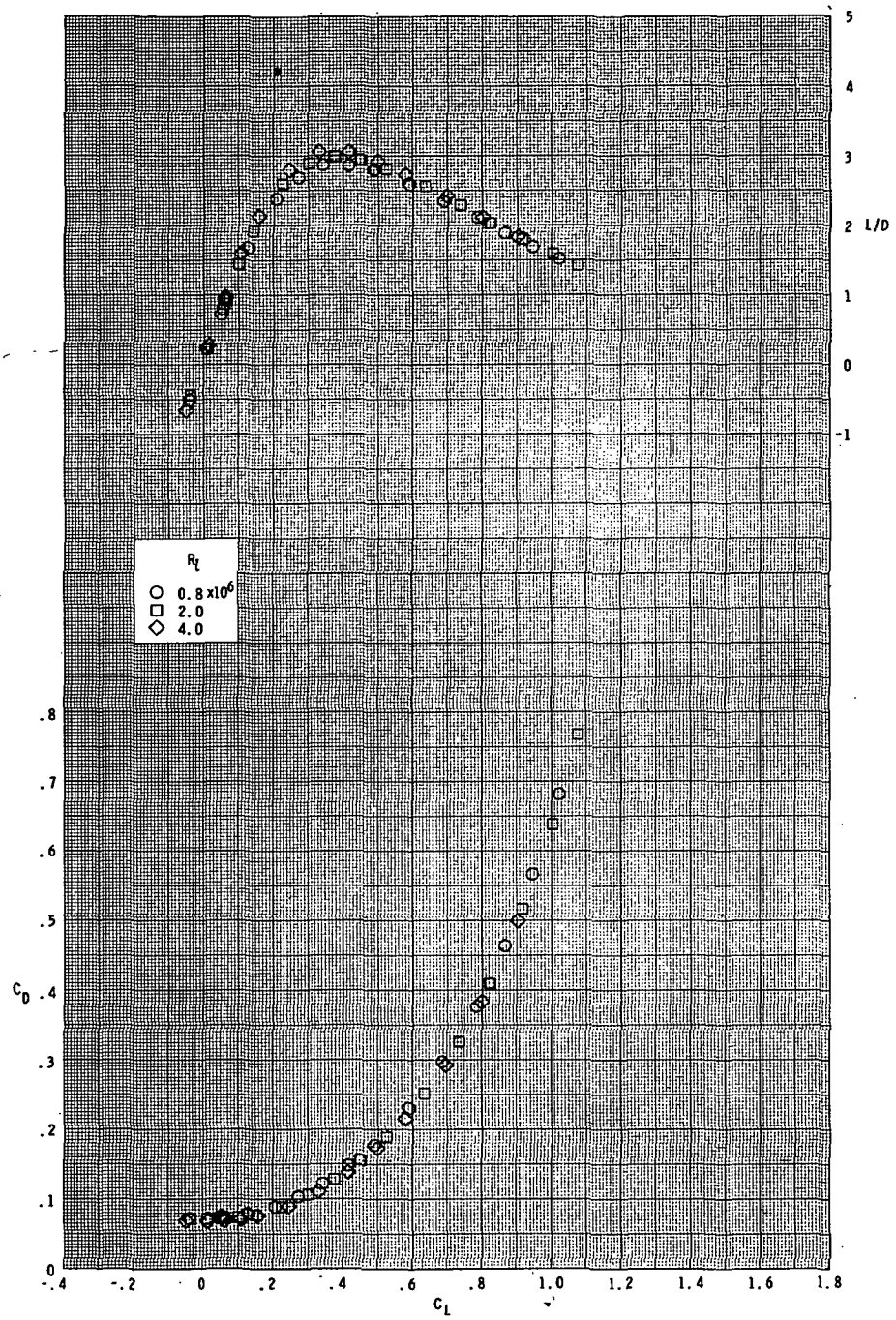

(a) Concluded.

Figure 7.- Continued.

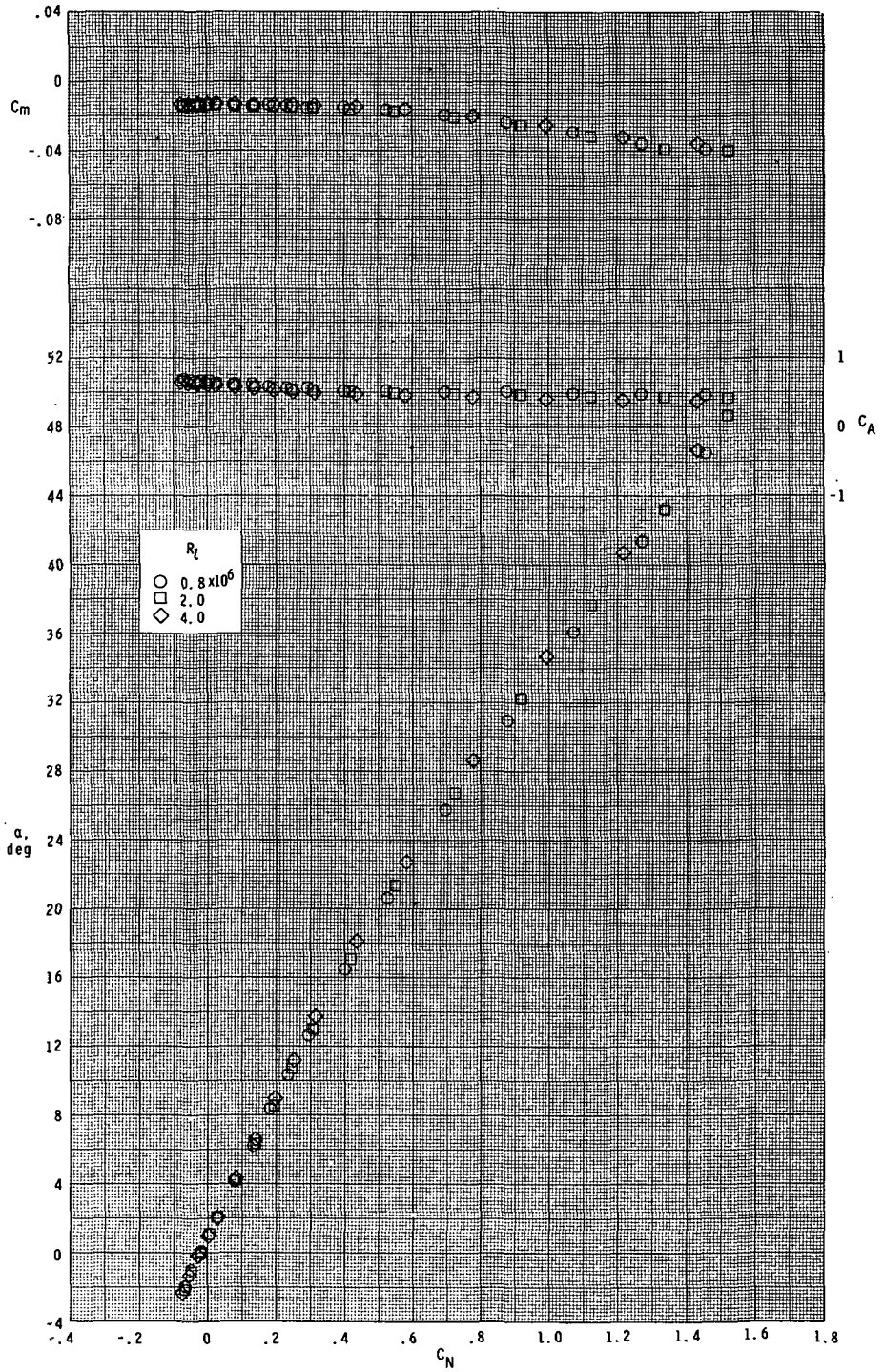

(b) M = 2.86.

Figure 7.- Continued.

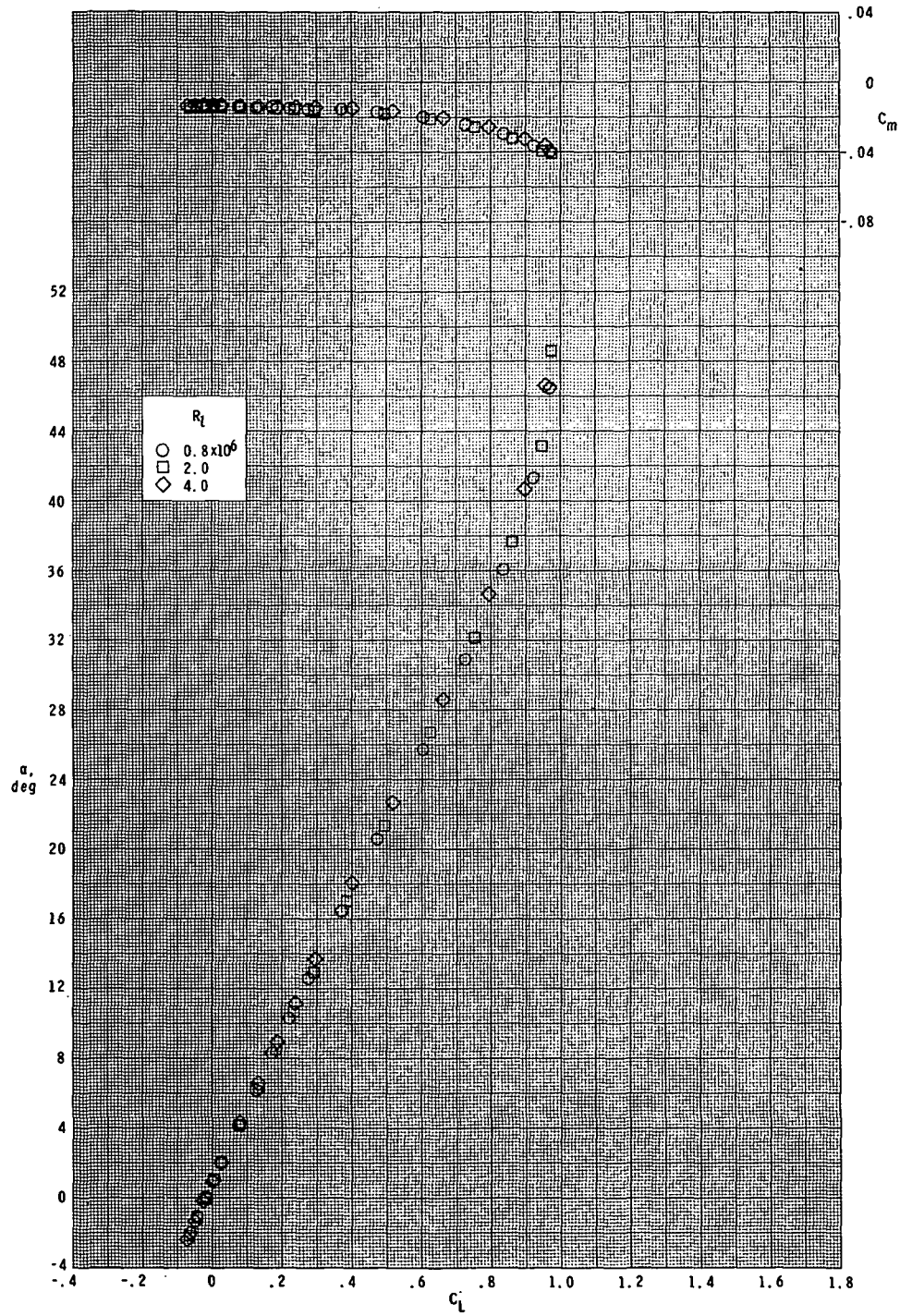

(b) Continued.

Figure 7.- Continued.

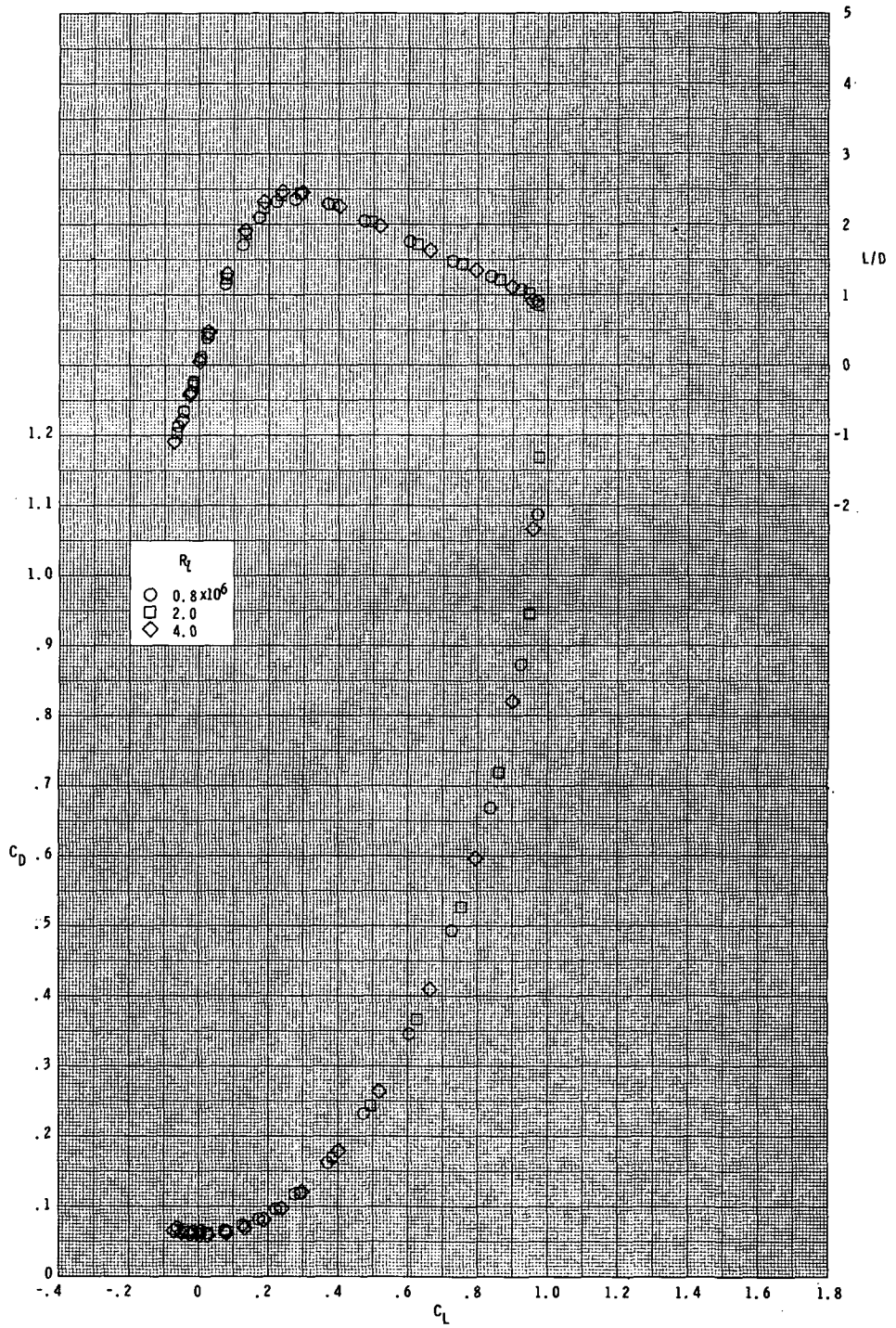

(b) Concluded.

Figure 7.- Continued.

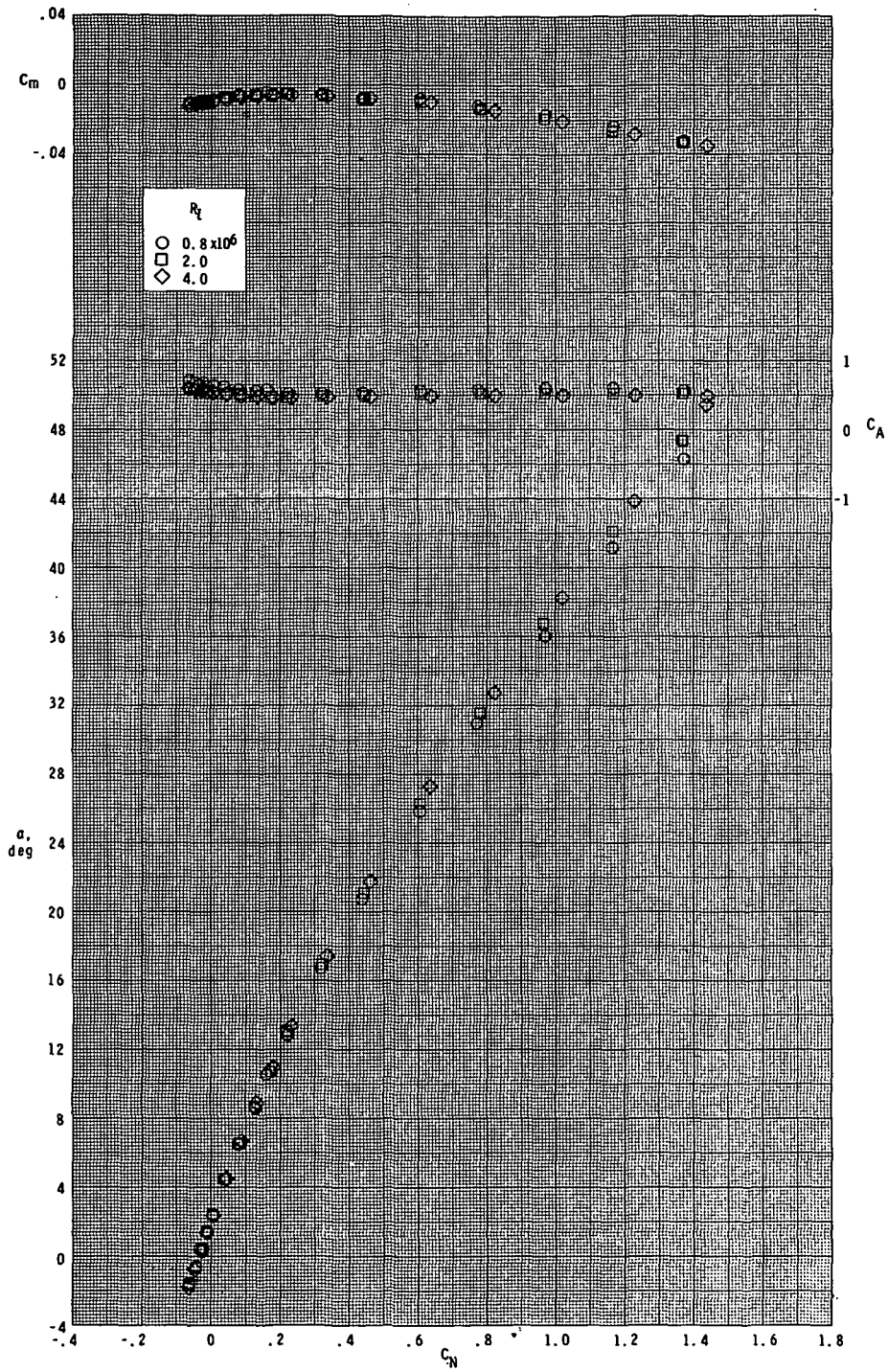

(c) M = 4.63.

Figure 7.- Continued.

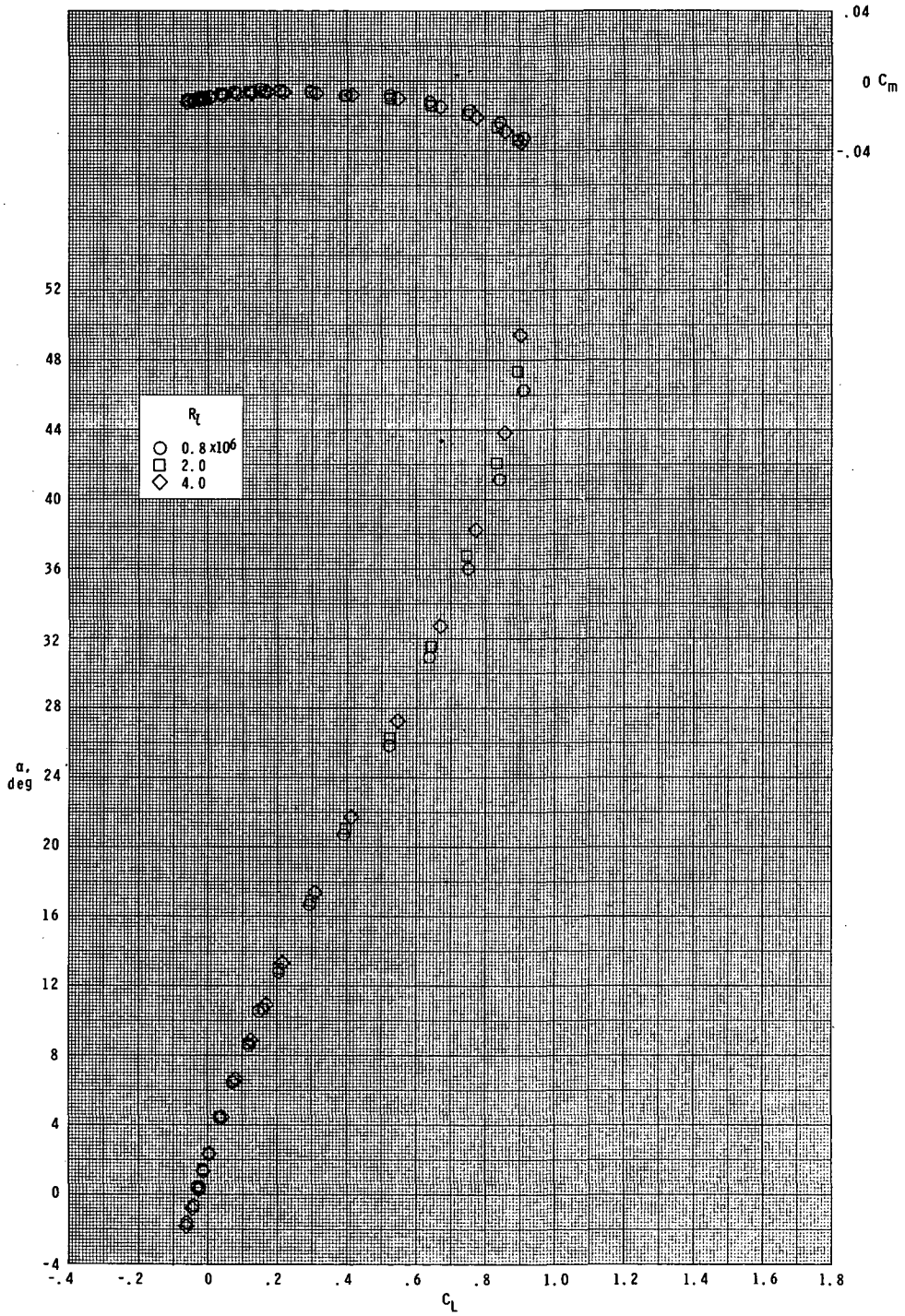

(c) Continued.

Figure 7.- Continued.

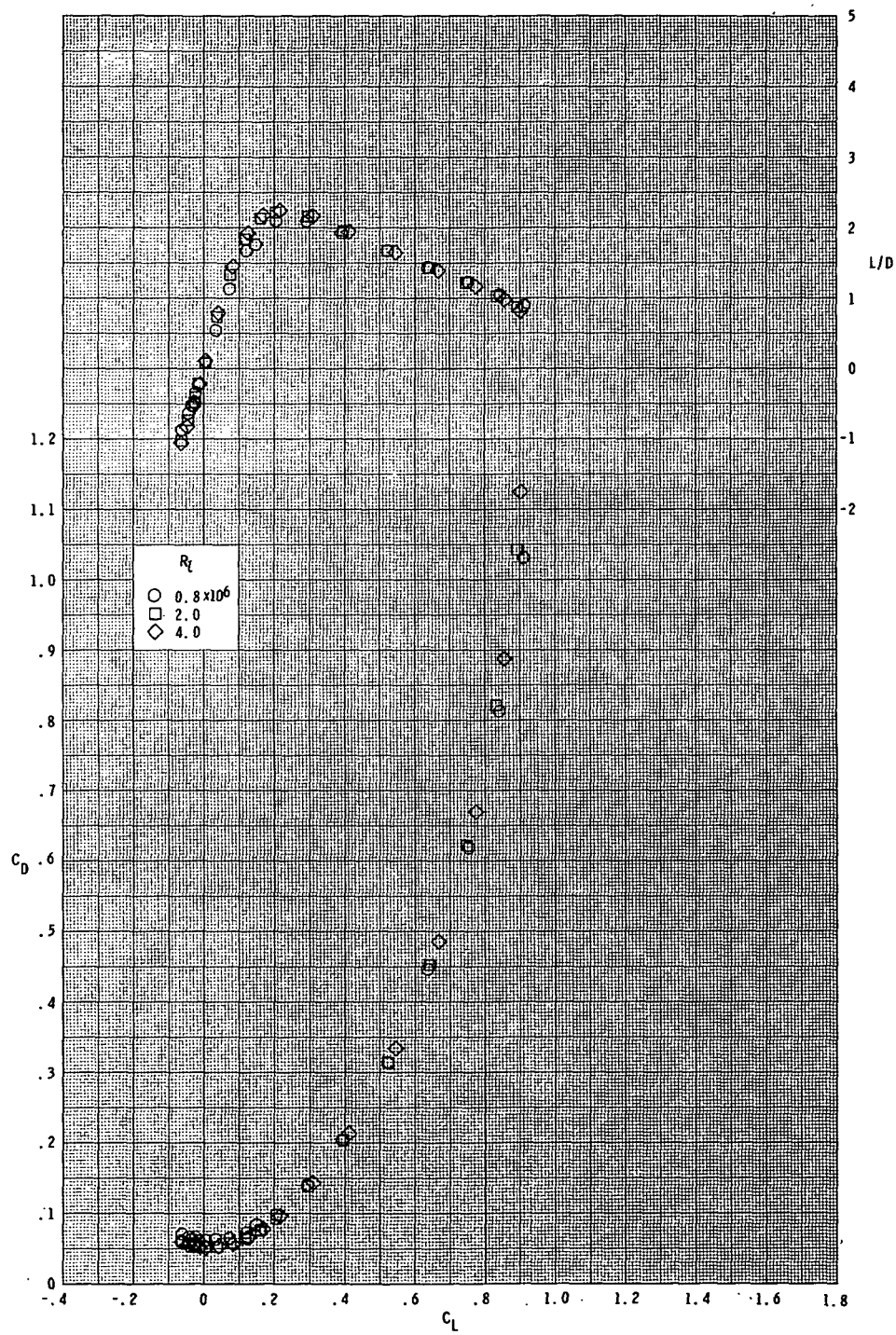

(c) Concluded.

Figure 7.- Concluded.

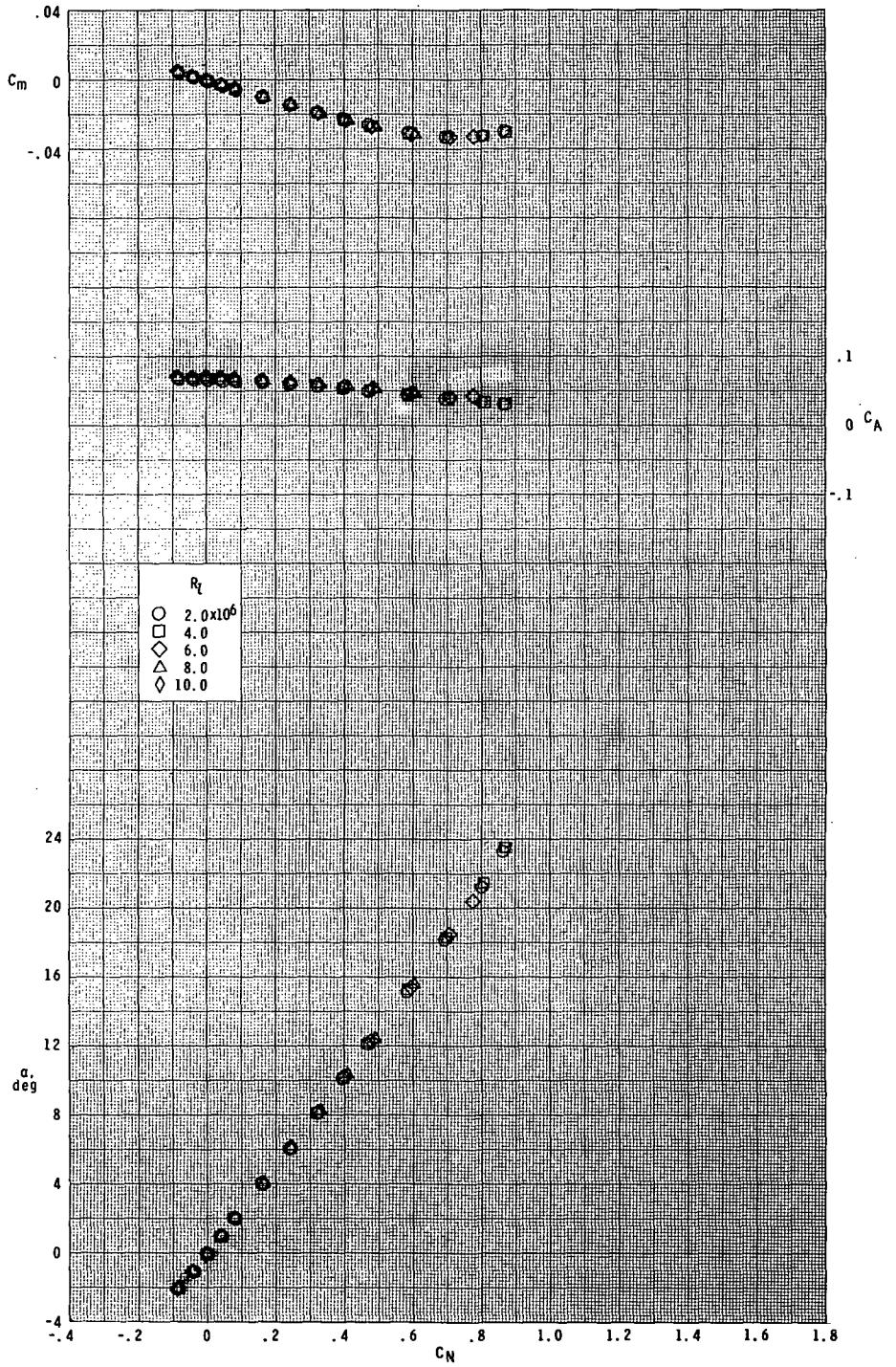

(a) M = 1.60.

Figure 8.- Effect of Reynolds number on longitudinal aerodynamic characteristics. Large model; $\delta_e = -10^o$.

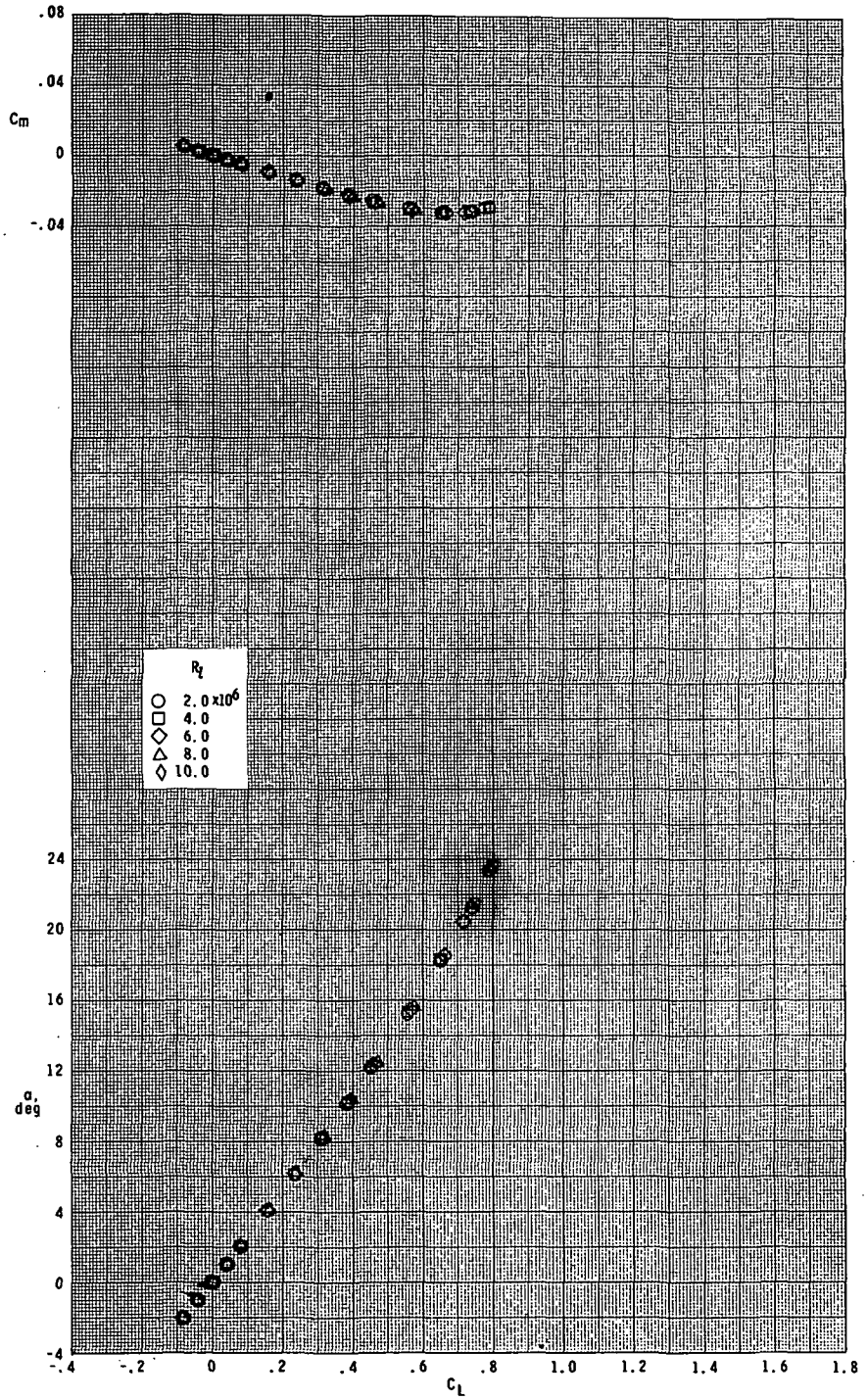

(a) Continued.

Figure 8.- Continued.

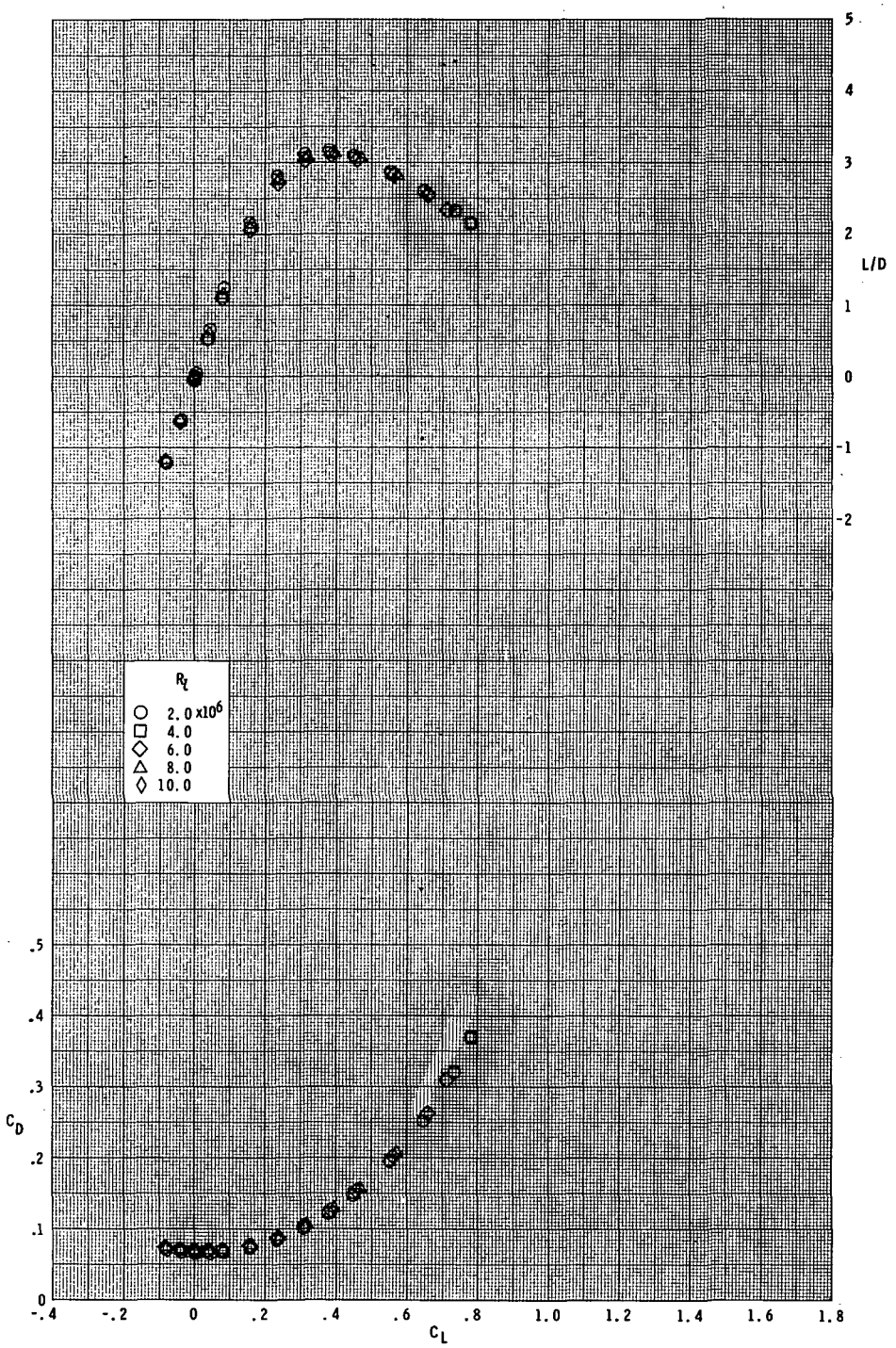

(a) Concluded.

Figure 8.- Continued.

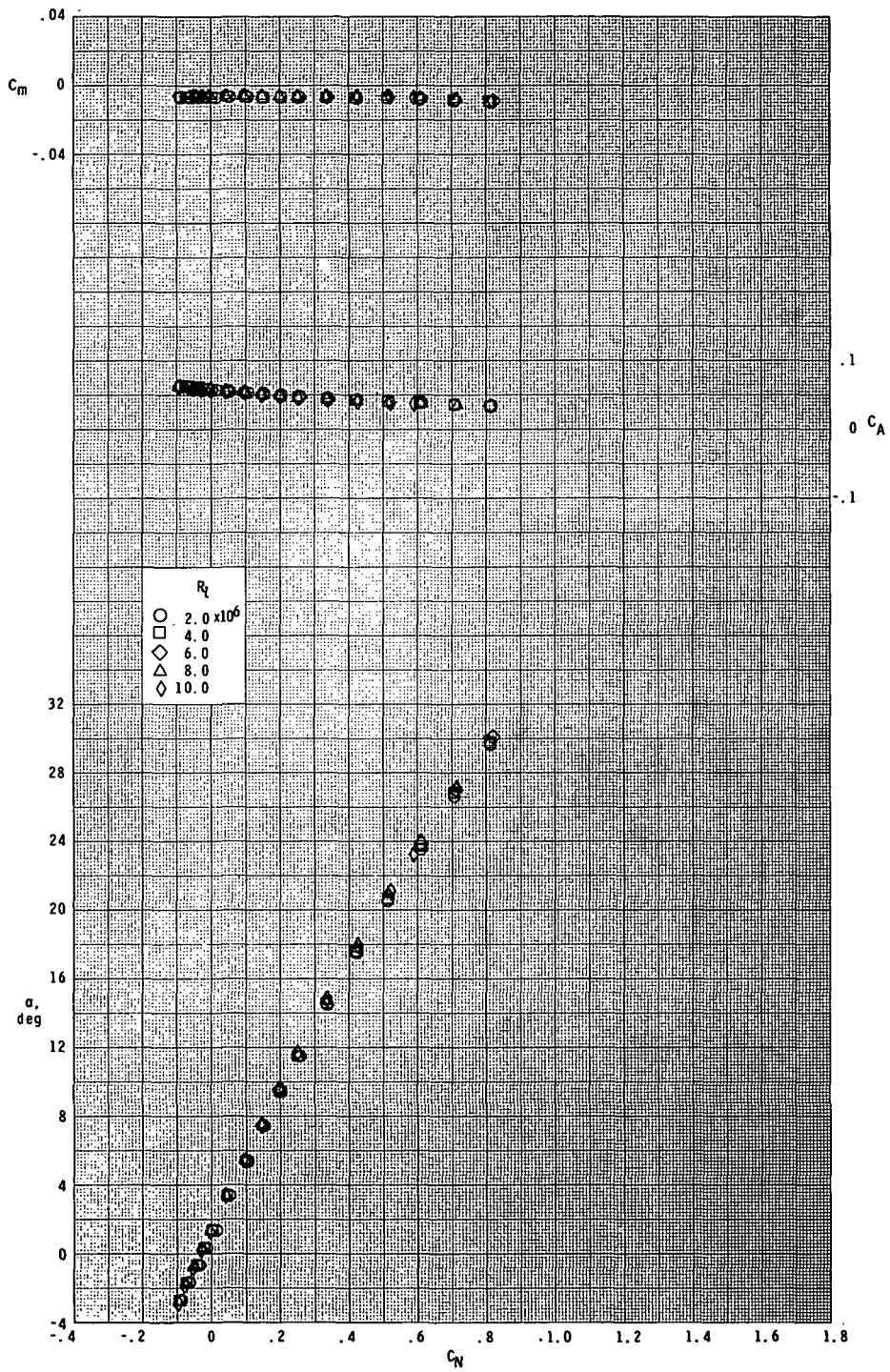

(b) M = 2.86.

Figure 8.- Continued.

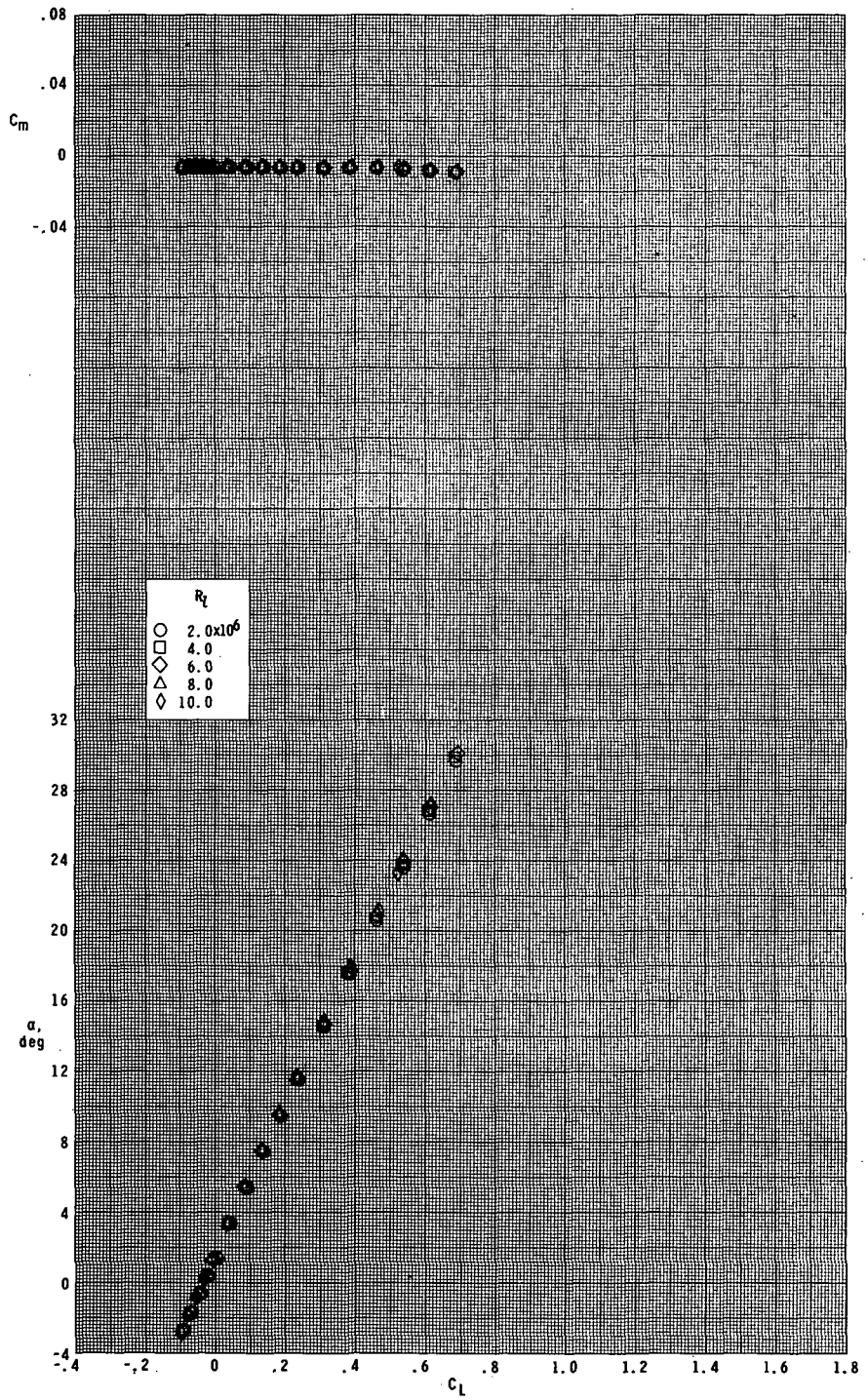

(b) Continued.

Figure 8.- Continued.

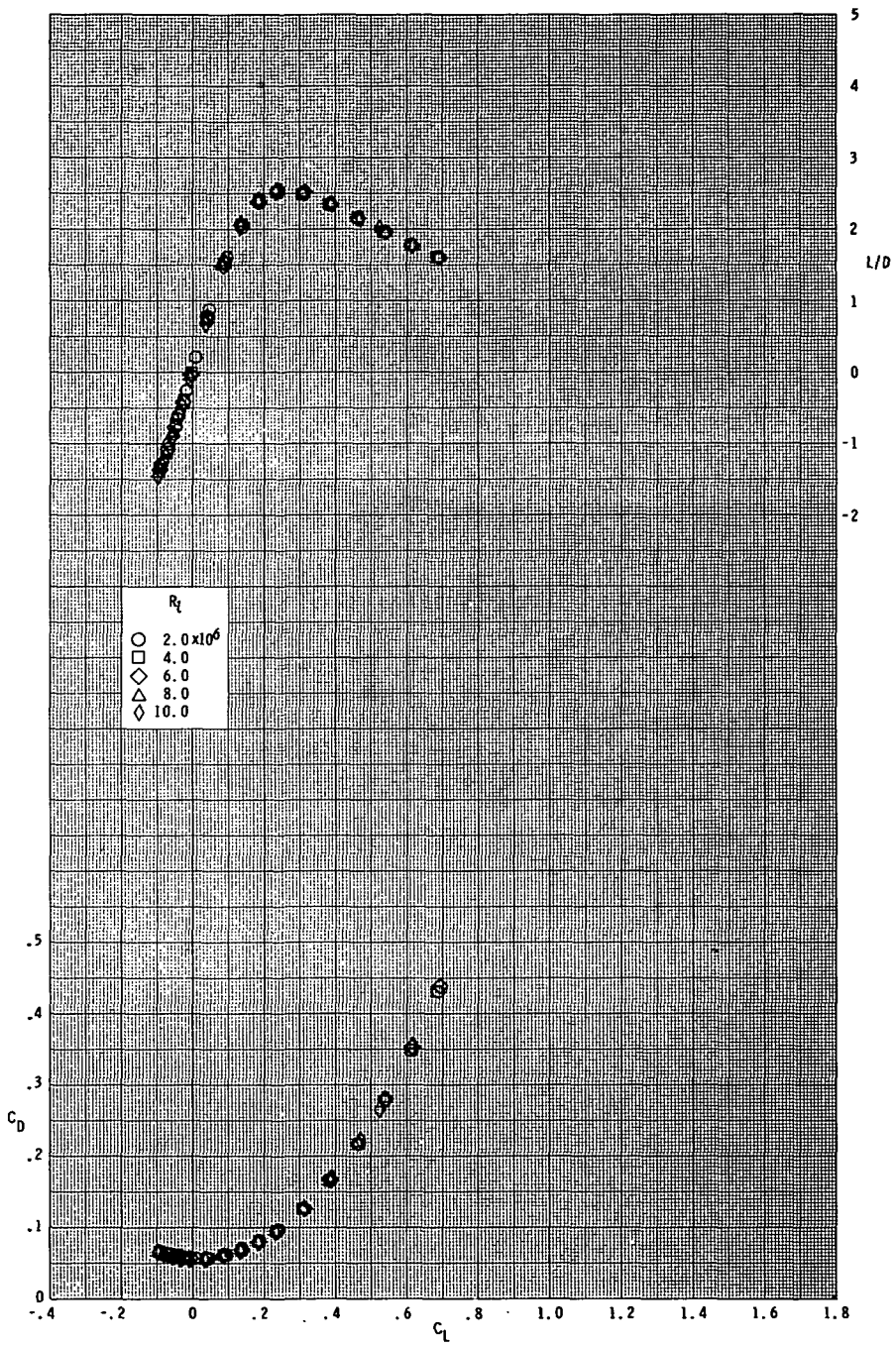

(b) Concluded.

Figure 8. - Continued.

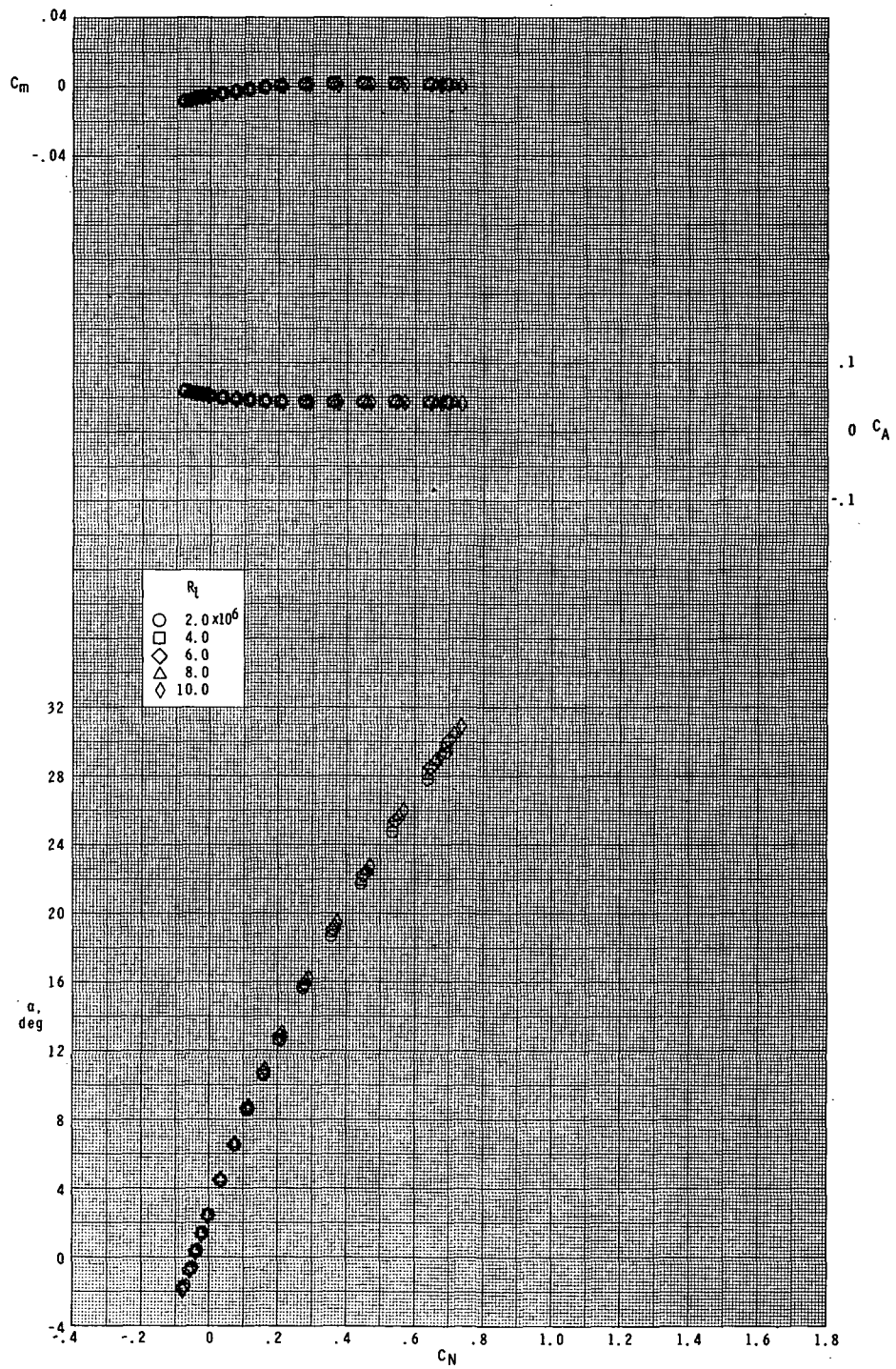

(c) M = 4.63.

Figure 8.- Continued.

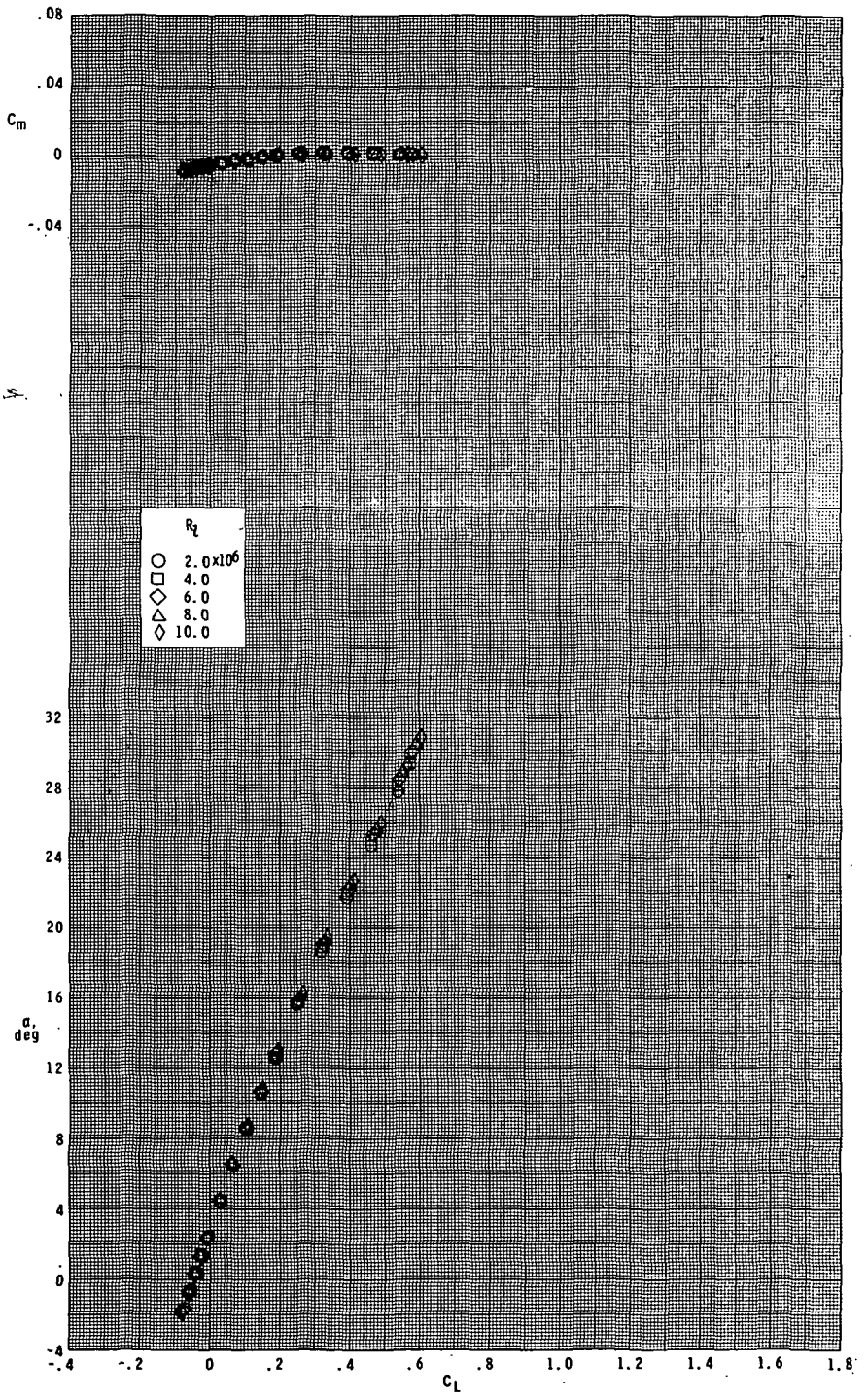

(c) Continued.

Figure 8.- Continued.

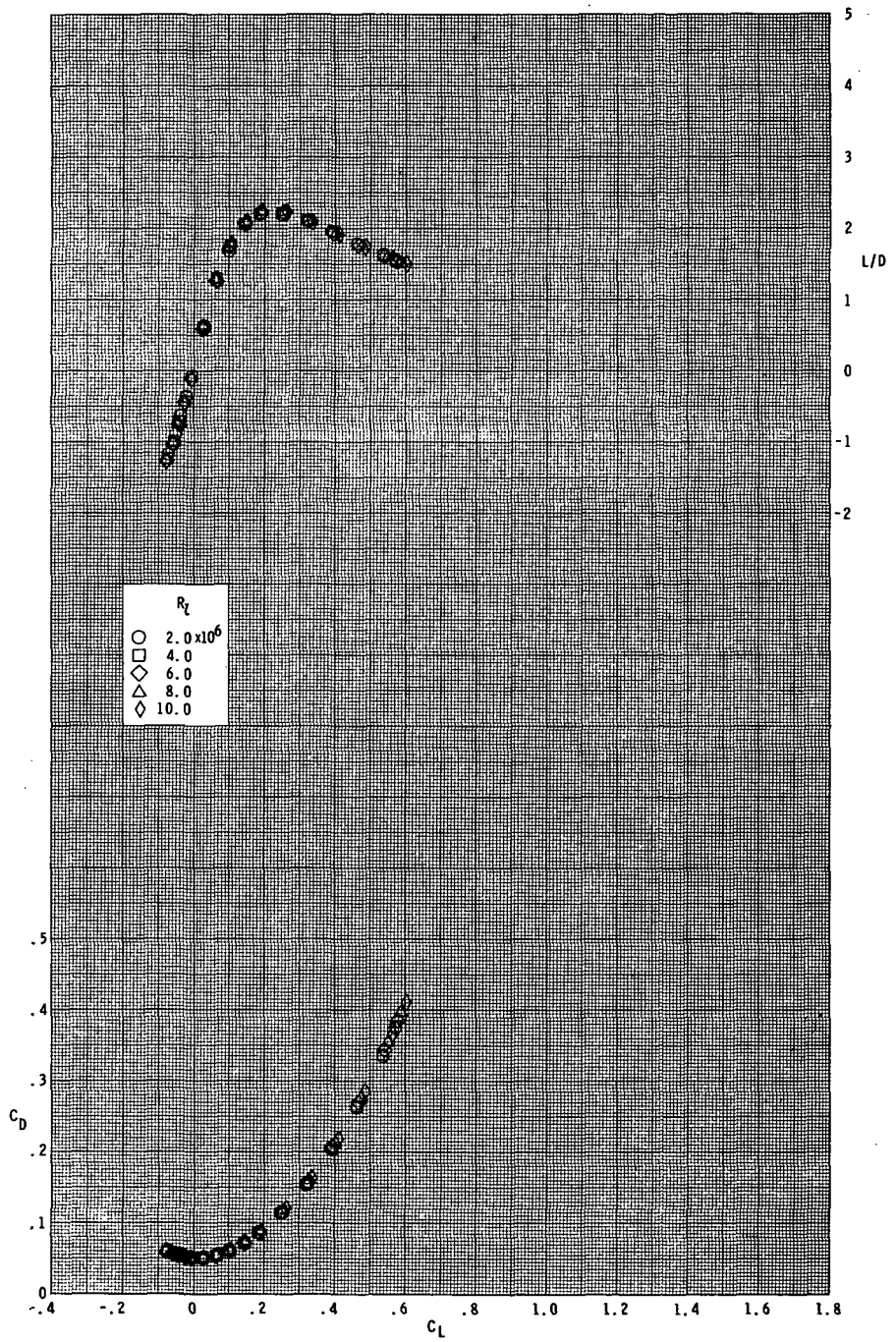

(c) Concluded.

Figure 8.- Concluded.

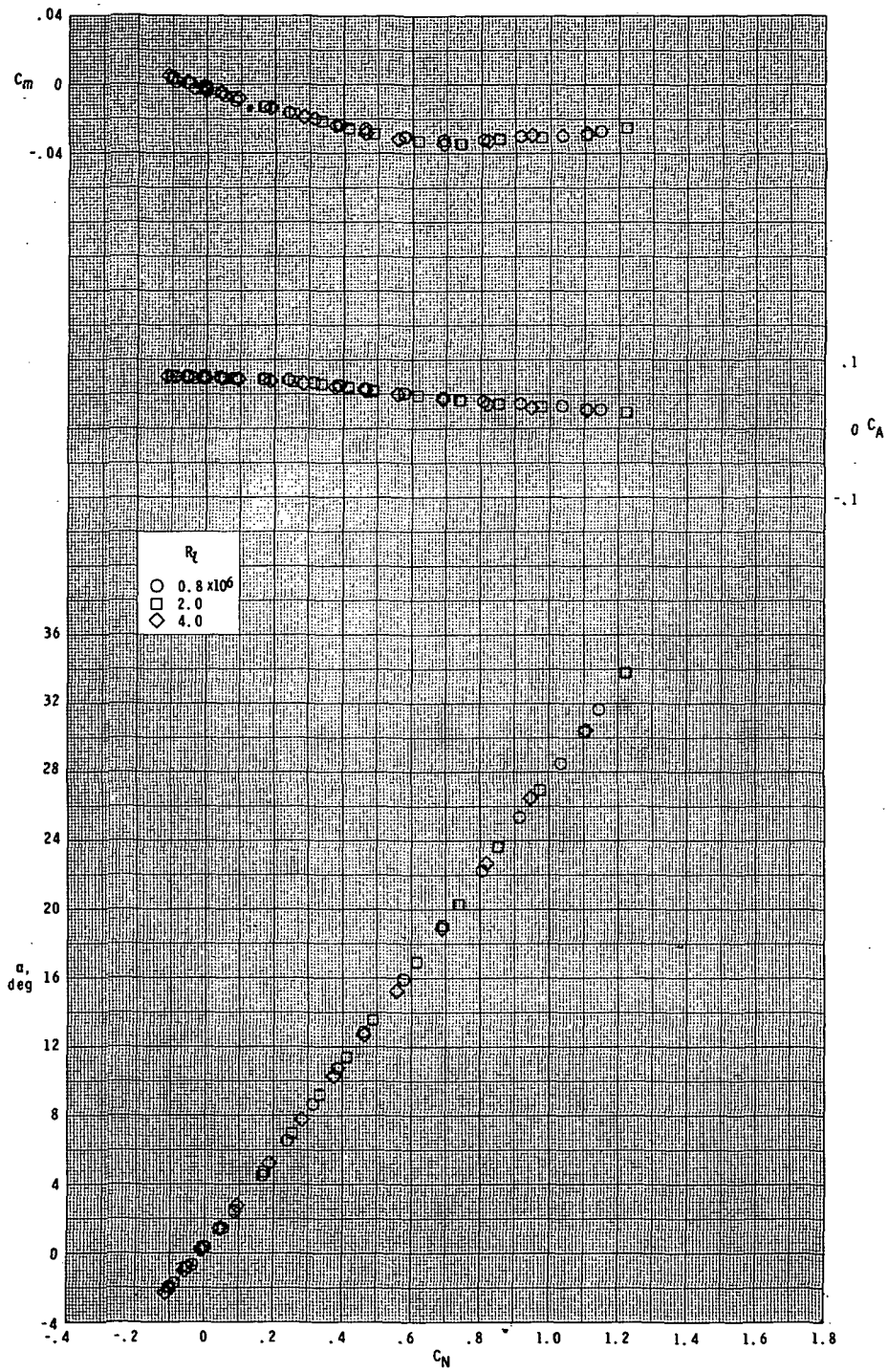

(a) M = 1.60.

Figure 9.- Effect of Reynolds number on longitudinal aerodynamic characteristics. Small model; $\delta_e = -10^o$.

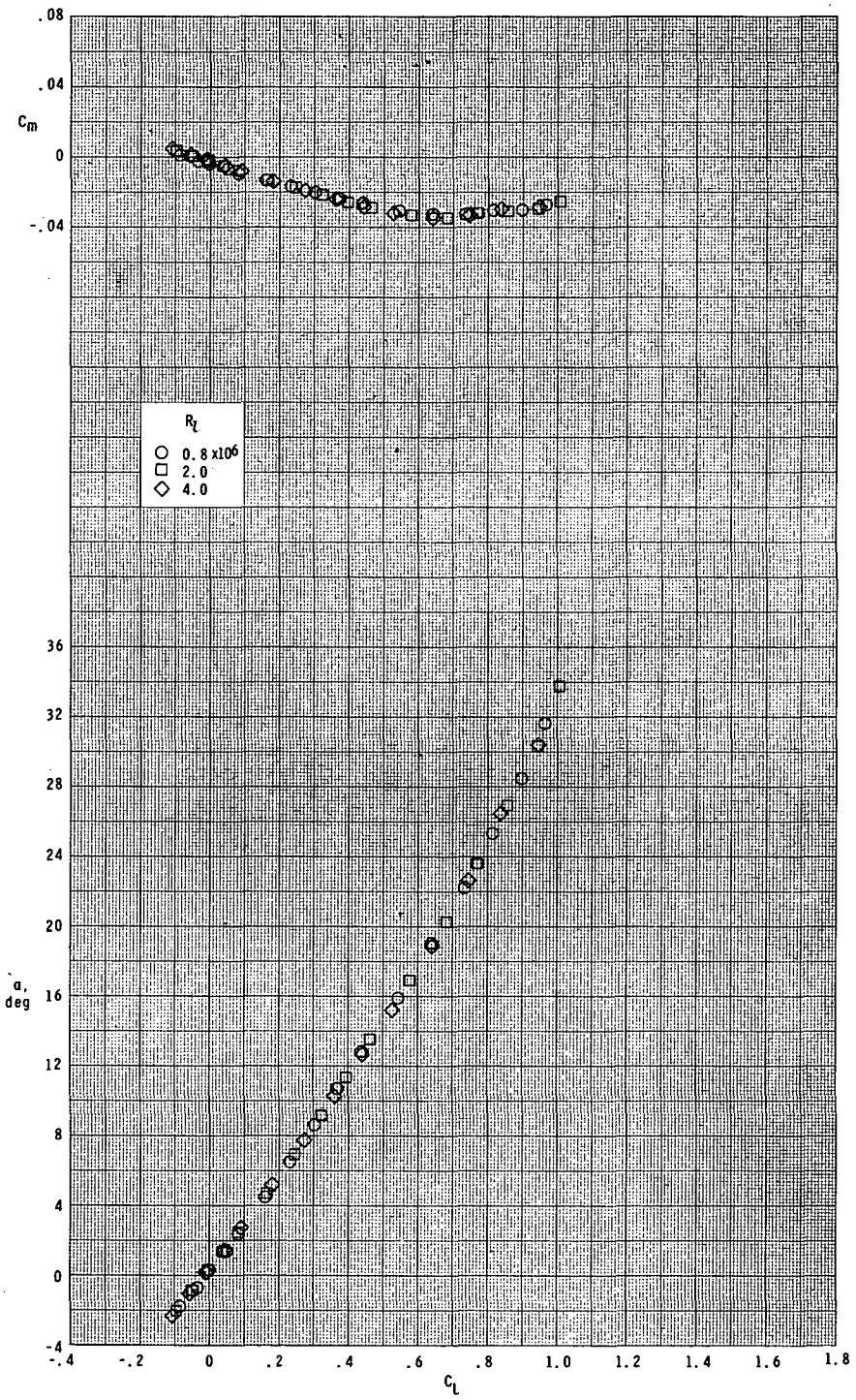

(a) Continued.

Figure 9.- Continued.

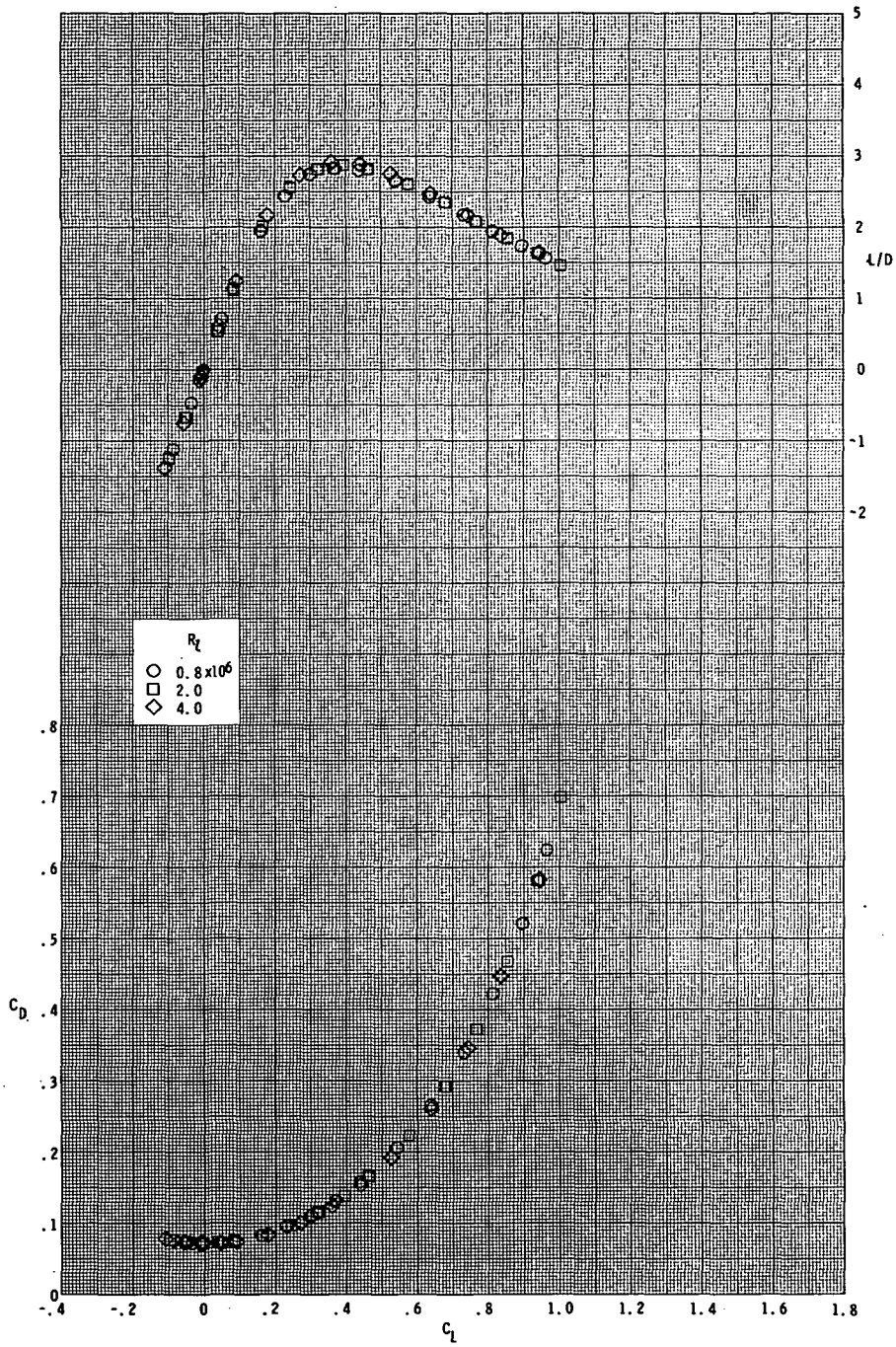

(a) Concluded.

Figure 9.- Continued.

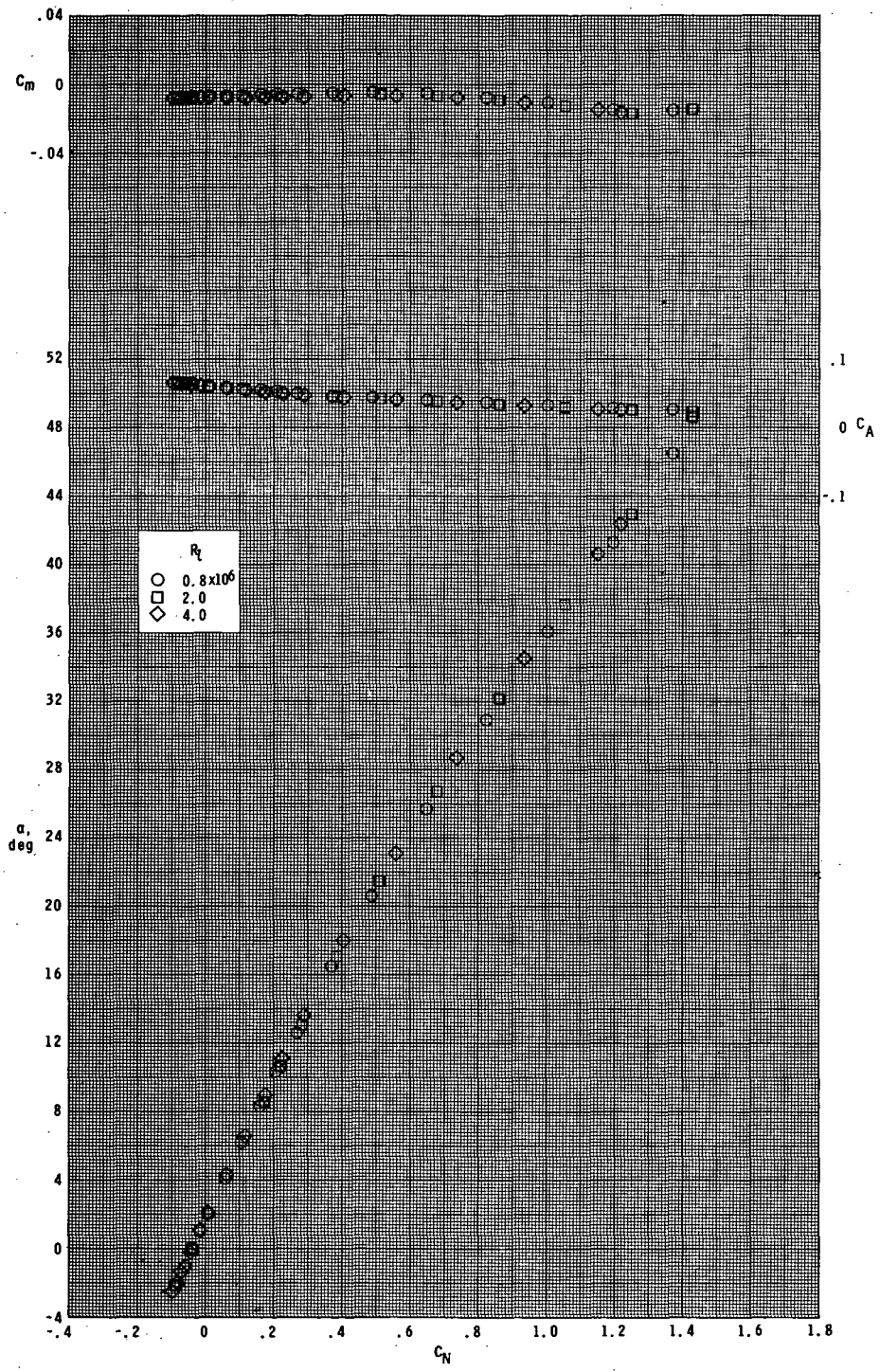

(b) M = 2.86.

Figure 9.- Continued.

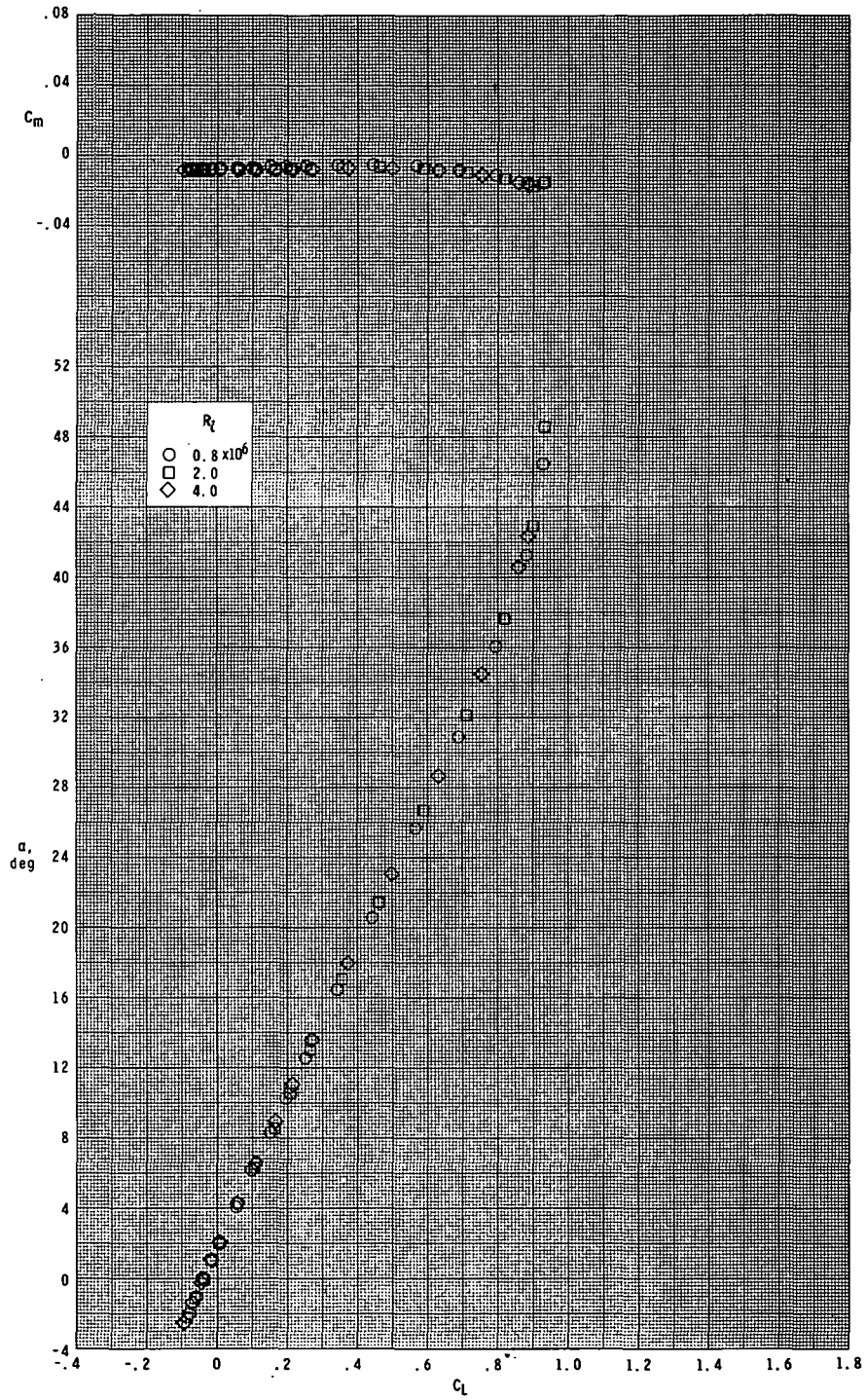

(b) Continued.

Figure 9.- Continued.

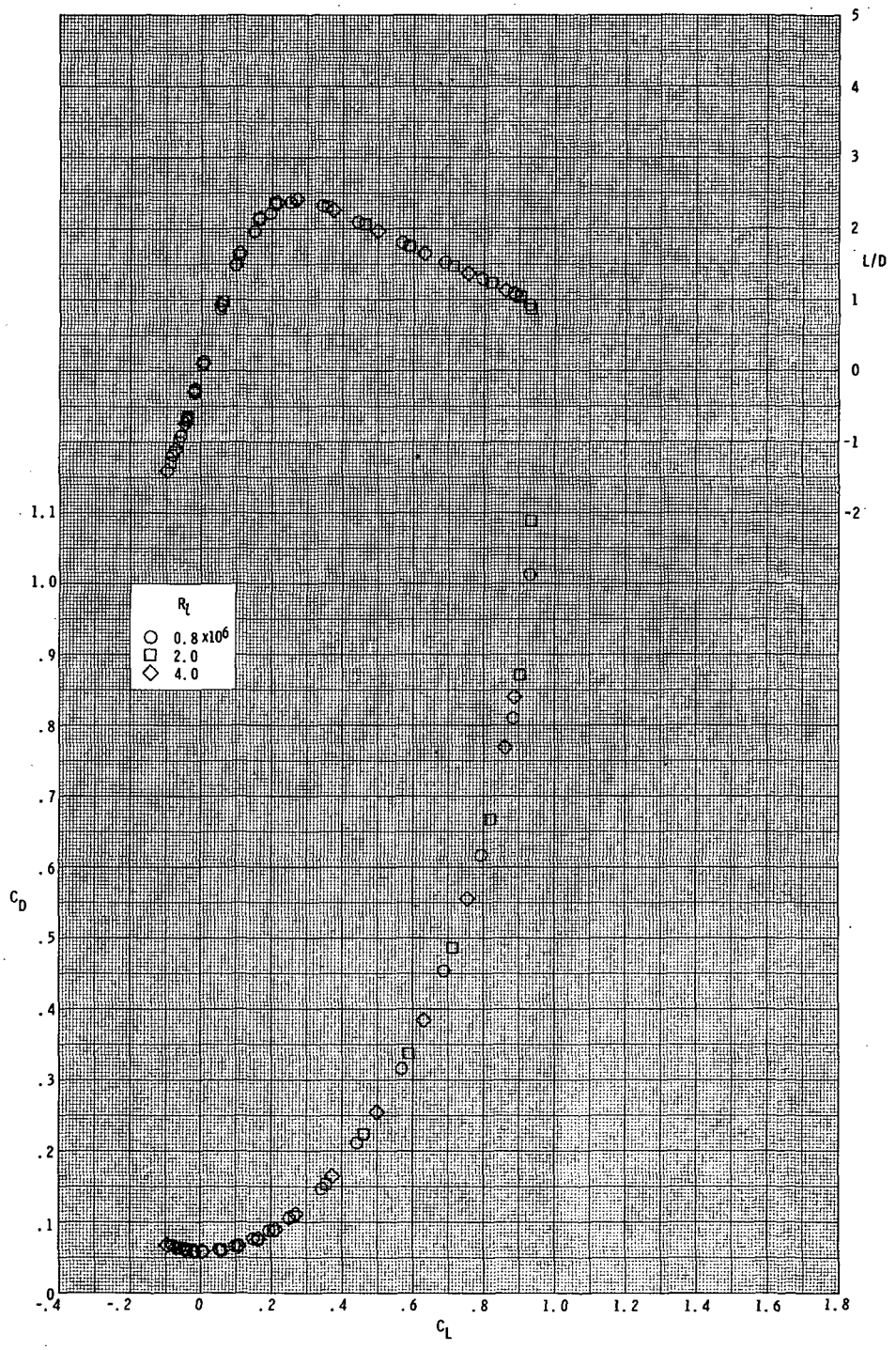

(b) Concluded.

Figure 9.- Continued.

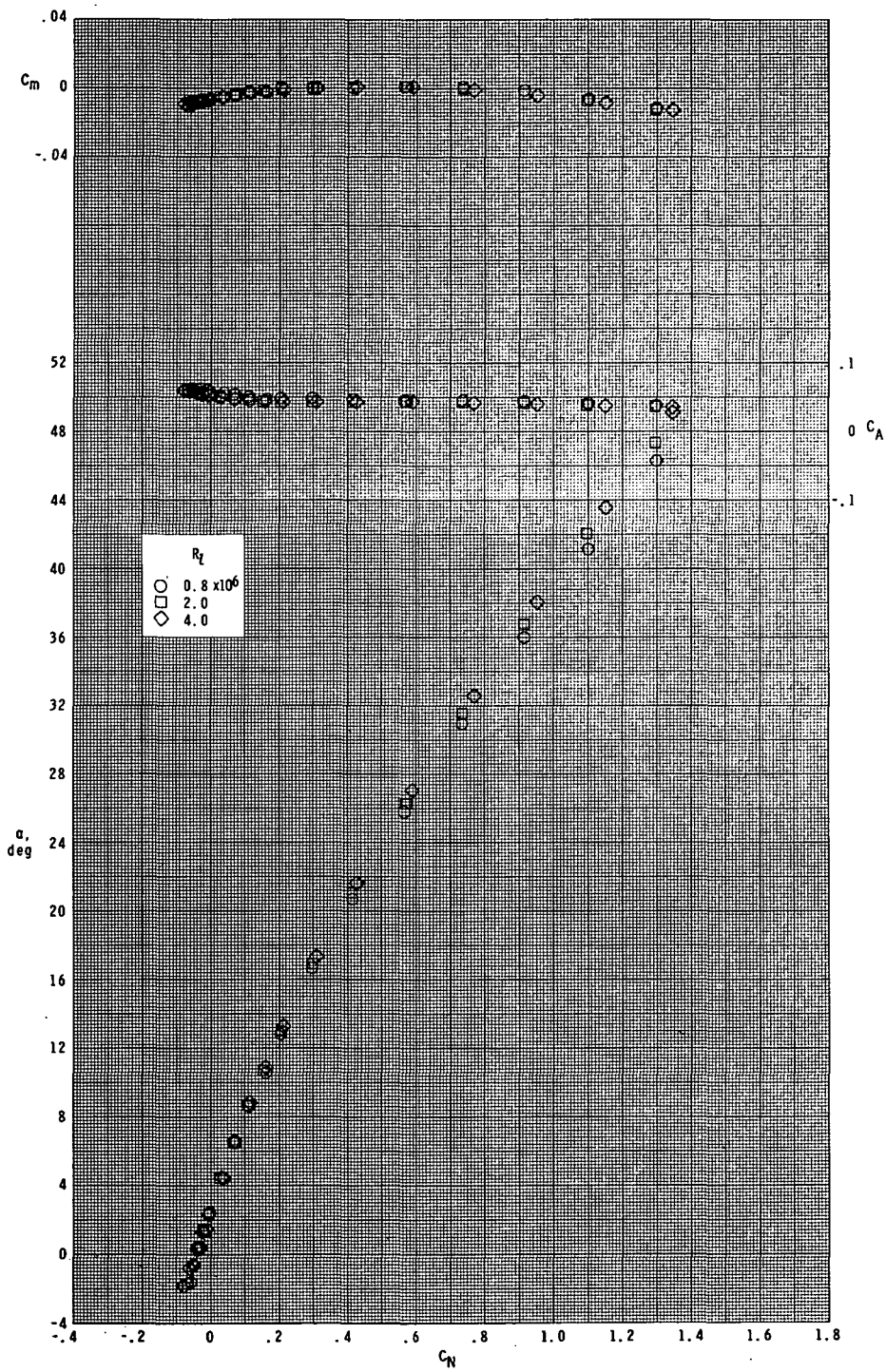

(c) M = 4.63.

Figure 9.- Continued.

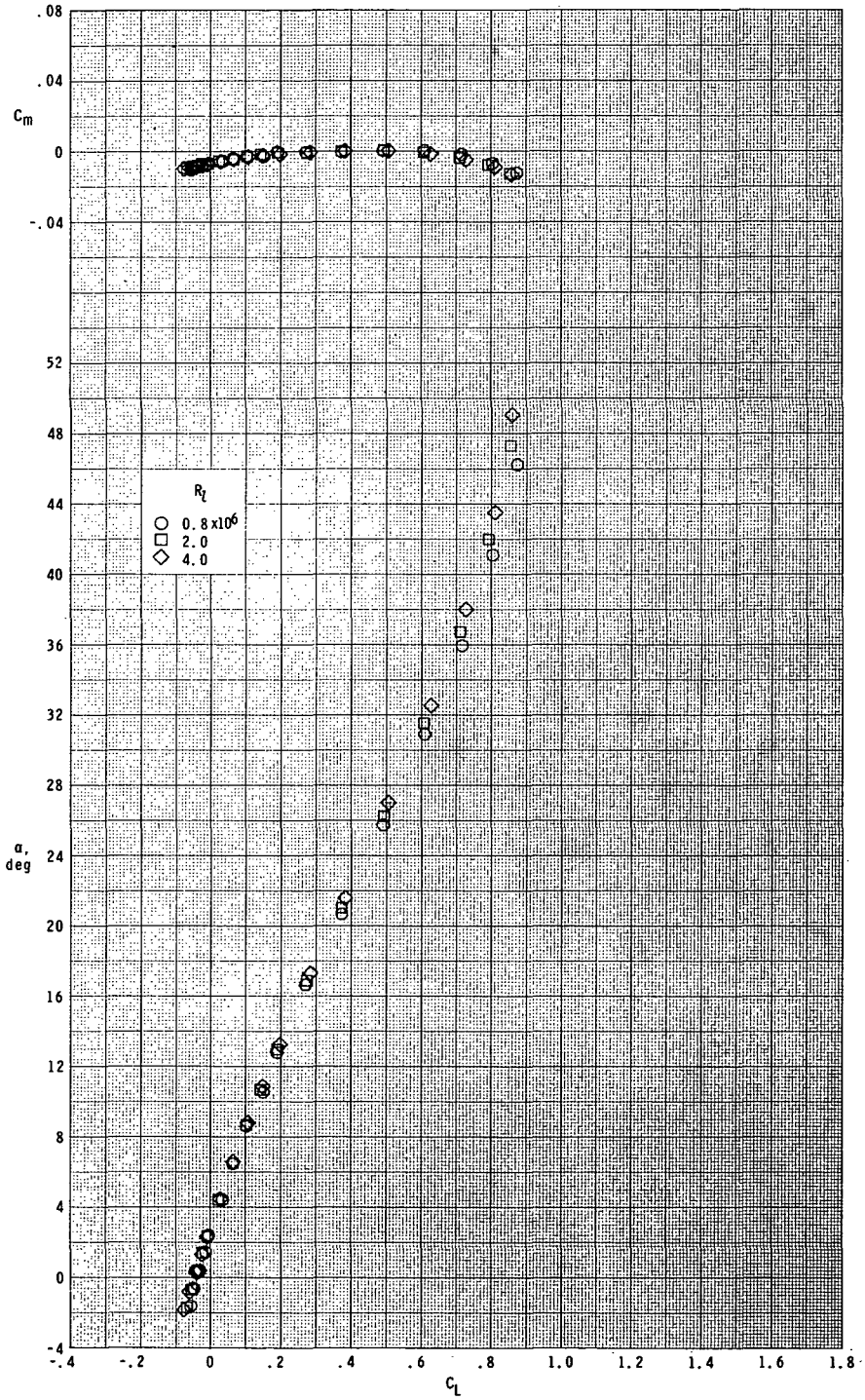

(c) Continued.

Figure 9.- Continued.

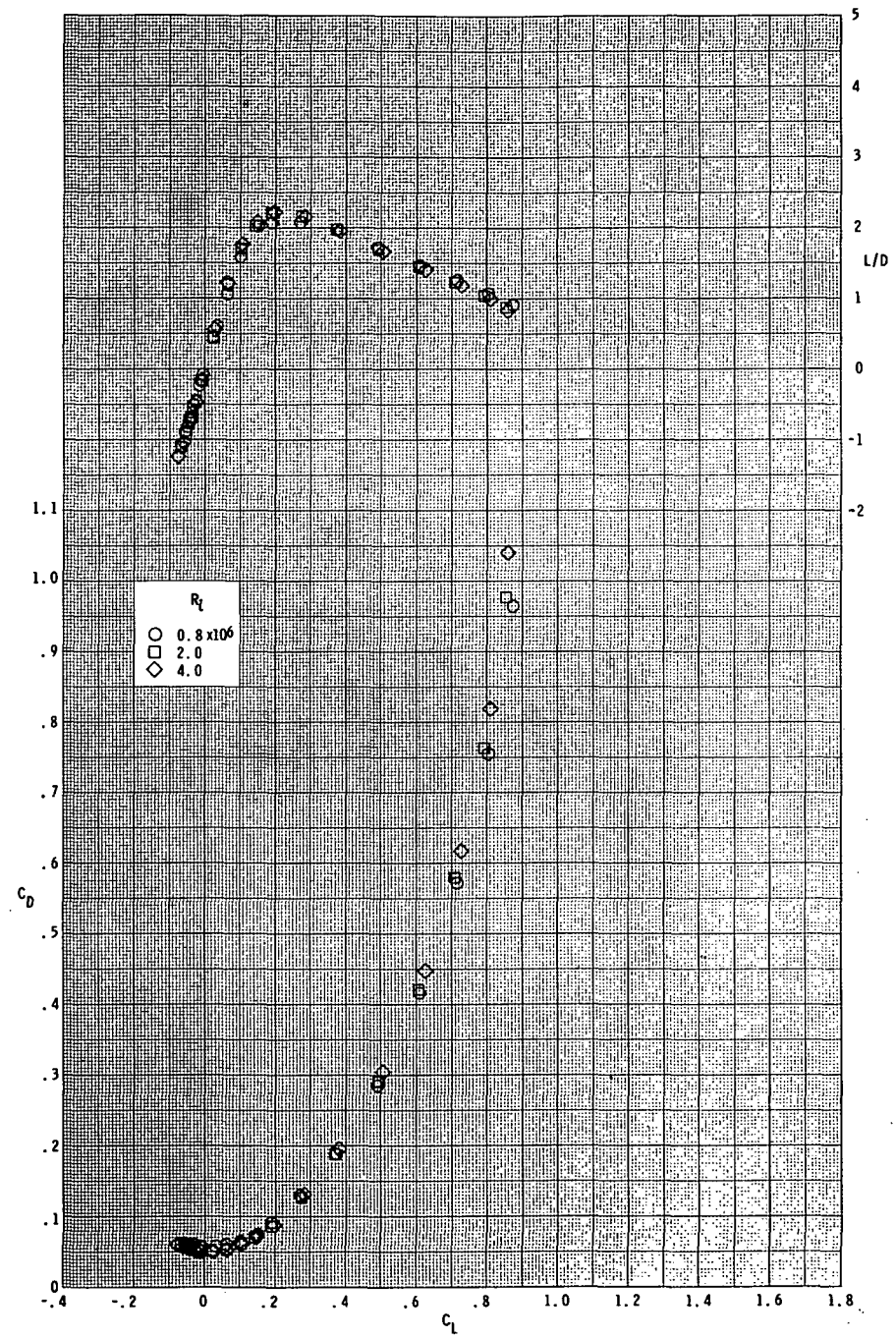

(c) Concluded.

Figure 9.- Concluded.

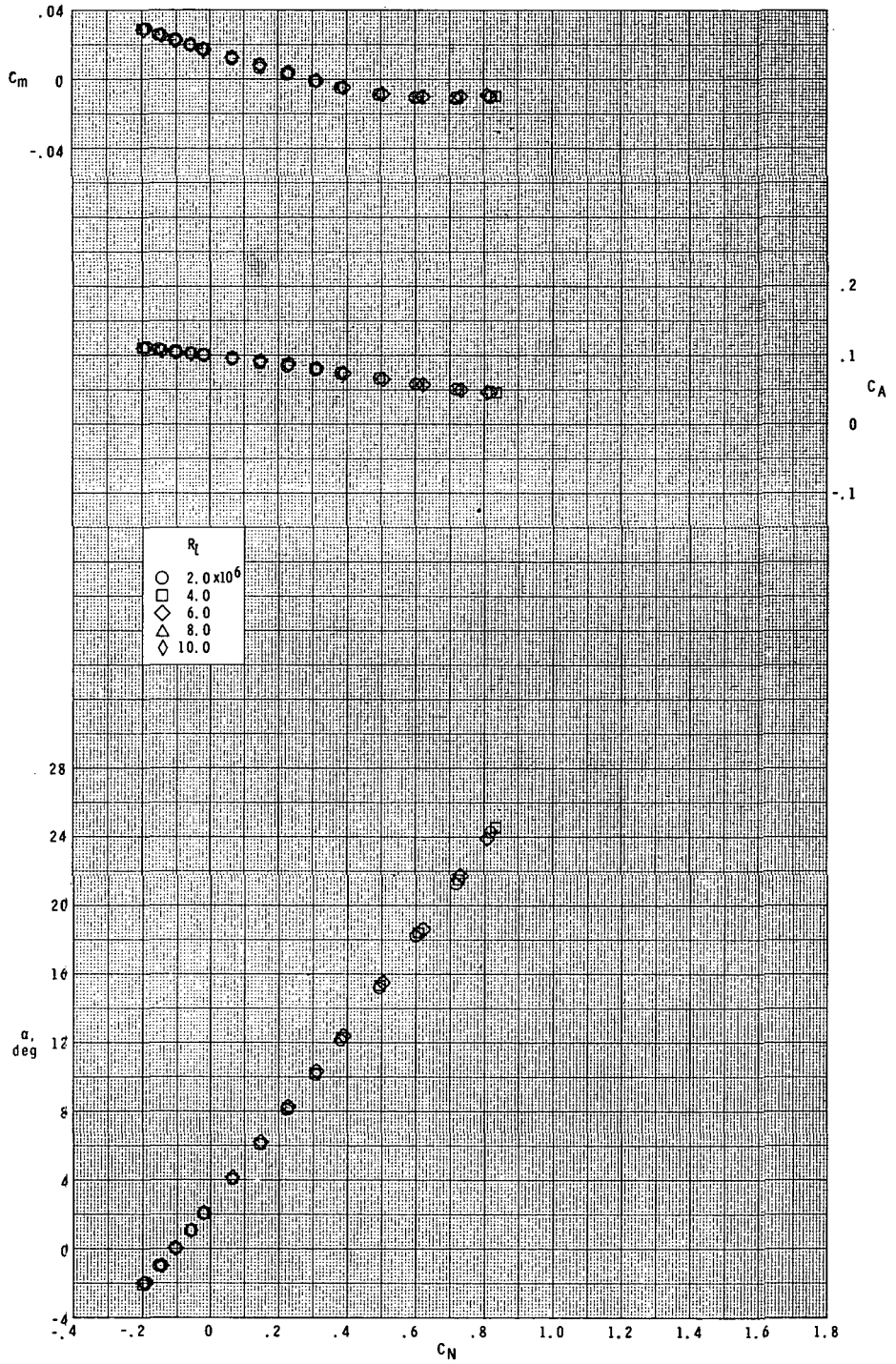

(a) M = 1.60.

Figure 10.- Effect of Reynolds number on longitudinal aerodynamic characteristics. Large model; $\delta_e = -30^o$.

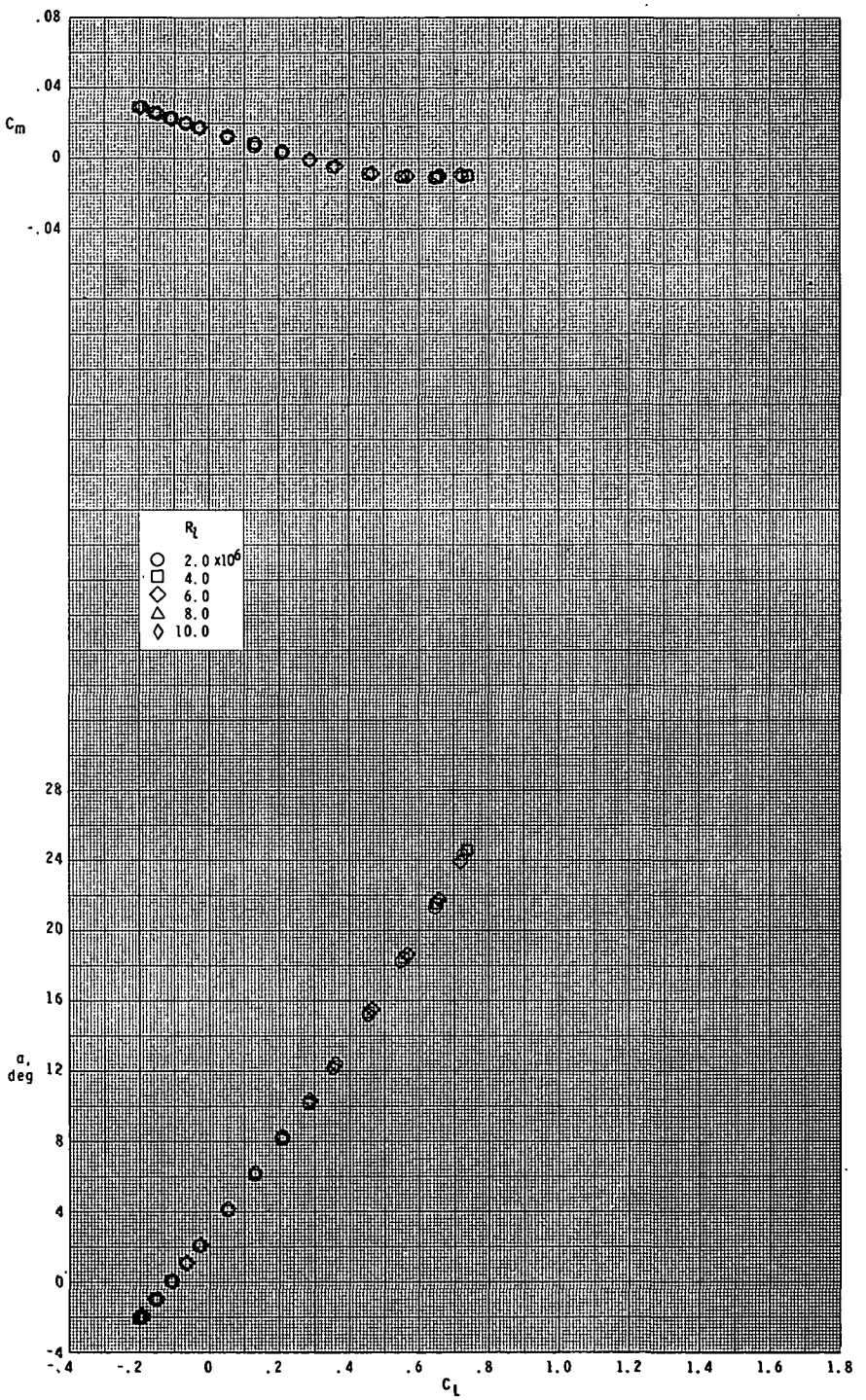

(a) Continued.

Figure 10. - Continued.

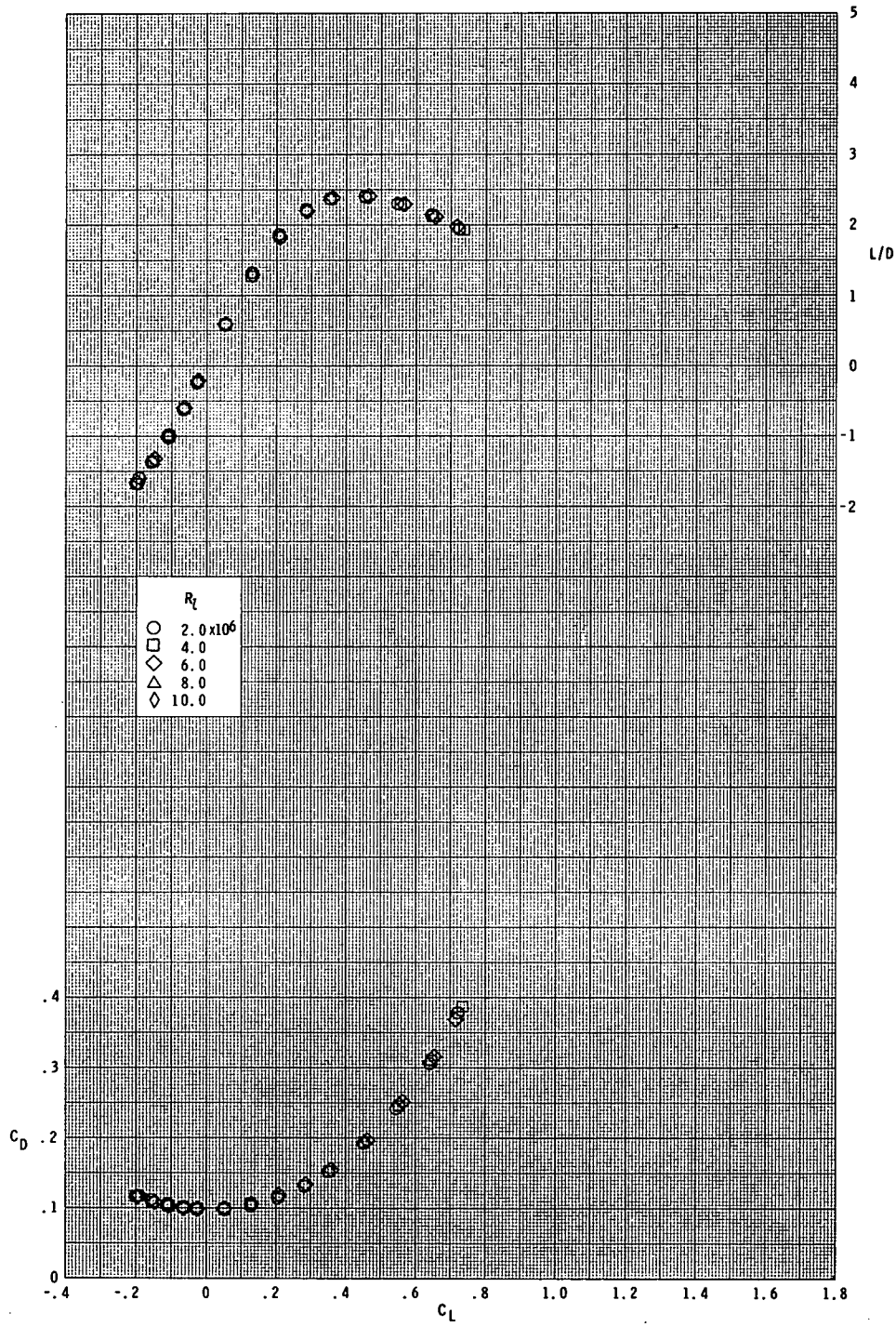

(a) Concluded.

Figure 10.- Continued.

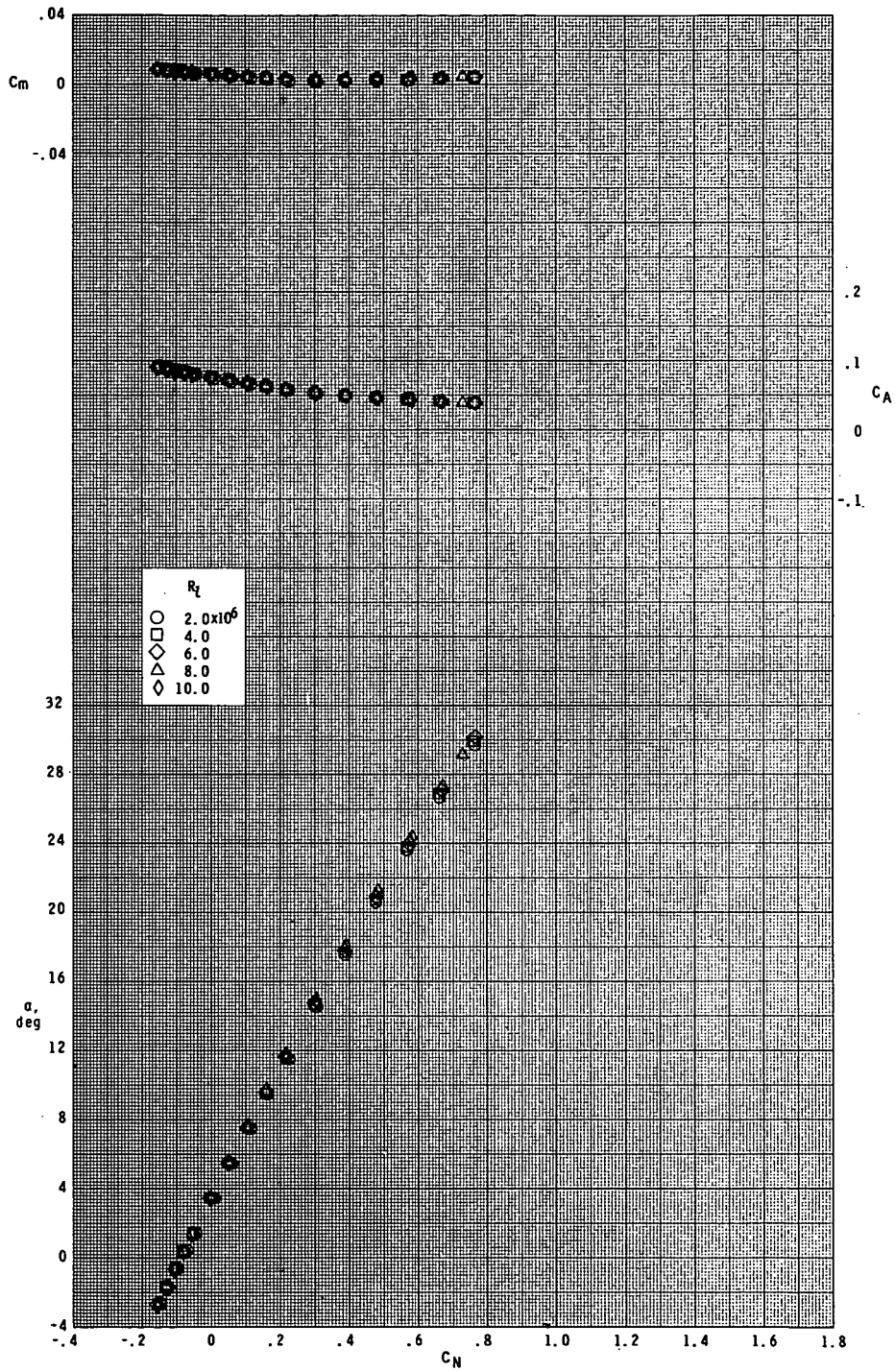

(b) M = 2.86.

Figure 10.- Continued.

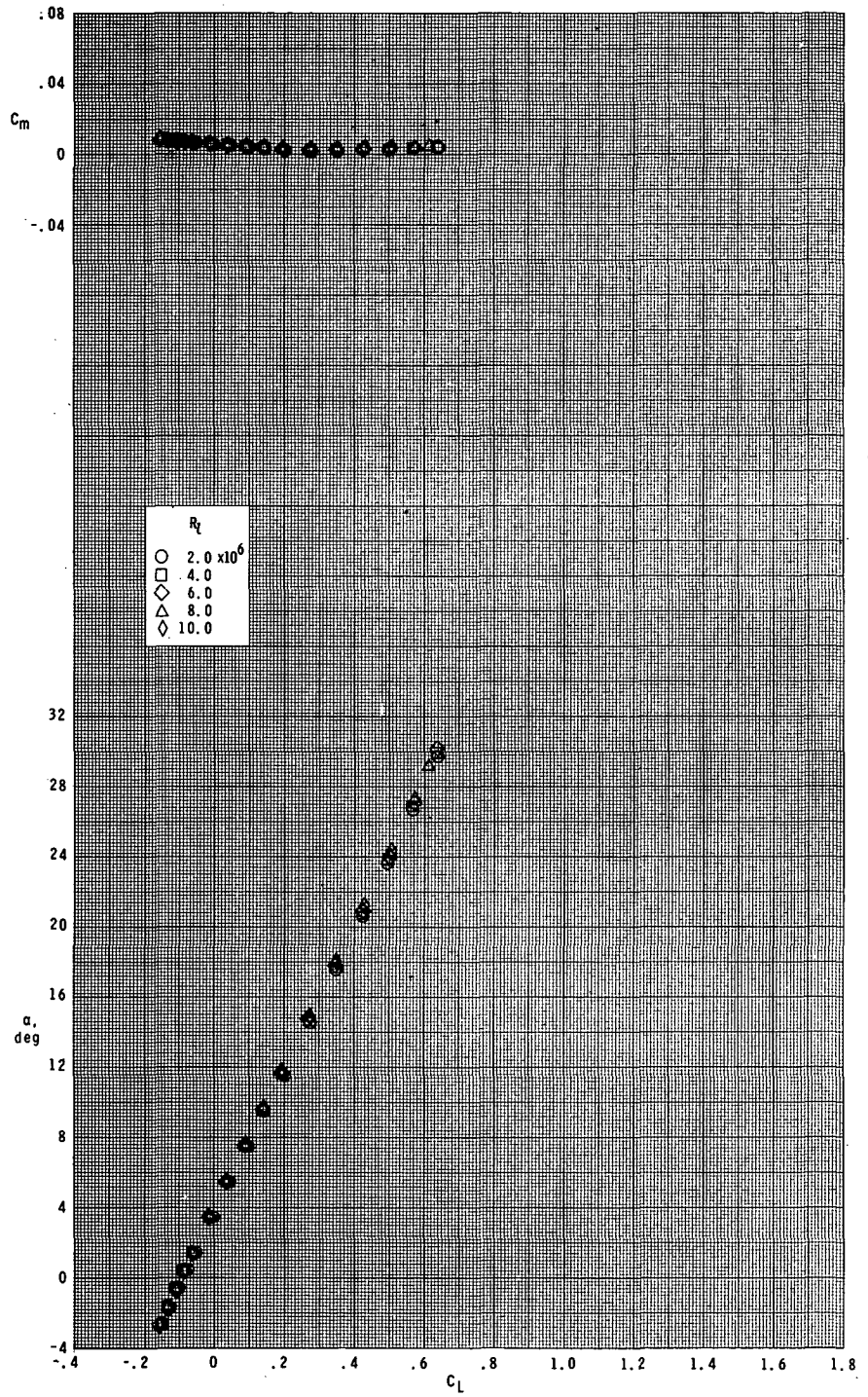

(b) Continued.

Figure 10.- Continued.

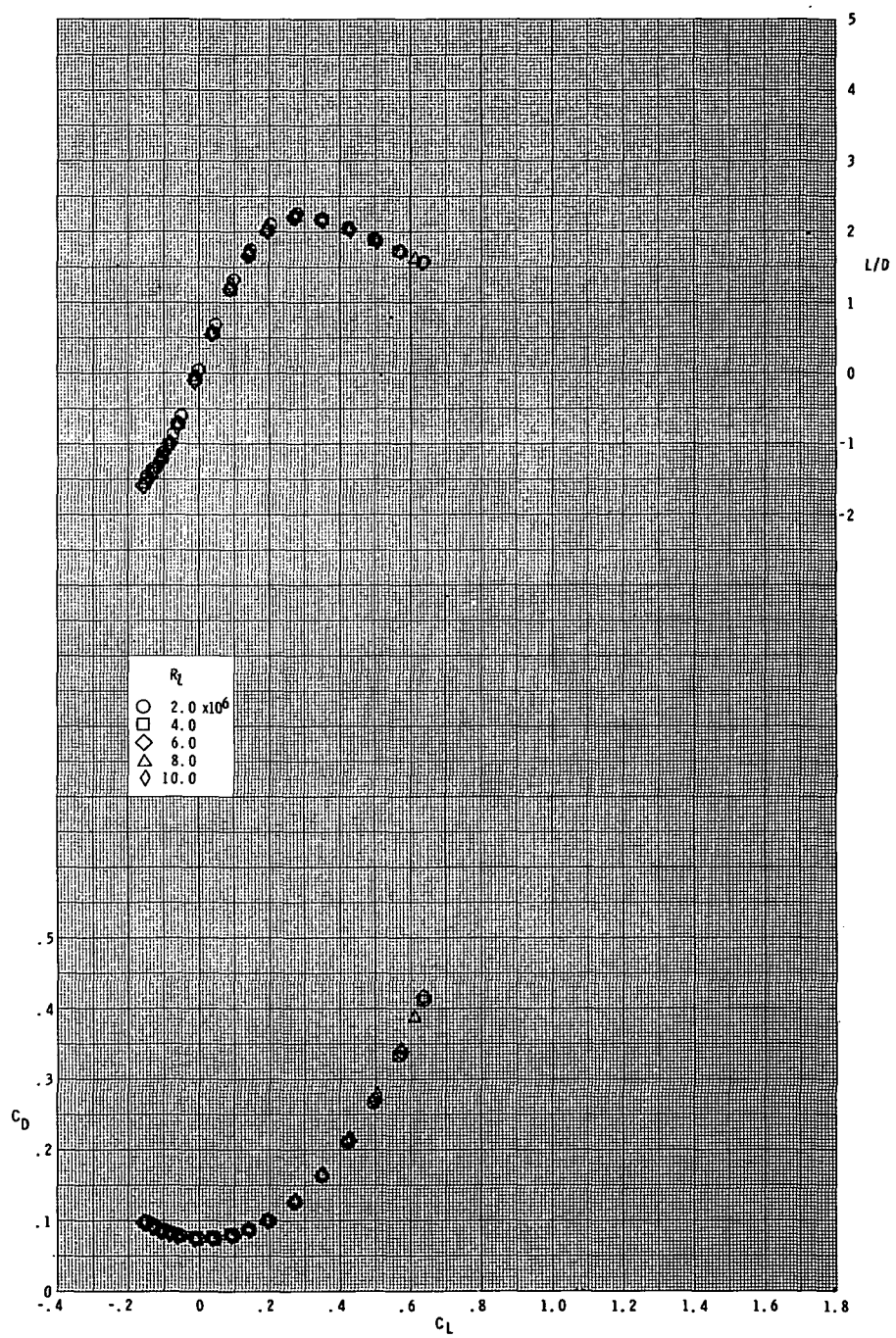

(b) Concluded.

Figure 10.- Continued.

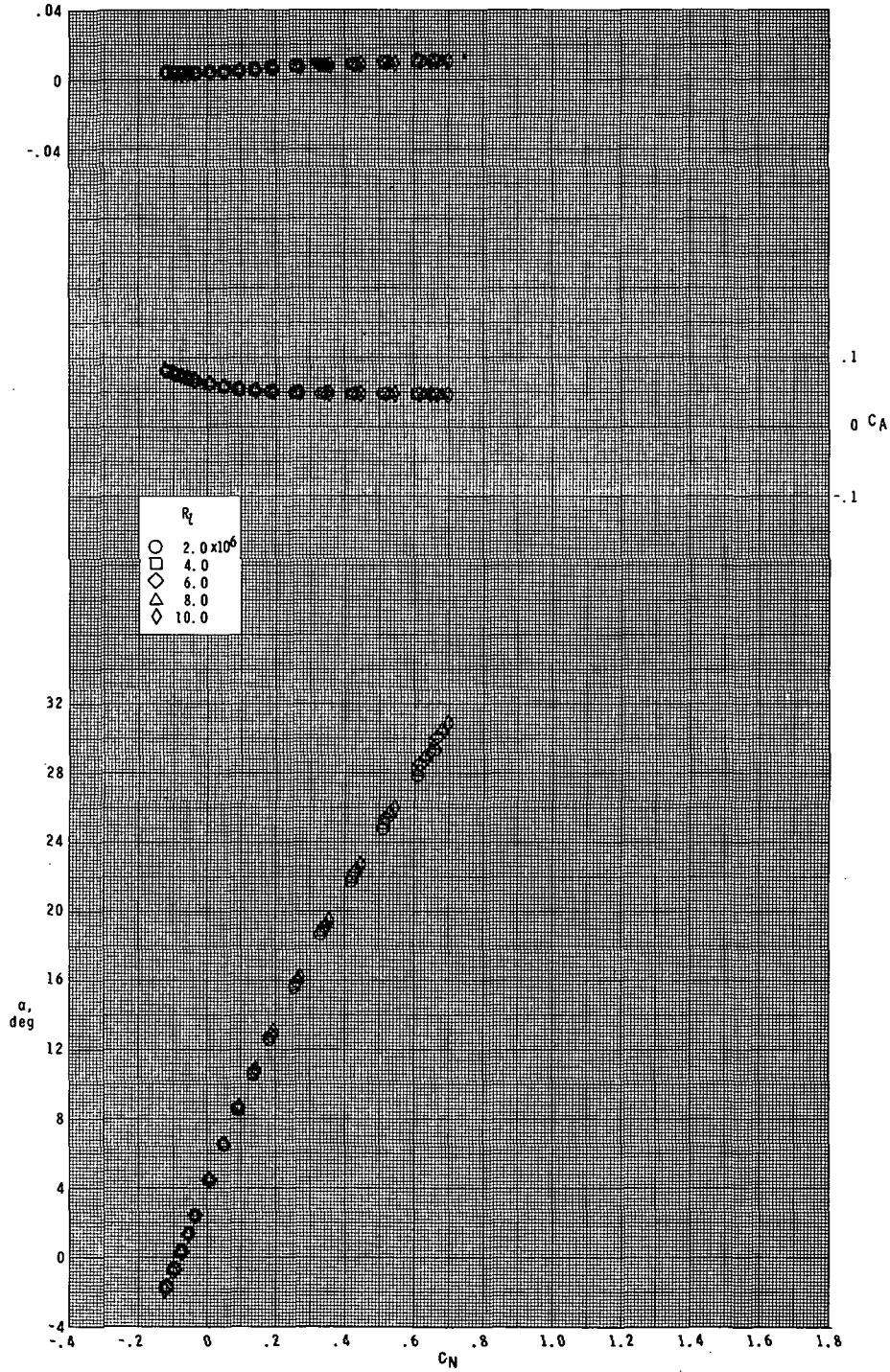

(c) M = 4.63.

Figure 10.- Continued.

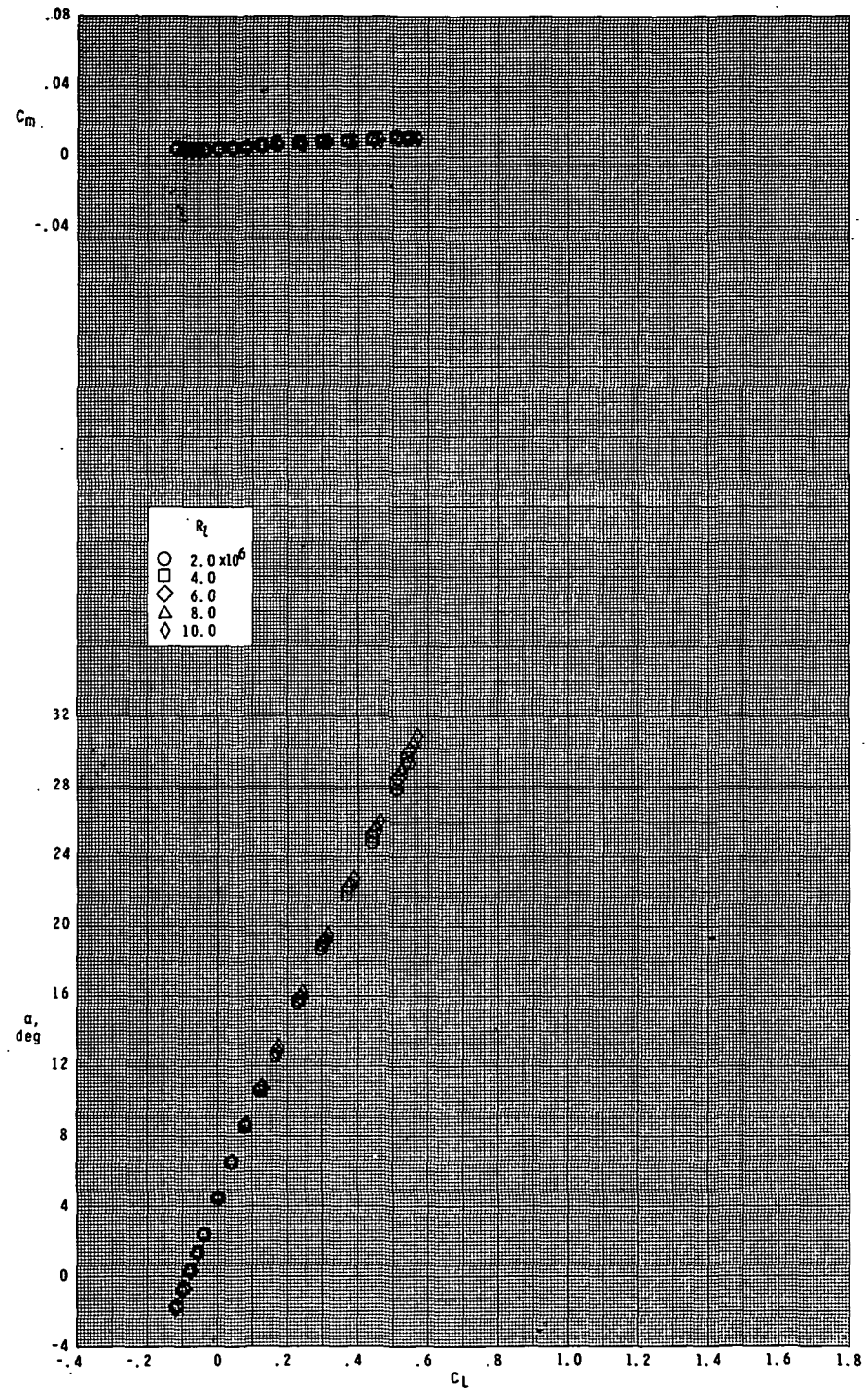

(c) Continued.

Figure 10.- Continued.

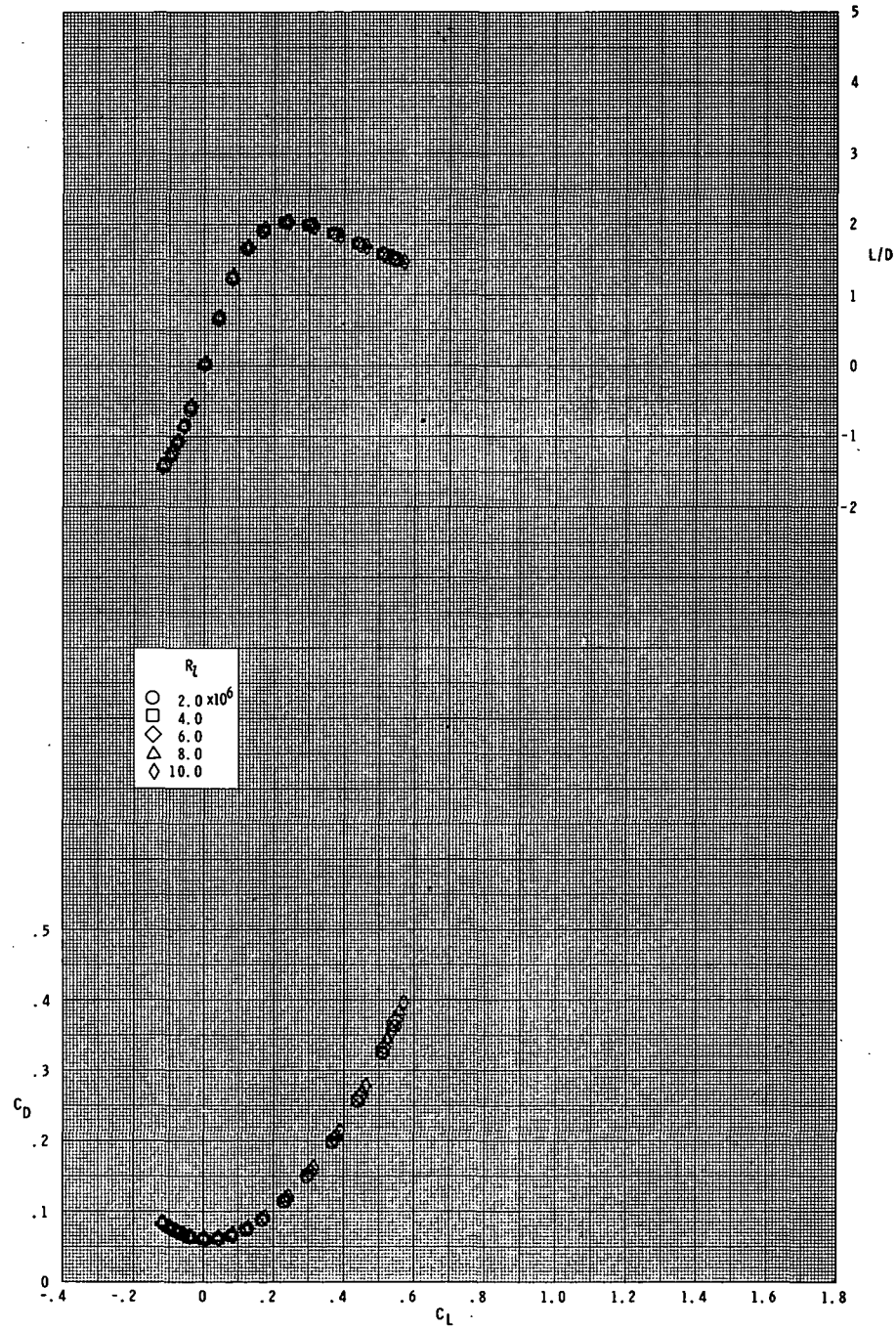

(c) Concluded.

Figure 10.- Concluded.

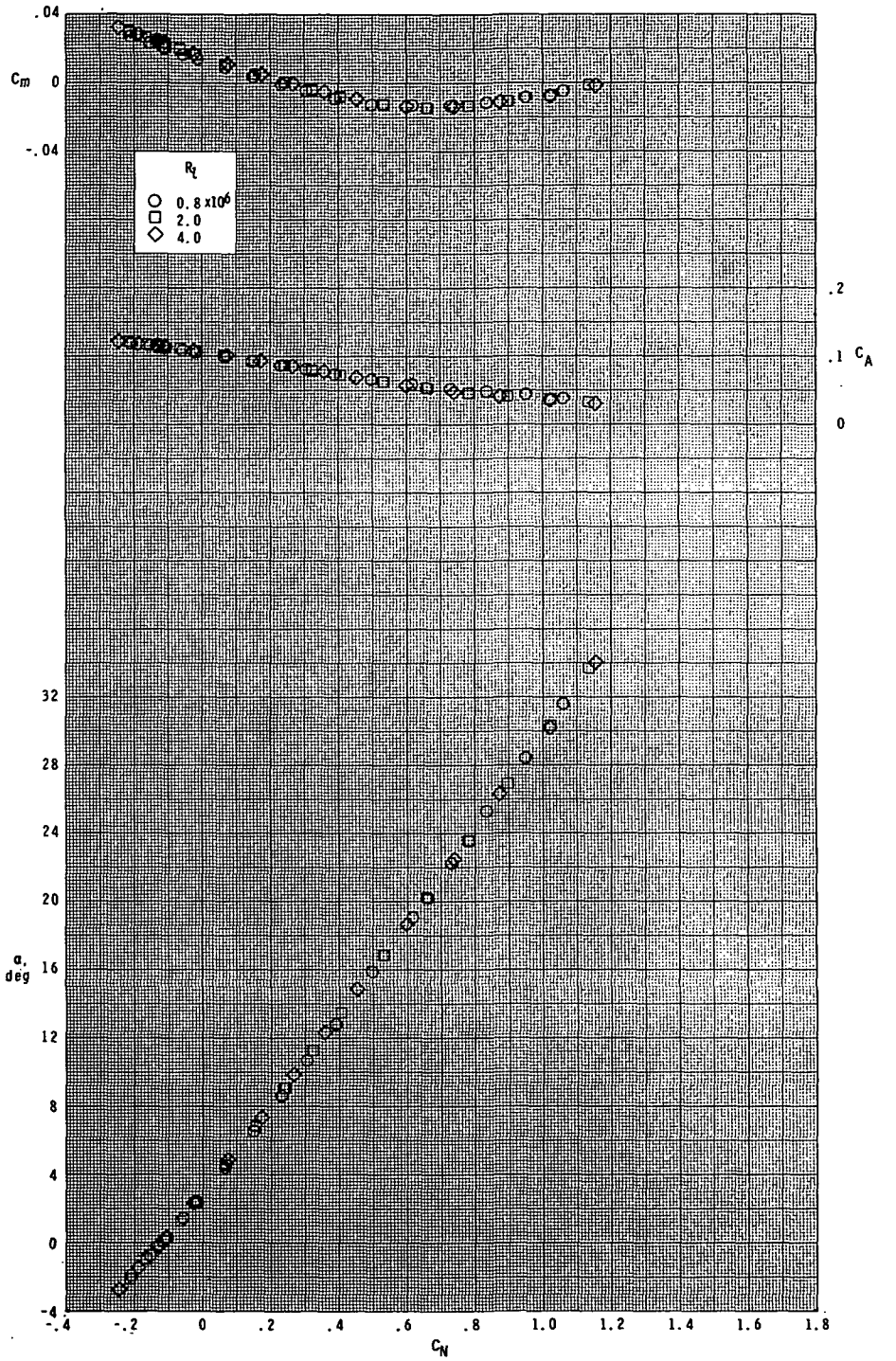

(a) M = 1.60.

Figure 11.- Effect of Reynolds number on longitudinal aerodynamic characteristics. Small model; $\delta_e = -30^o$.

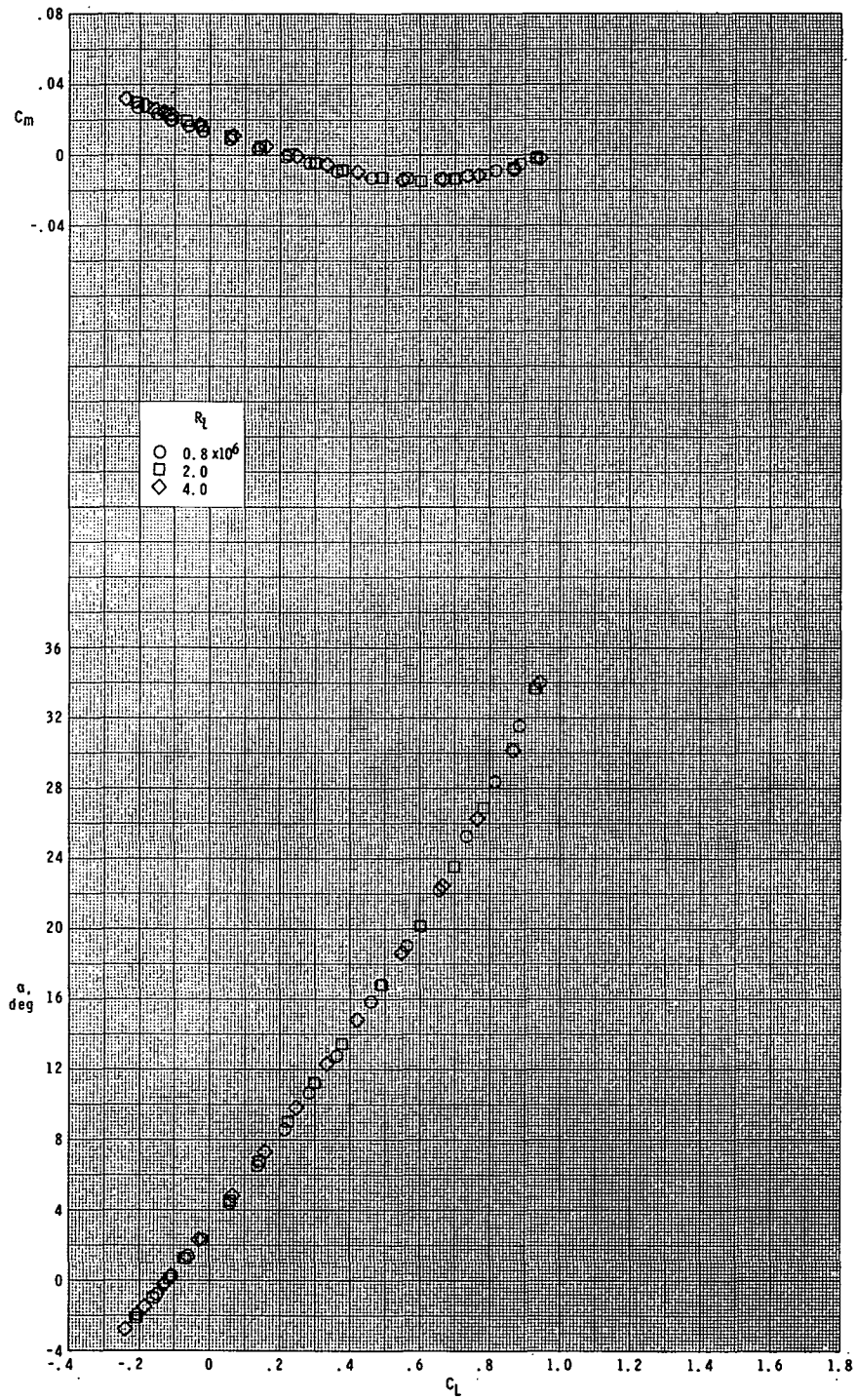

(a) Continued.

Figure 11.- Continued.

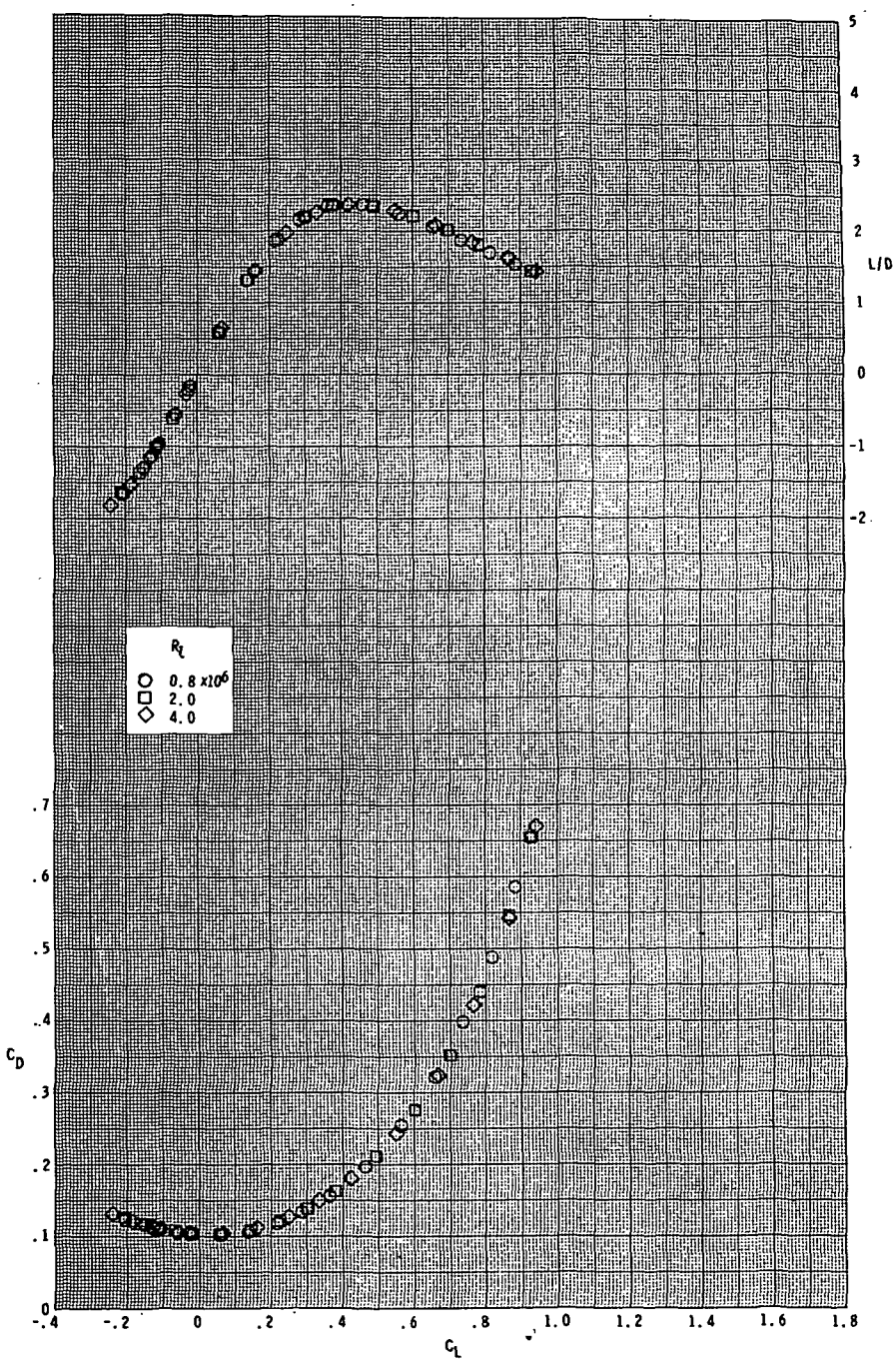

(a) Concluded.

Figure 11.- Continued.

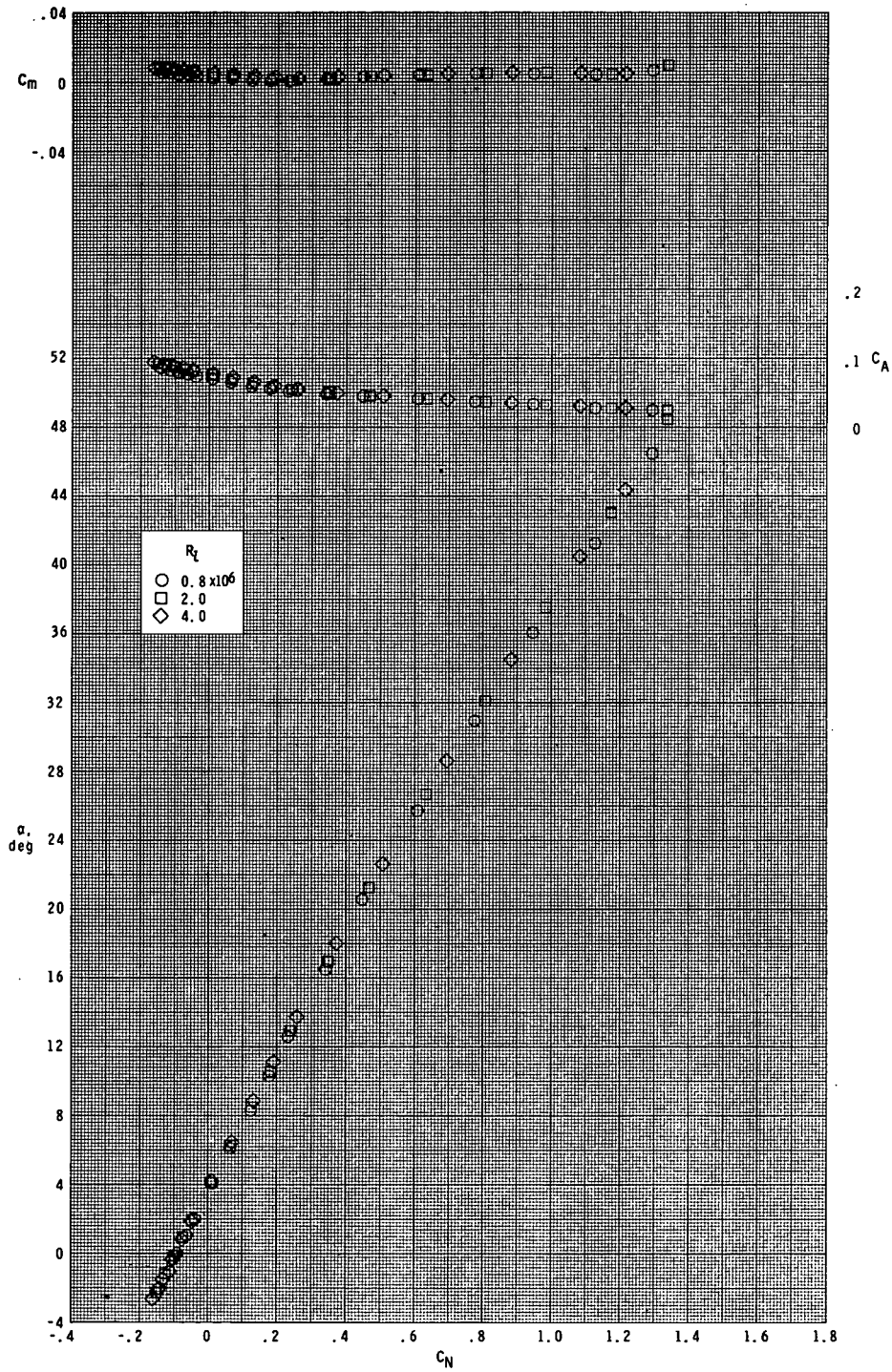

(b) M = 2.86.

Figure 11.- Continued.

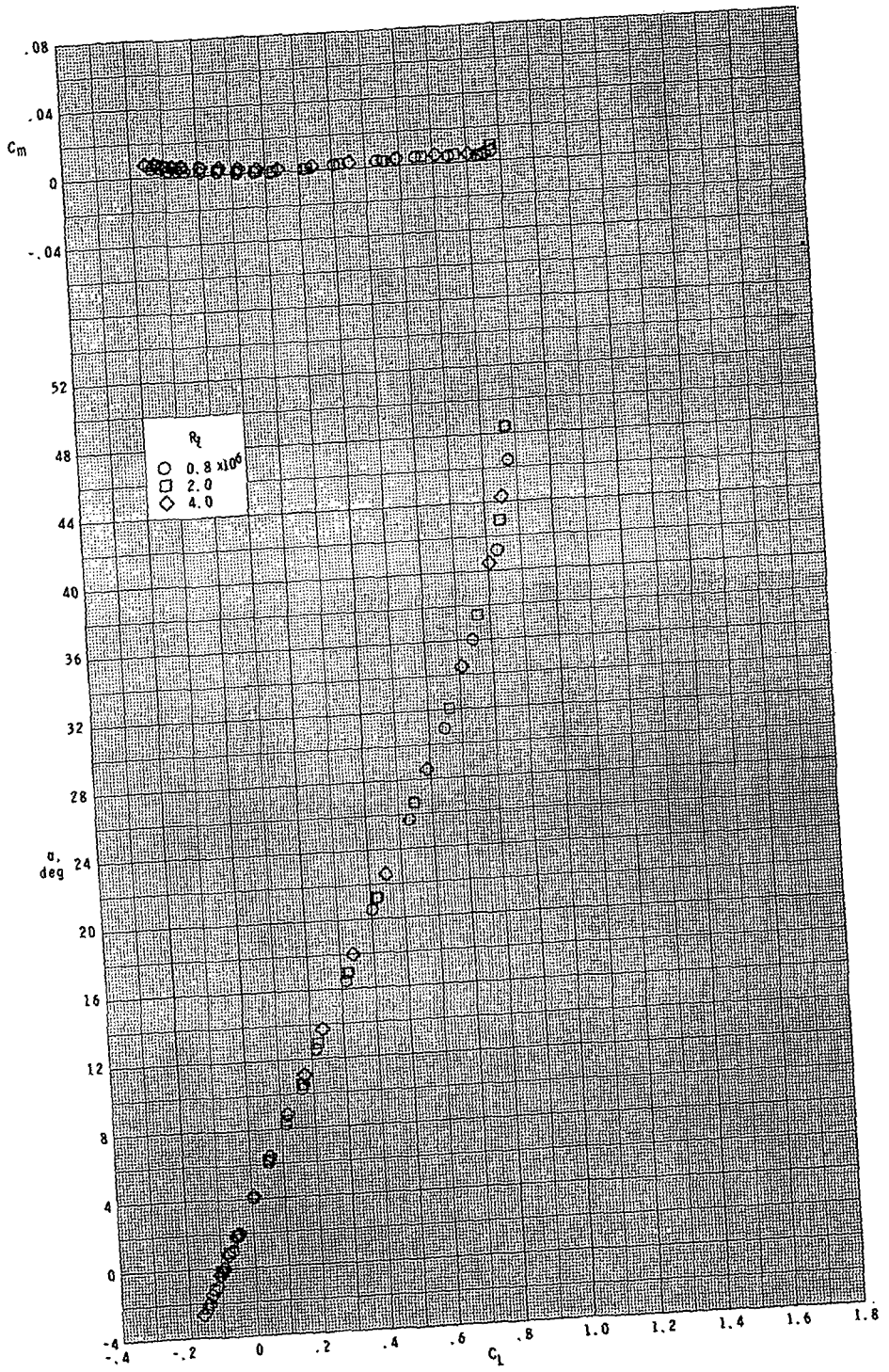

(b) Continued.

Figure 11.- Continued.

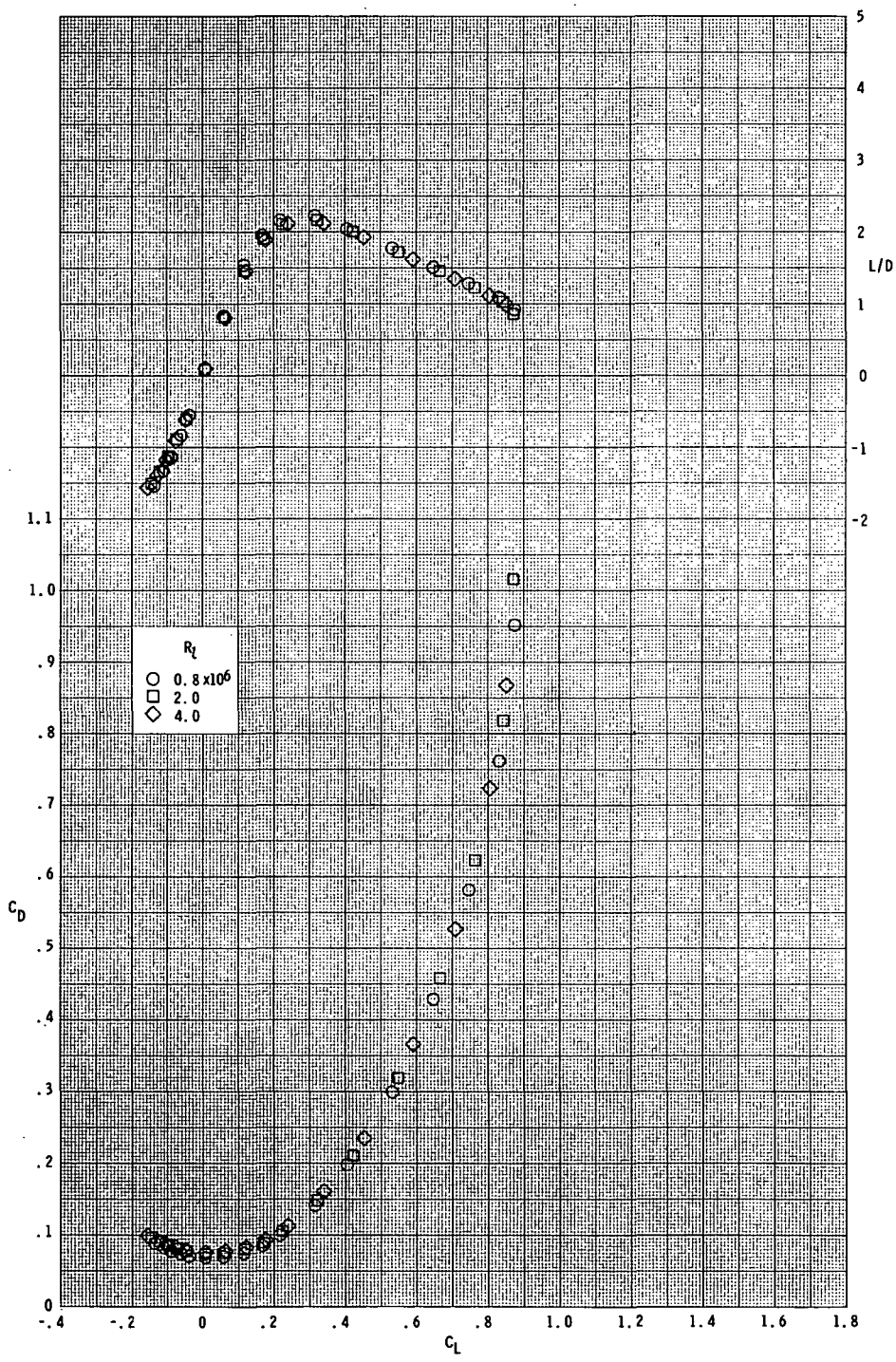

(b) Concluded.

Figure 11.- Continued.

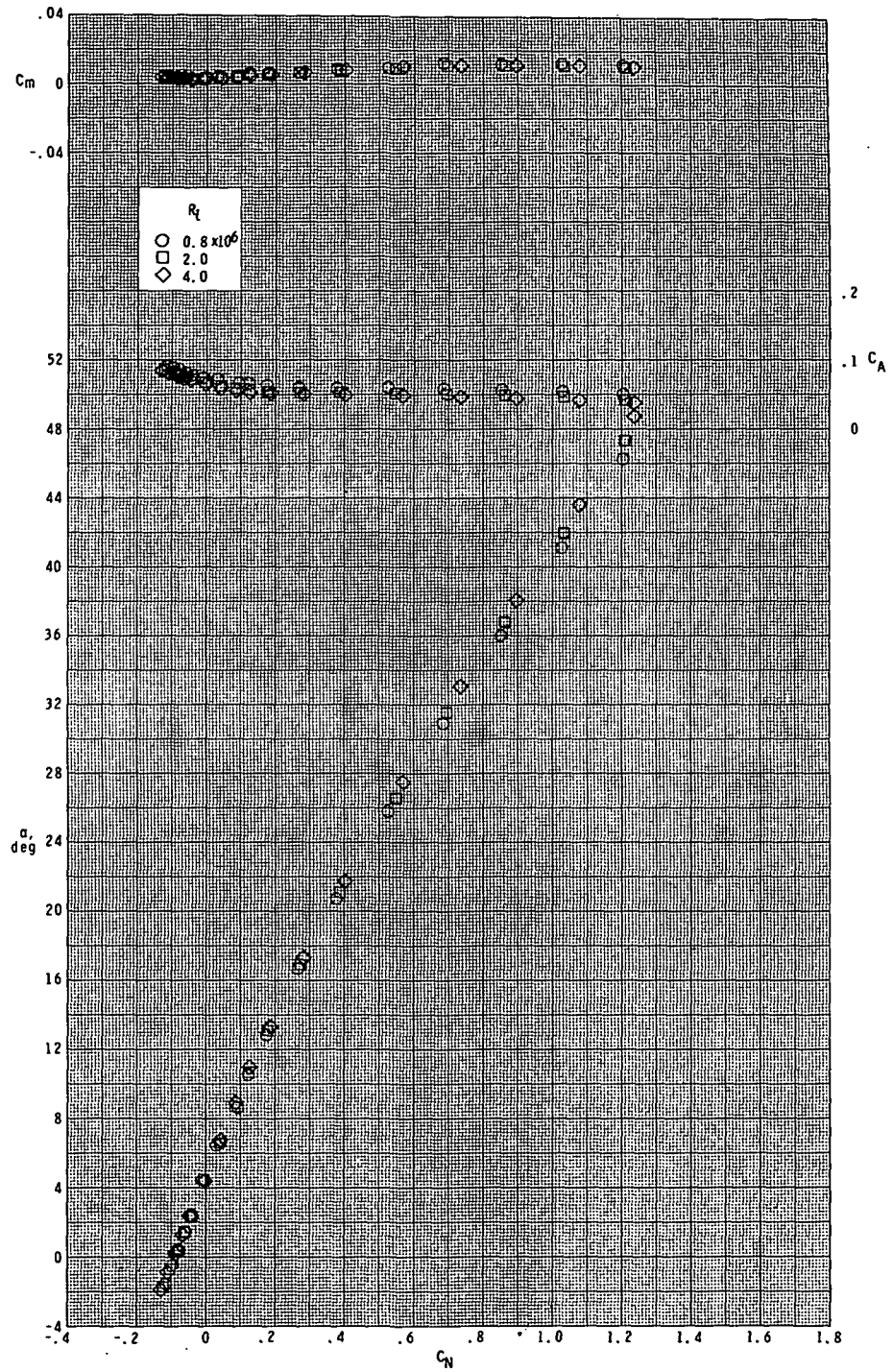

(c) M = 4.63.

Figure 11.- Continued.

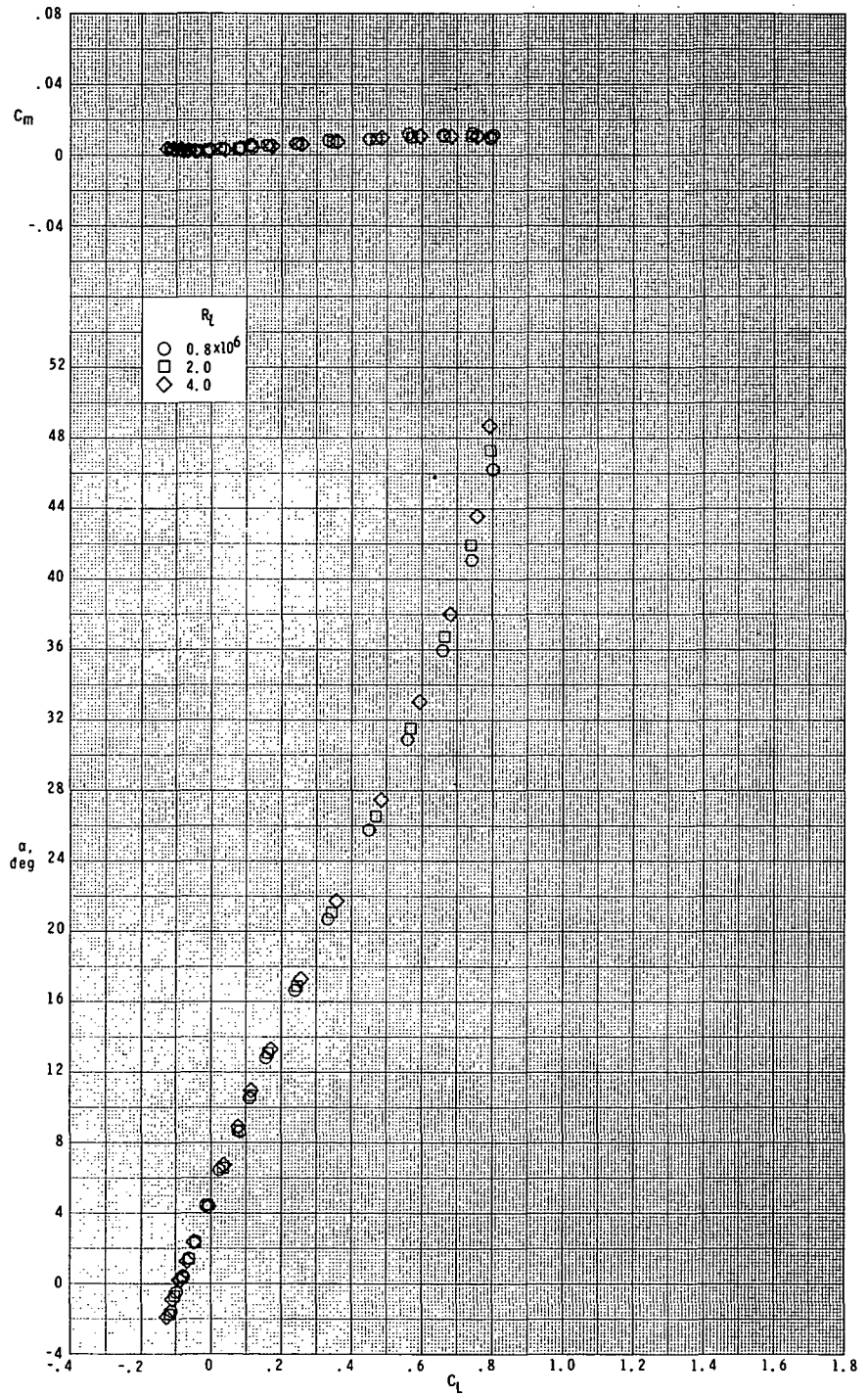

(c) Continued.

Figure 11.- Continued.

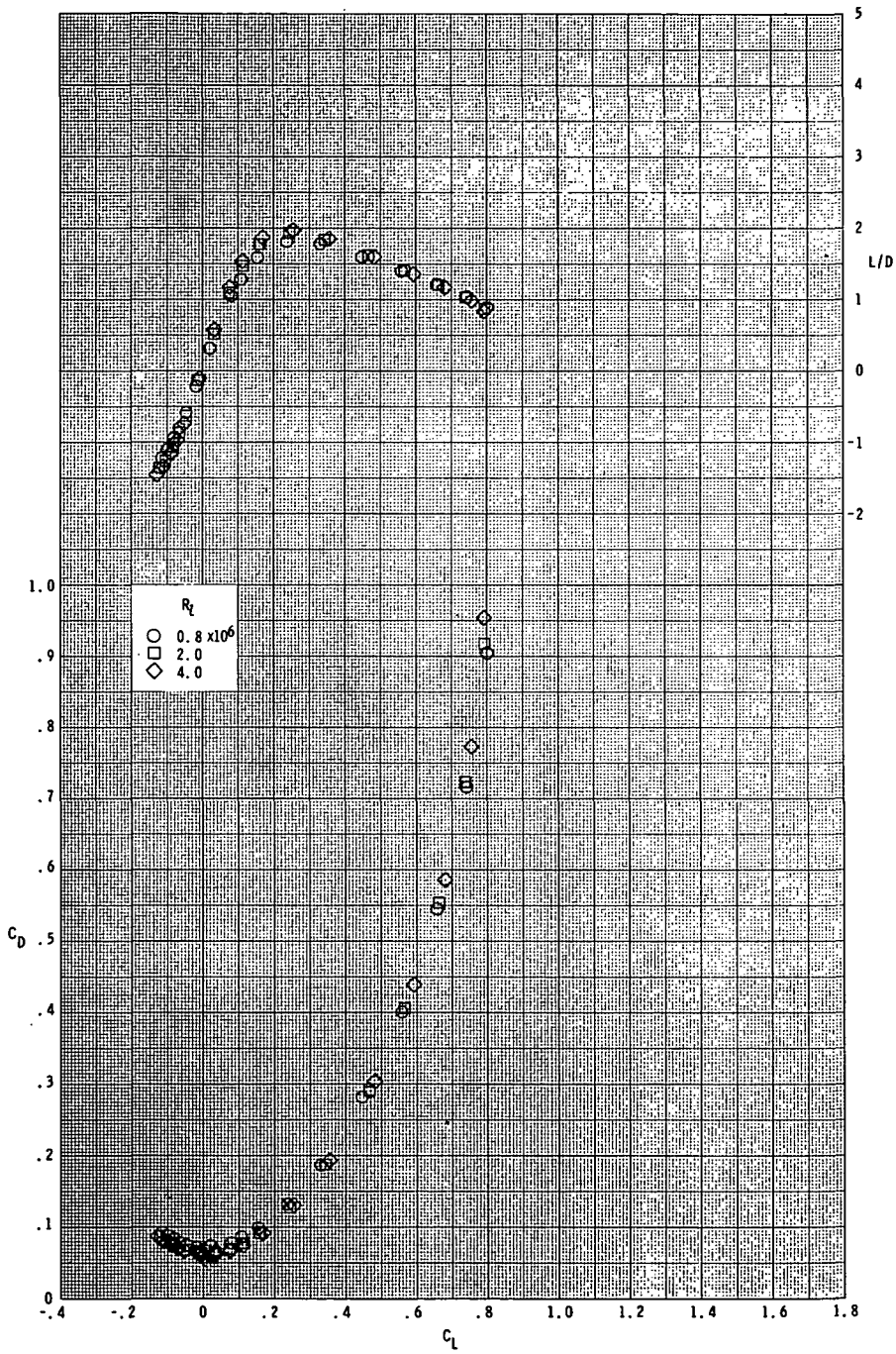

(c) Concluded.

Figure 11.- Concluded.

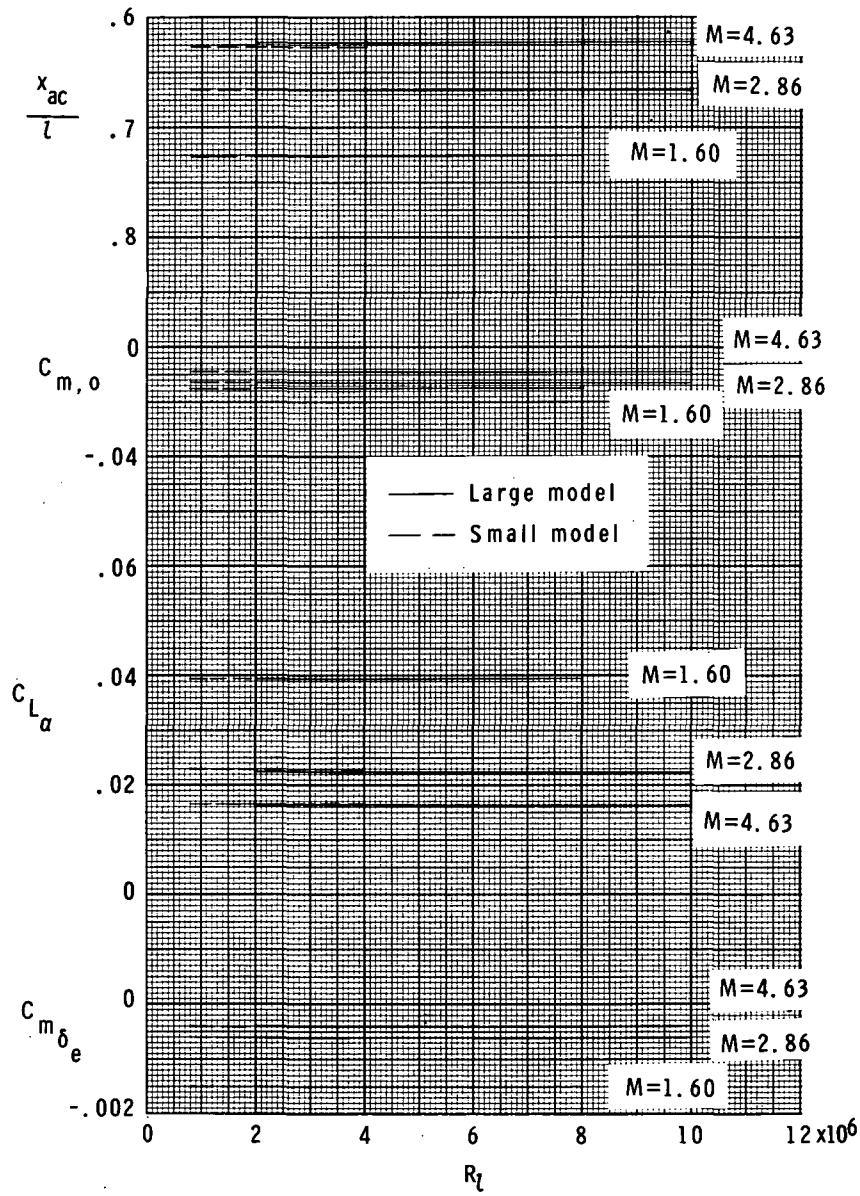

(a) $\alpha \approx 0^{o}$.

Figure 12.- Summary of longitudinal aerodynamic characteristics.

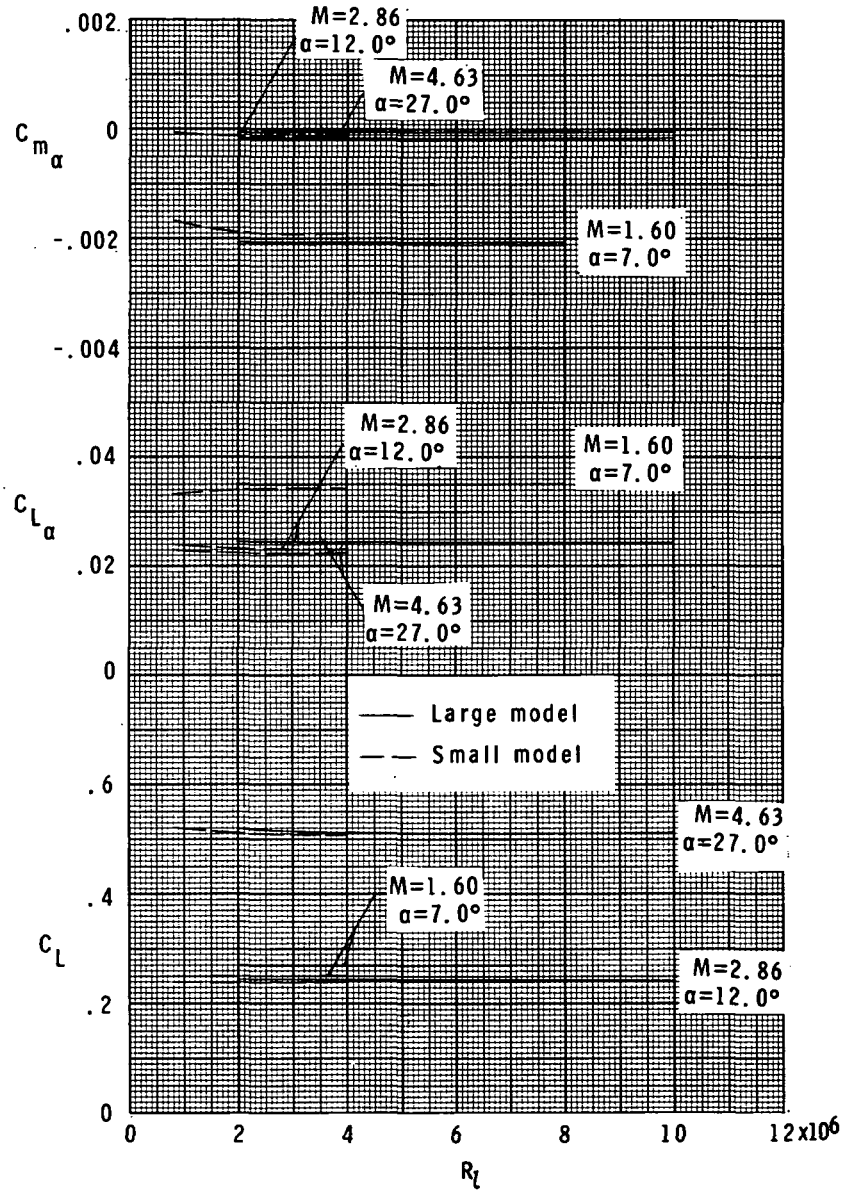

(b) Flight α-schedule for nominal operational high cross-range mission. (See ref. 1.)

Figure 12.- Concluded.

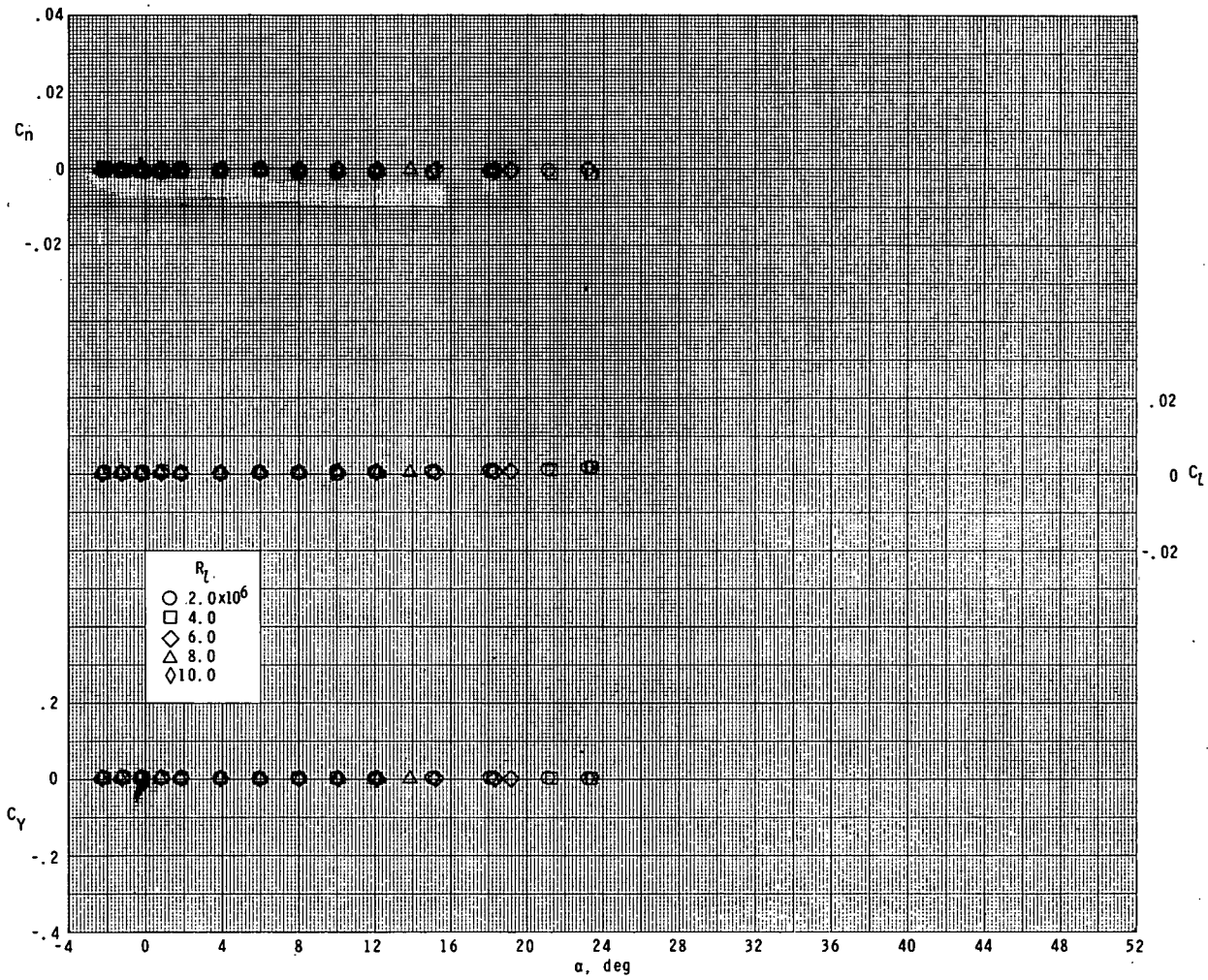

(a) M = 1.60.

Figure 13.- Effect of Reynolds number on lateral aerodynamic characteristics. Large model; $\delta_e = 0^o$.

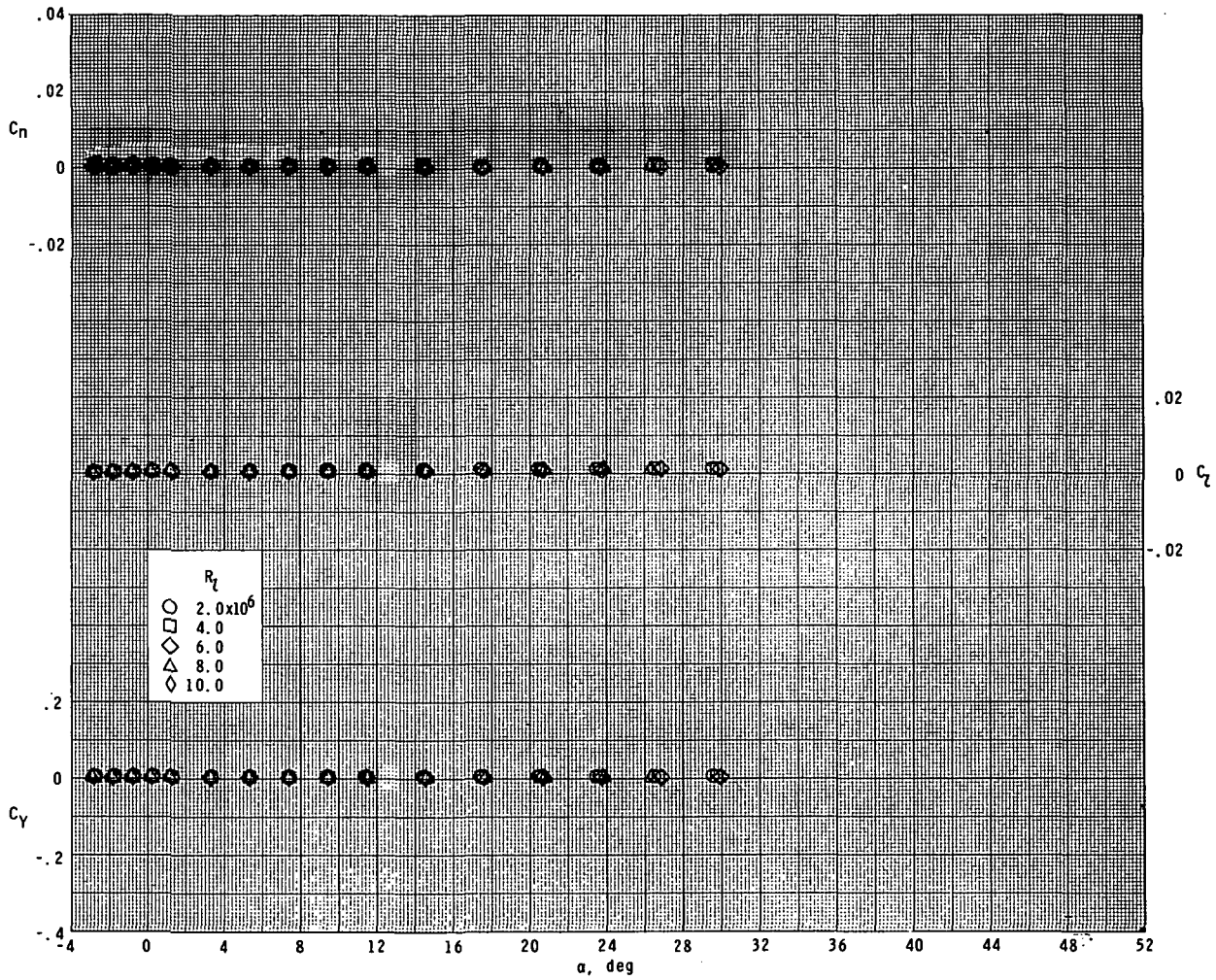

(b) M = 2.86.

Figure 13.- Continued.

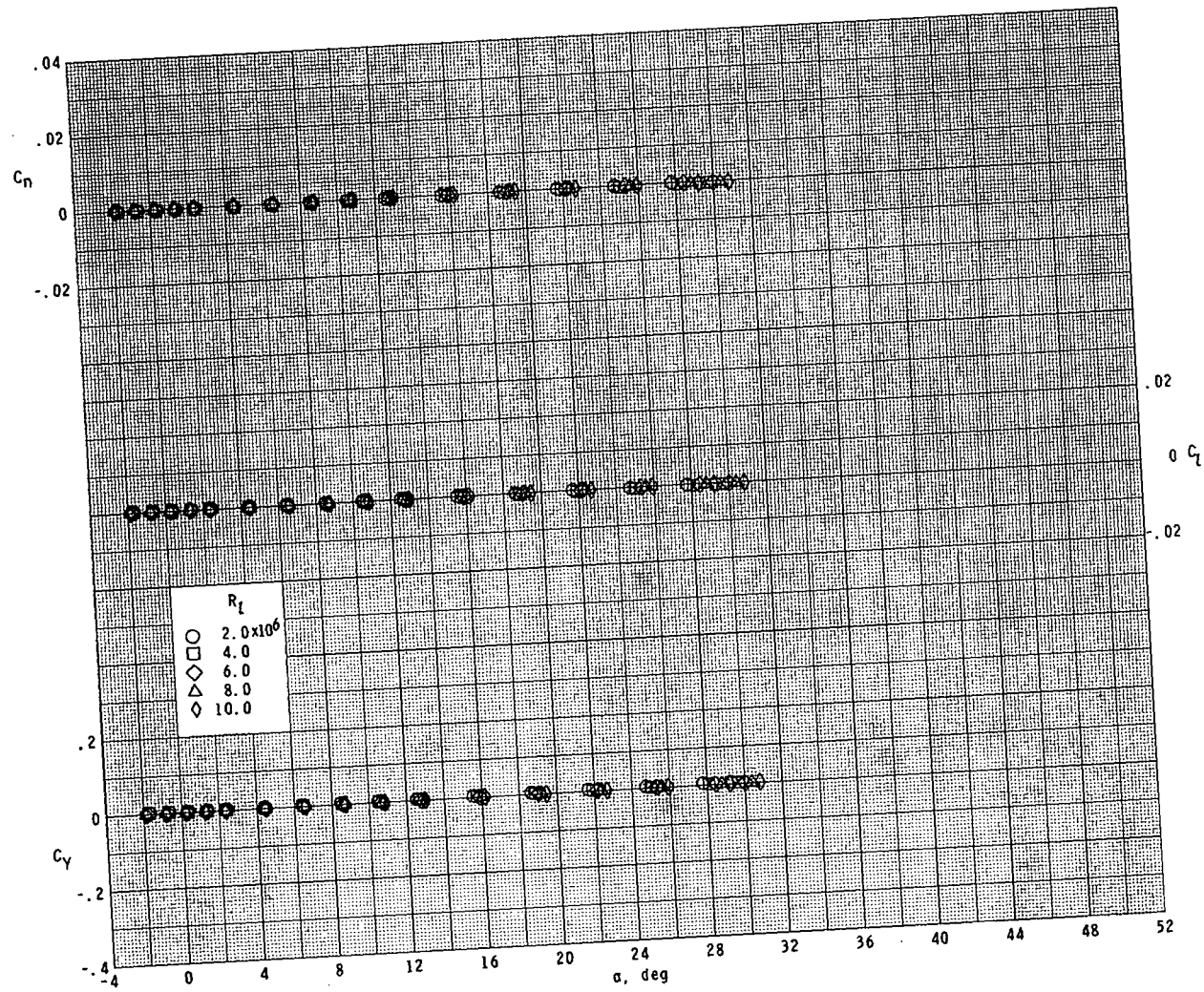

(c) M = 4.63.

Figure 13.- Concluded.

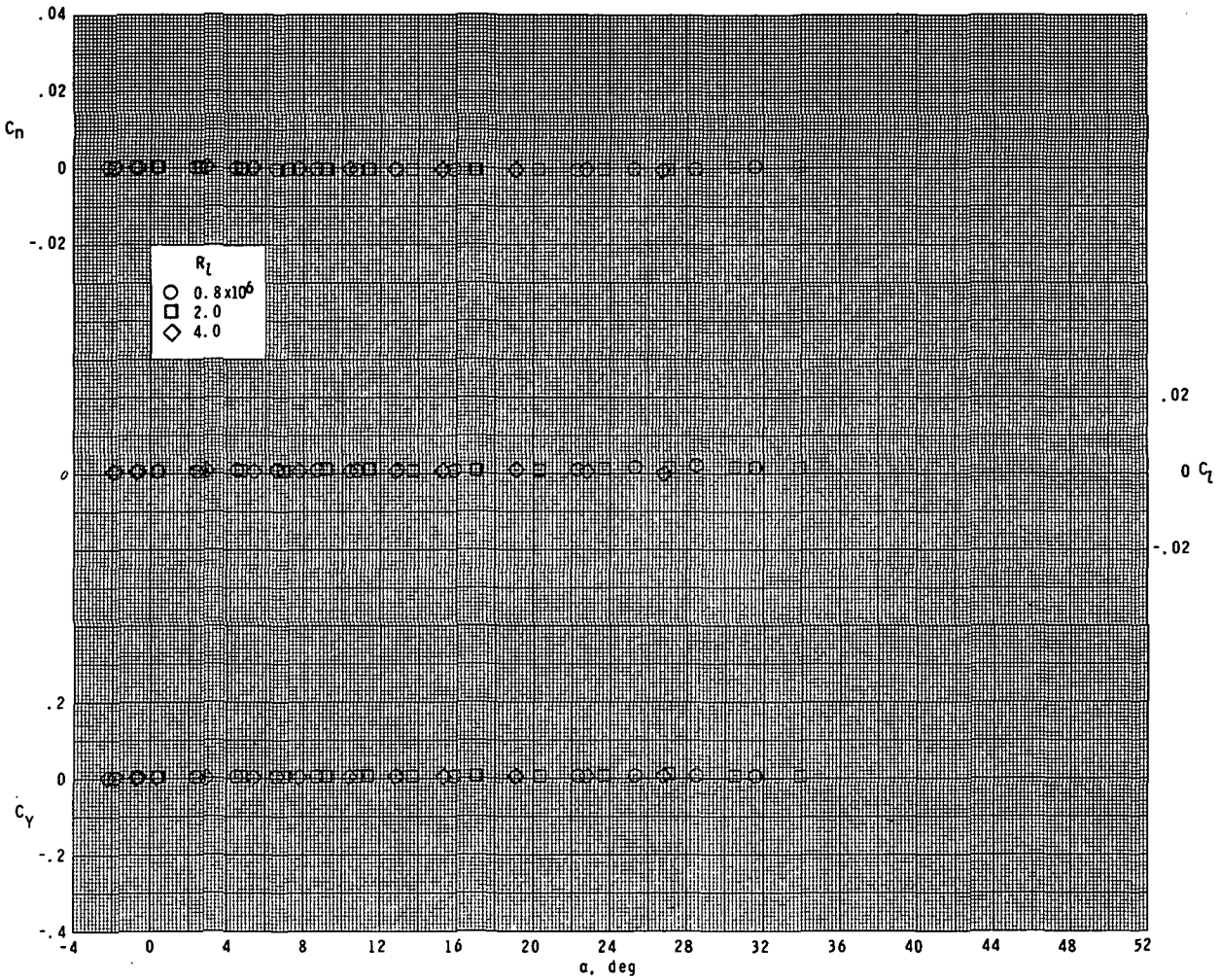

(a) M = 1.60.

Figure 14.- Effect of Reynolds number on lateral aerodynamic characteristics. Small model; $\delta_e = 0^o$.

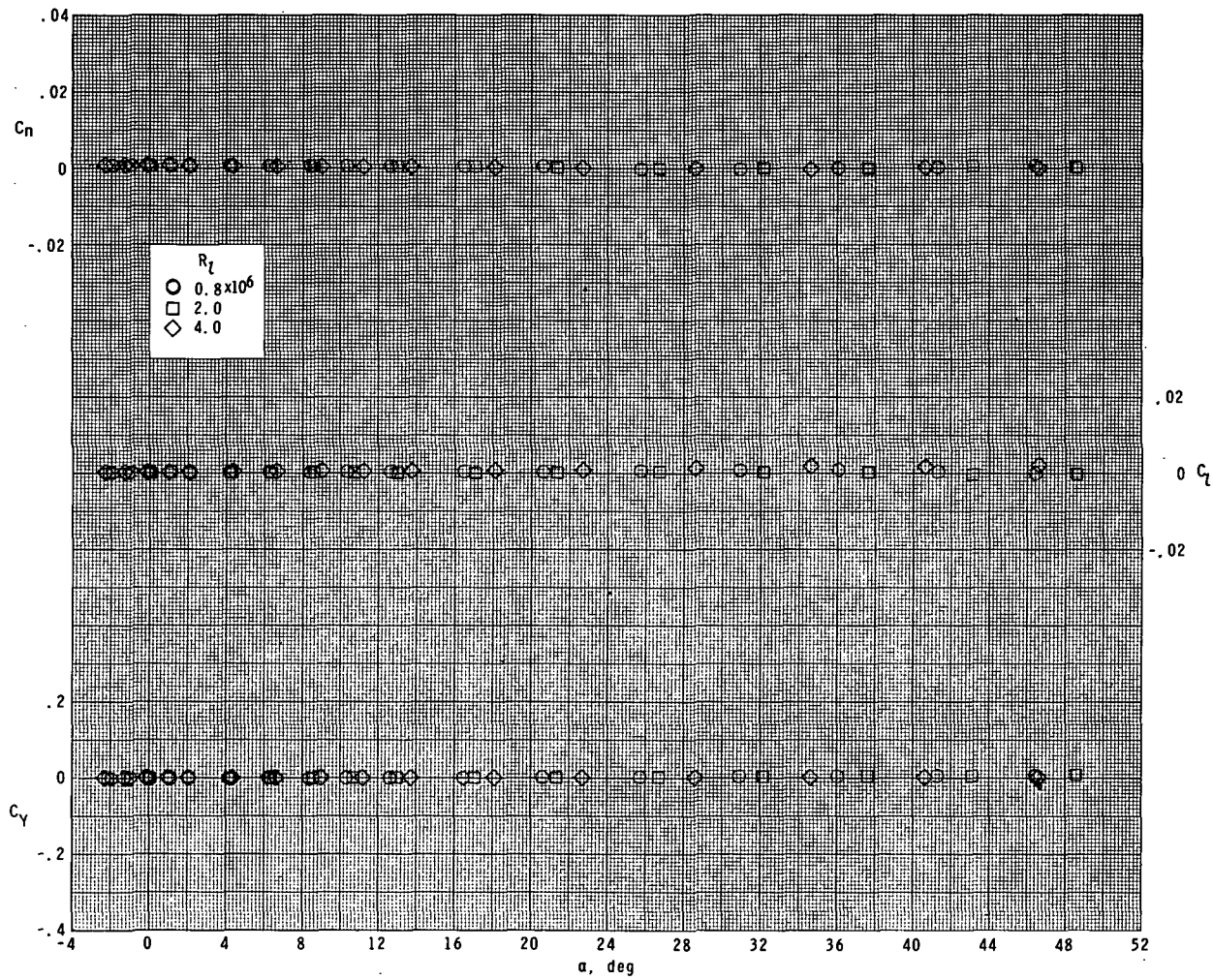

(b) M = 2.86.

Figure 14.- Continued.

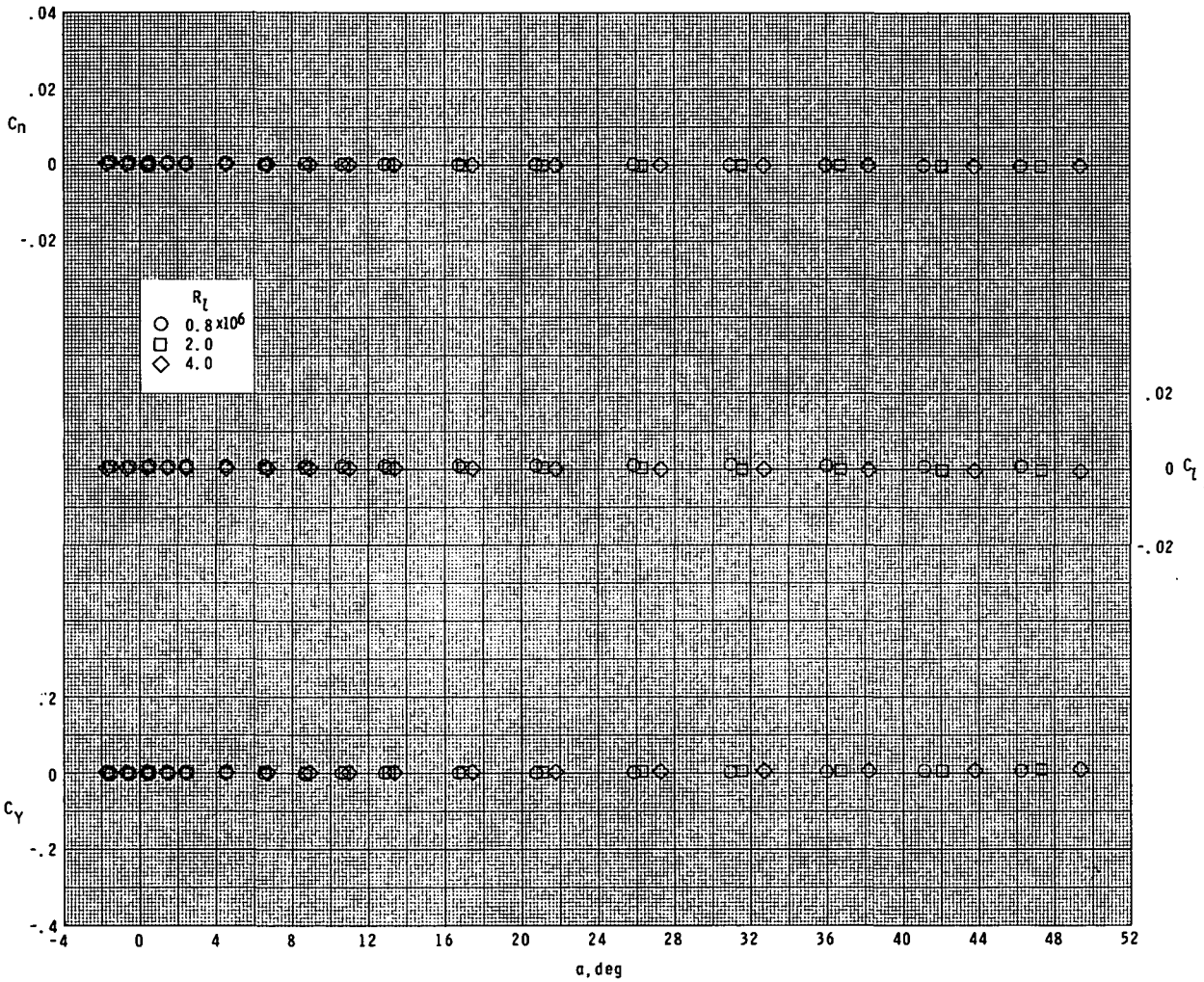

(c) M = 4.63.

Figure 14.- Concluded.

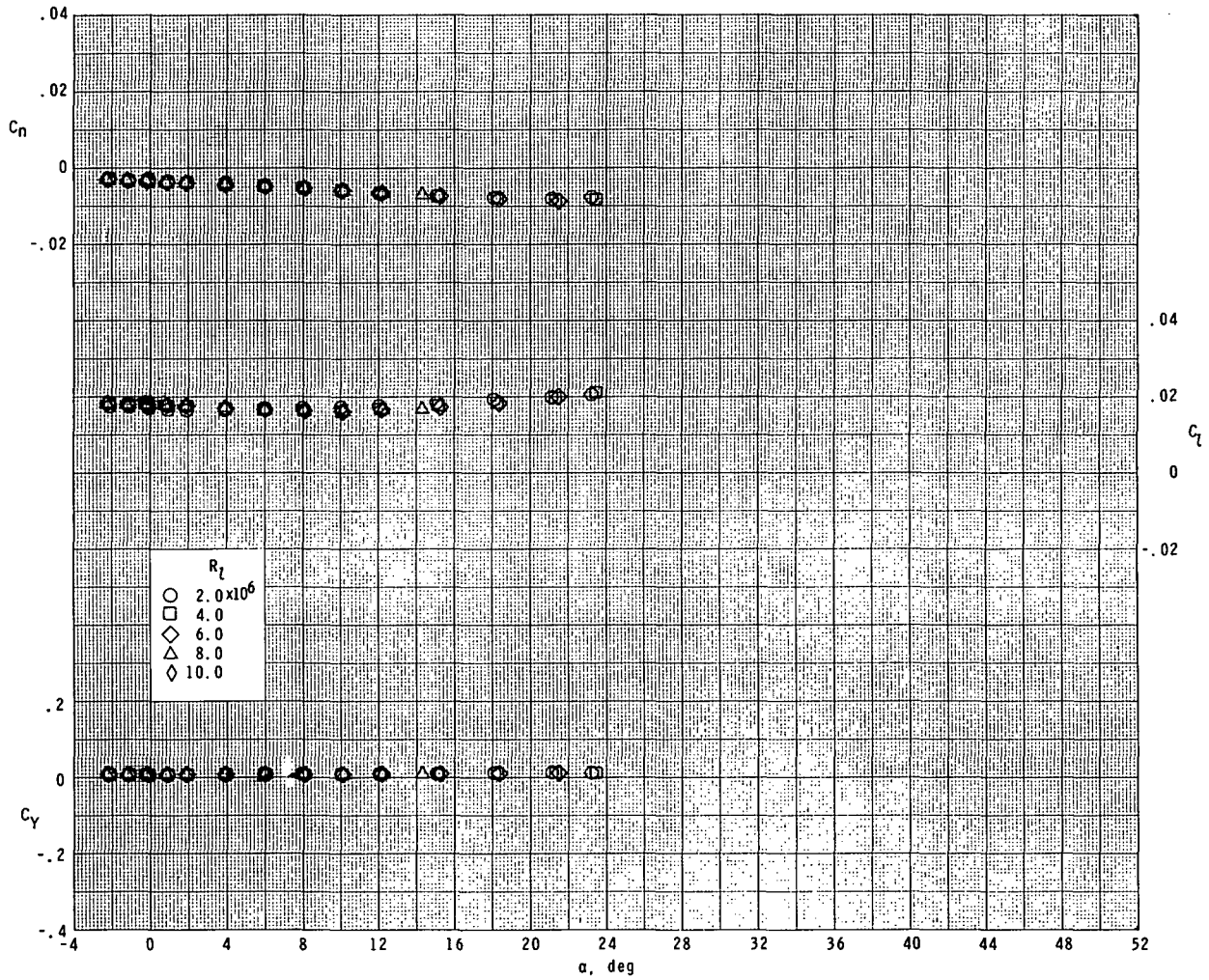

(a) M = 1.60.

Figure 15.- Effect of Reynolds number on lateral aerodynamic characteristics. Large model; $\delta_{e,L} = 10^{o}$ and $\delta_{e,R} = -10^{o}$.

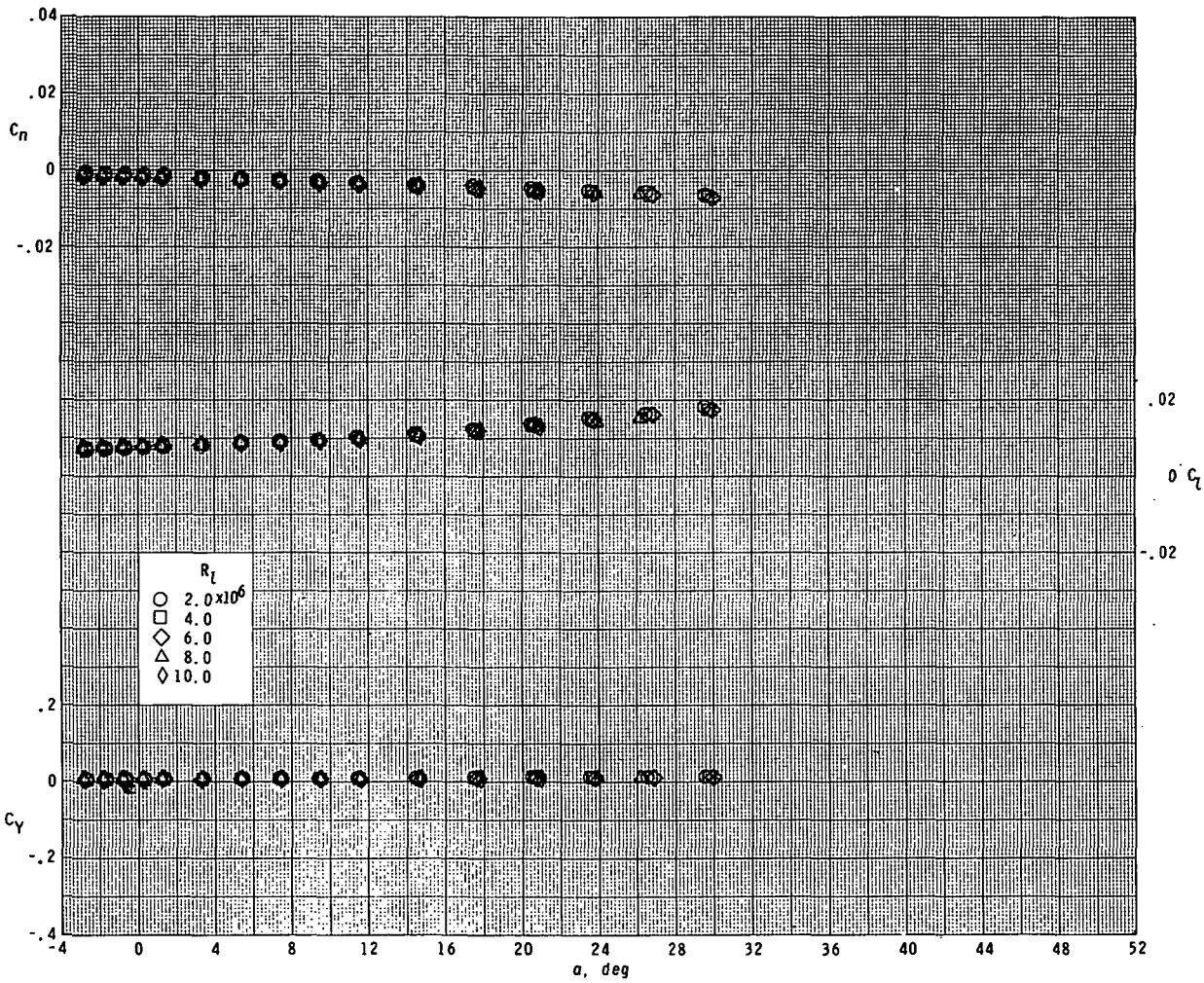

(b) M = 2.86.

Figure 15.- Continued.

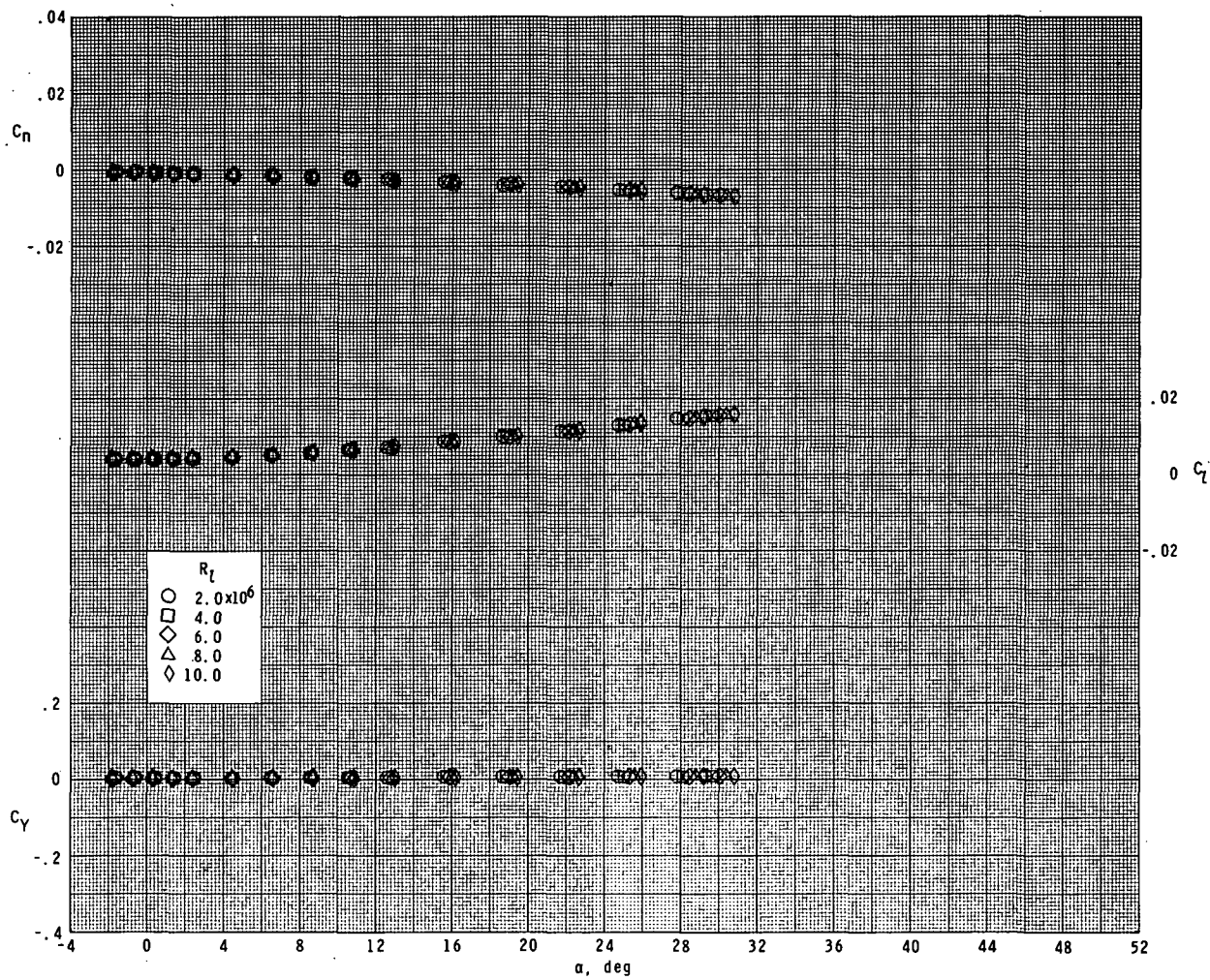

(c) M = 4.63.

Figure 15.- Concluded.

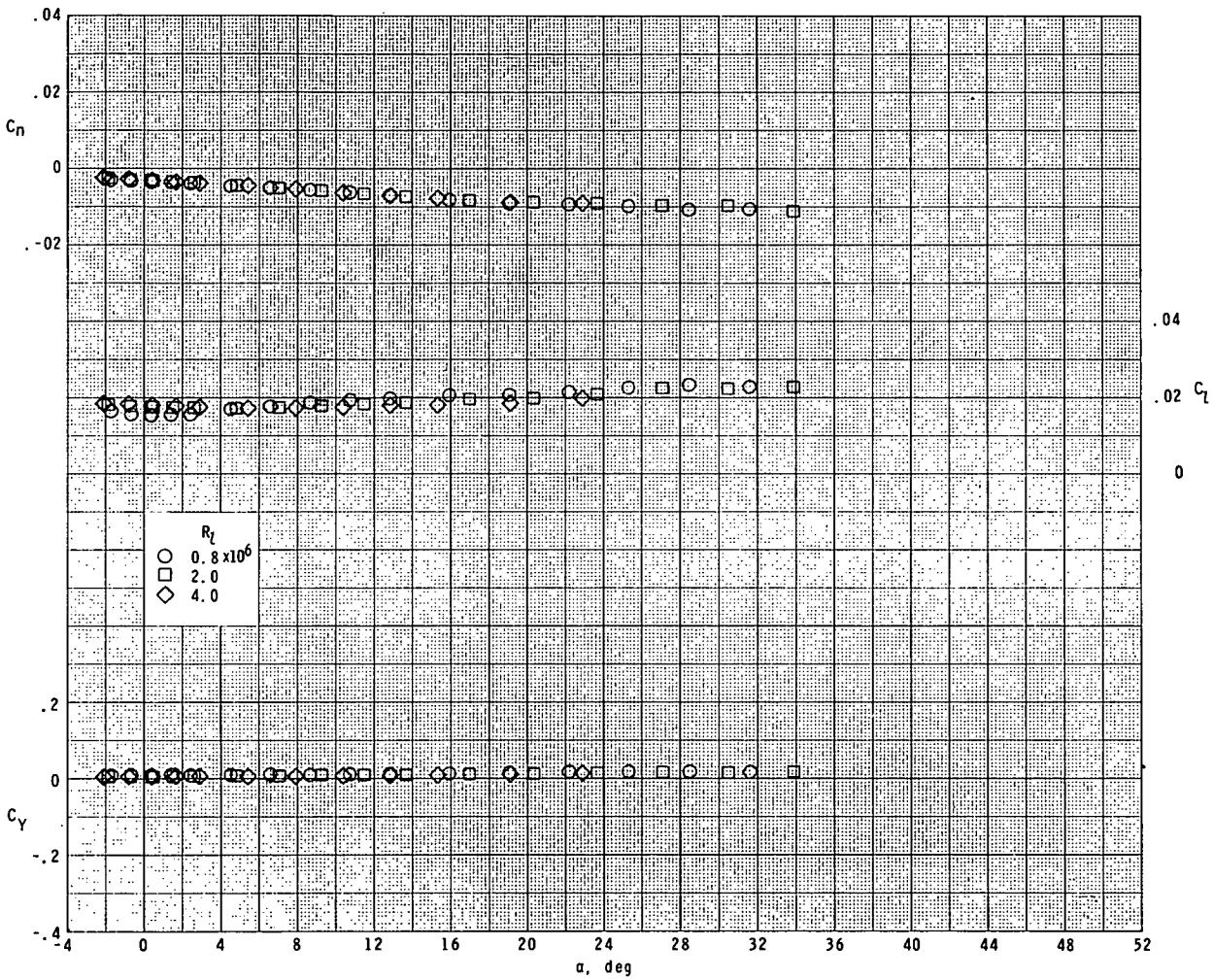

(a) M = 1.60.

Figure 16.- Effect of Reynolds number on lateral aerodynamic characteristics. Small model; $\delta_{e,L} = 10^{o}$ and $\delta_{e,R} = -10^{o}$.

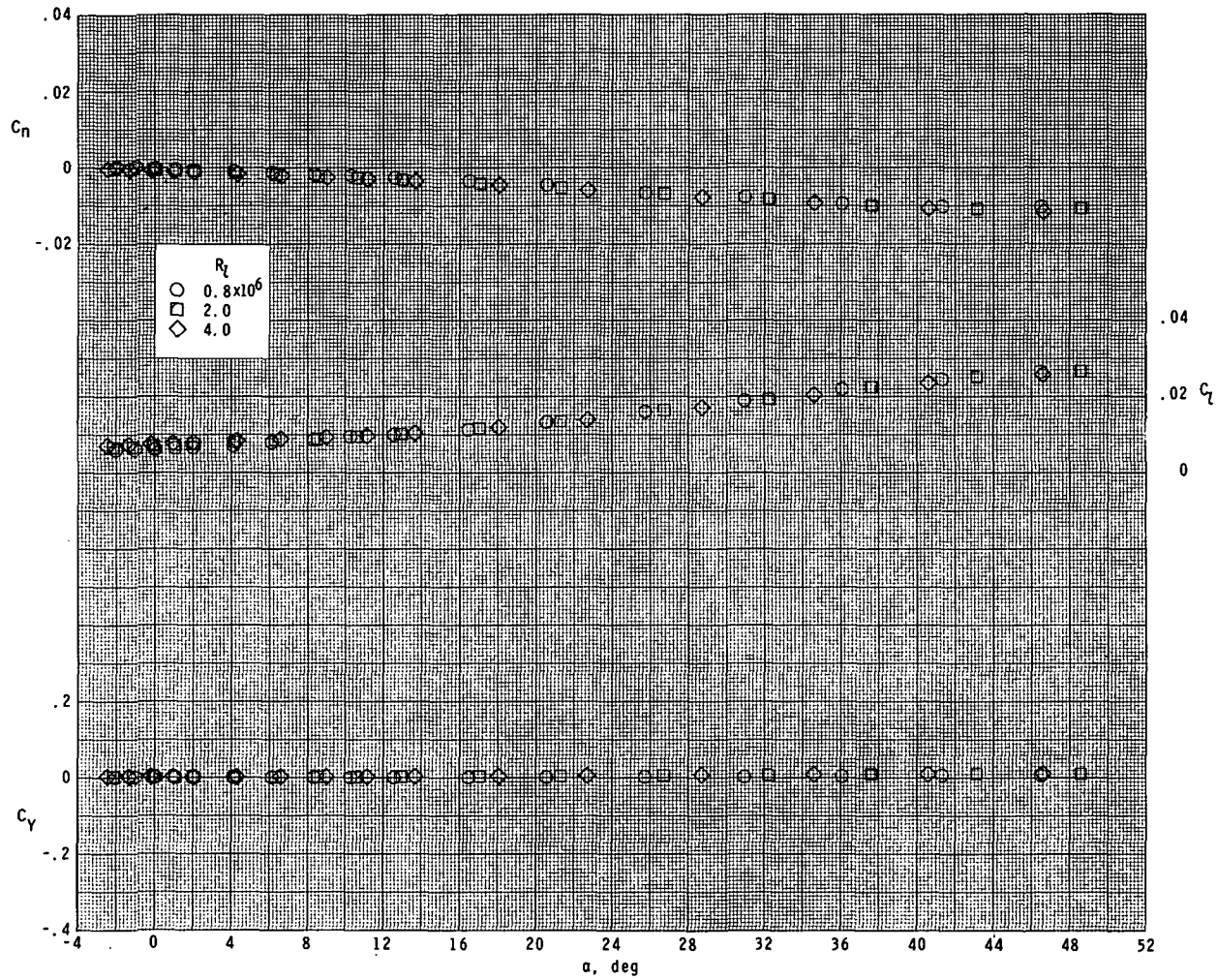

(b) M = 2.86.

Figure 16.- Continued.

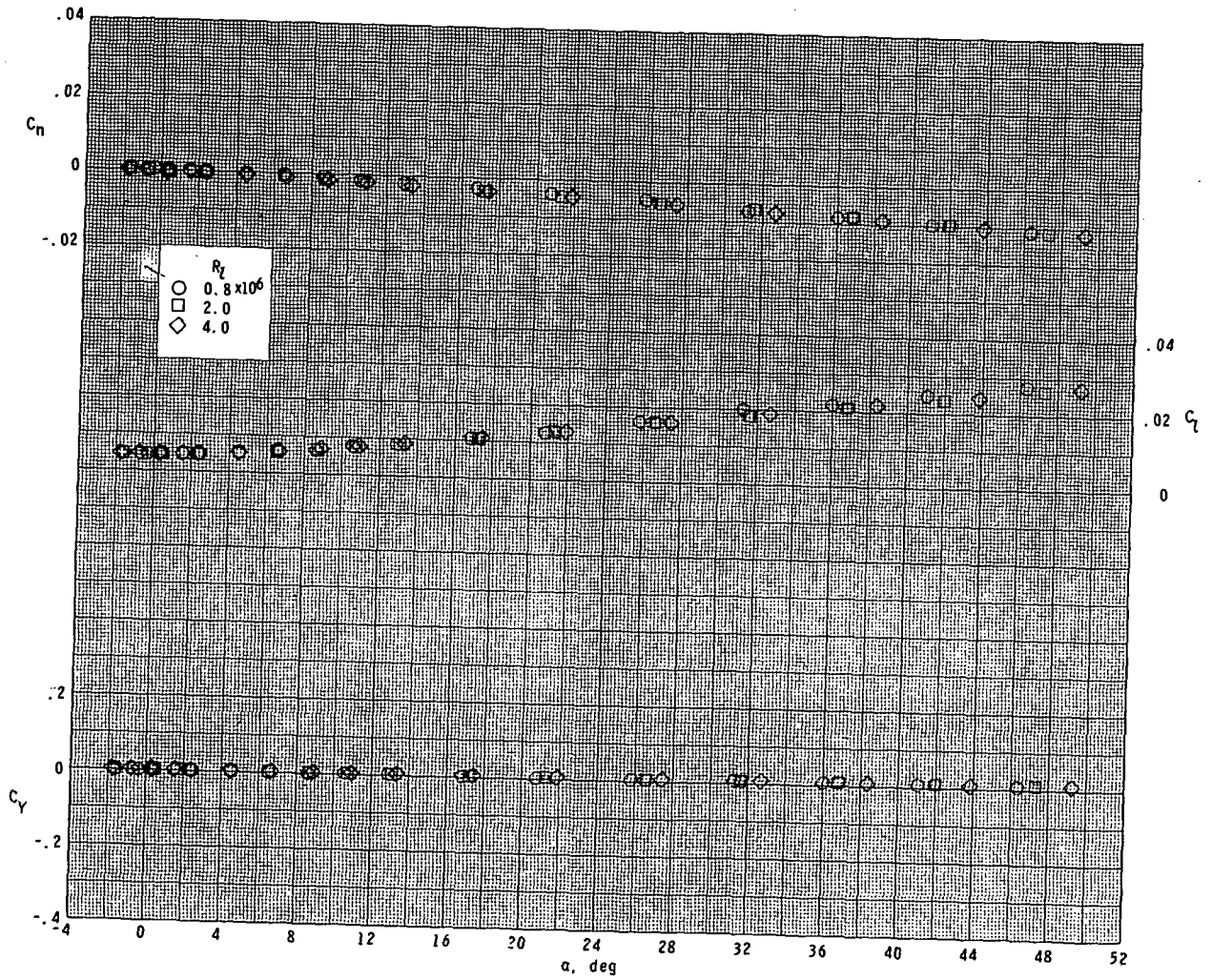

(c) M = 4.63.

Figure 16.- Concluded.

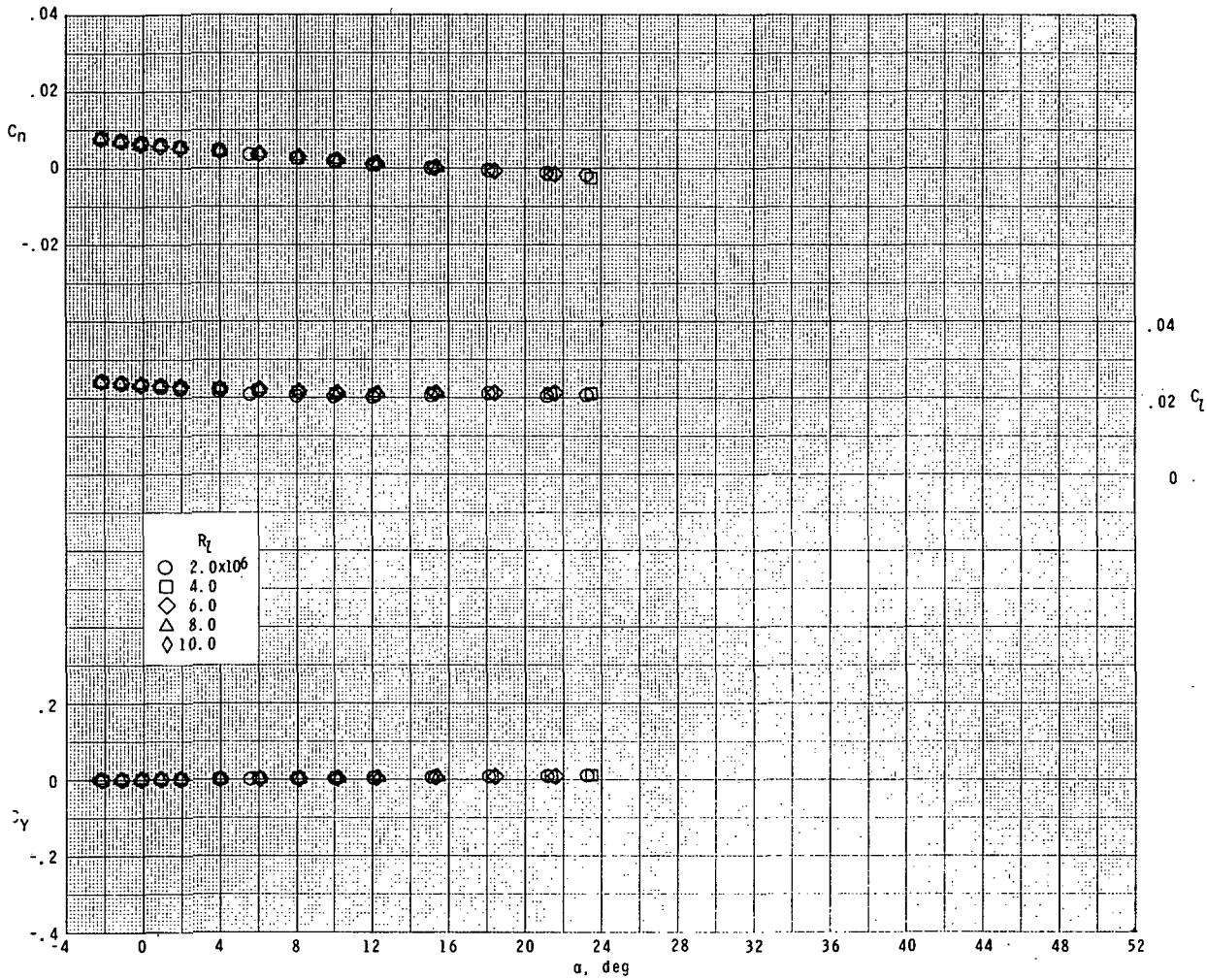

(a) M = 1.60.

Figure 17.- Effect of Reynolds number on lateral aerodynamic characteristics. Large model; $\delta_{e,L} = 0^{o}$ and $\delta_{e,R} = -30^{o}$.

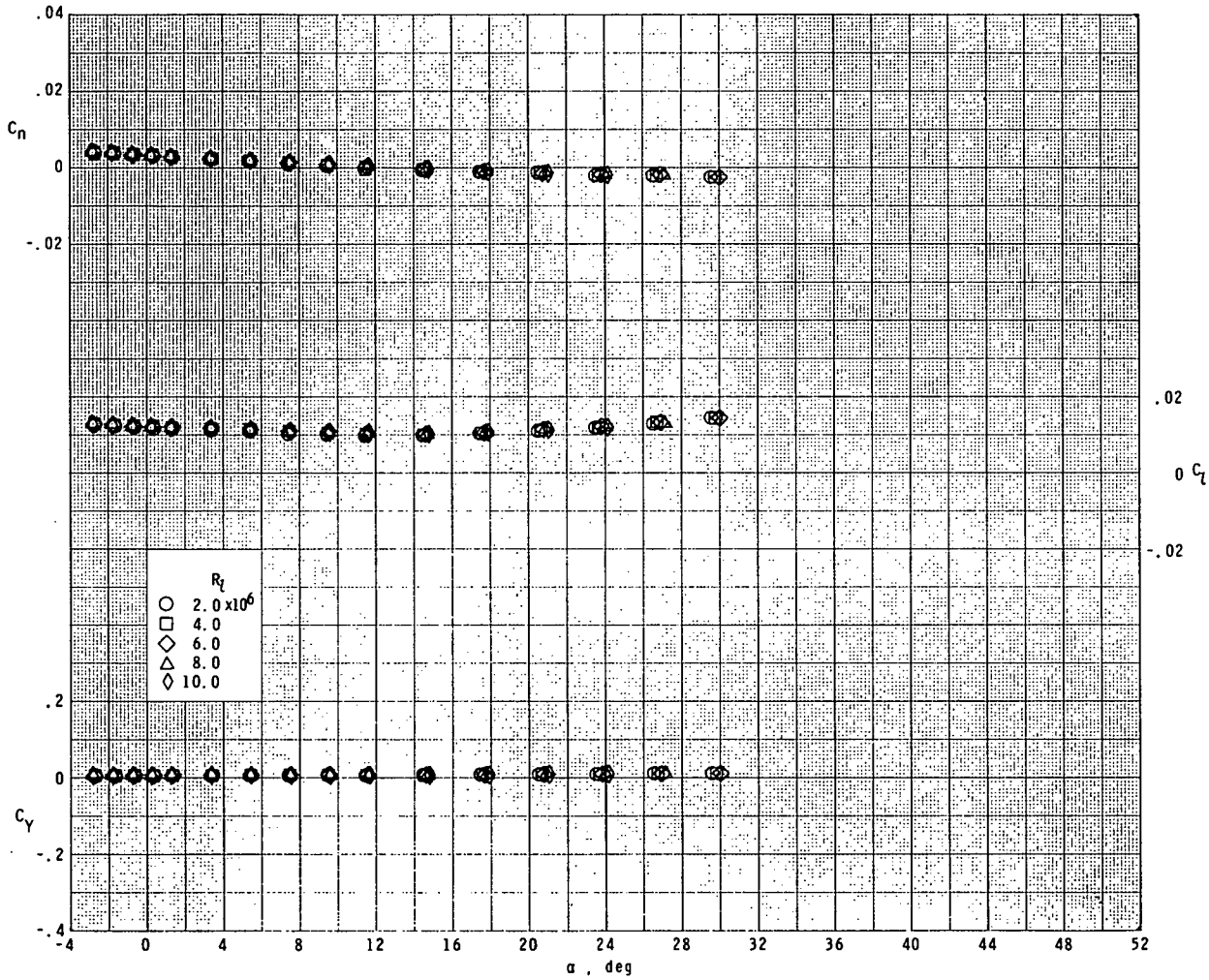

(b) M = 2.86.

Figure 17.- Continued.

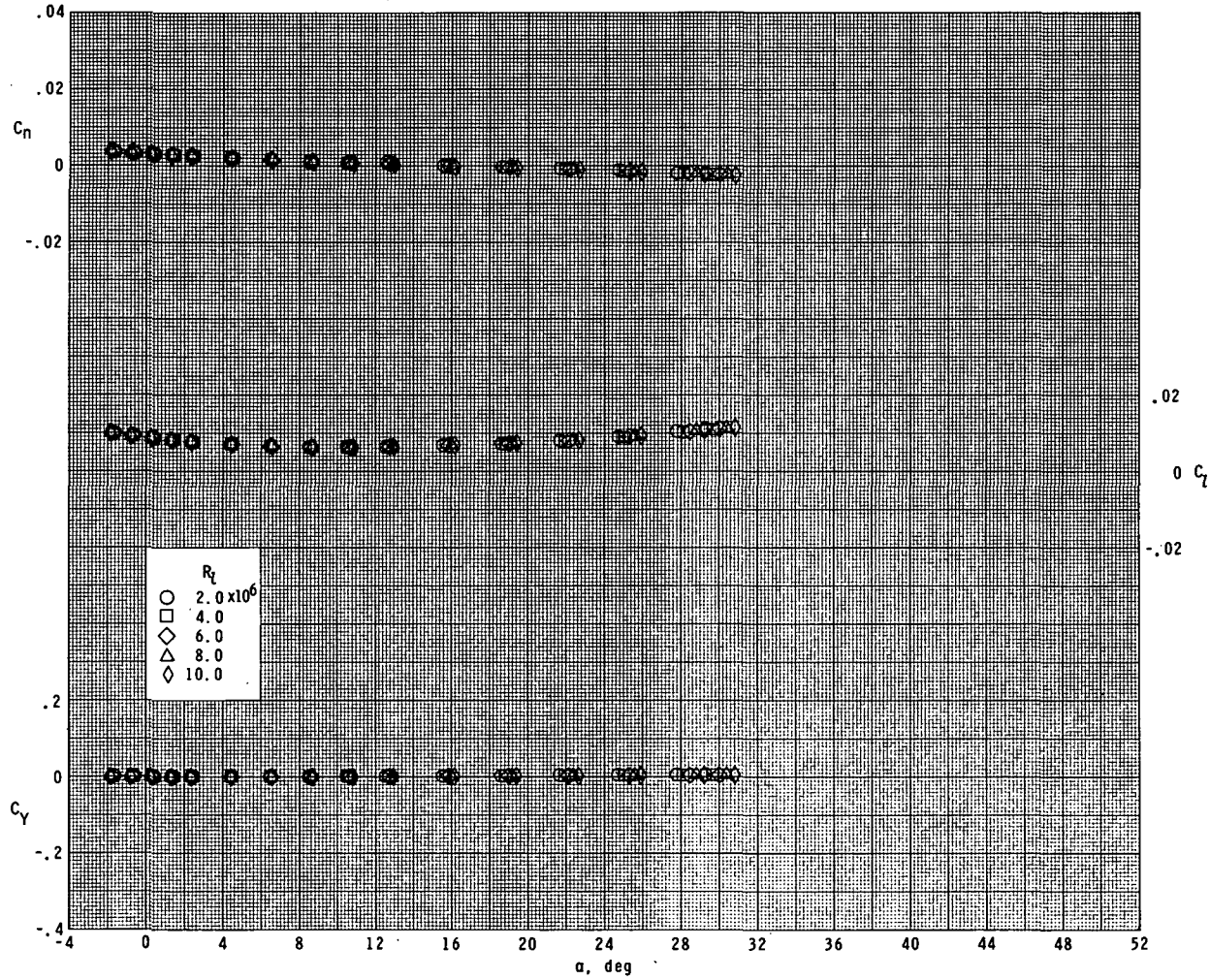

(c) M = 4.63.

Figure 17. - Concluded.

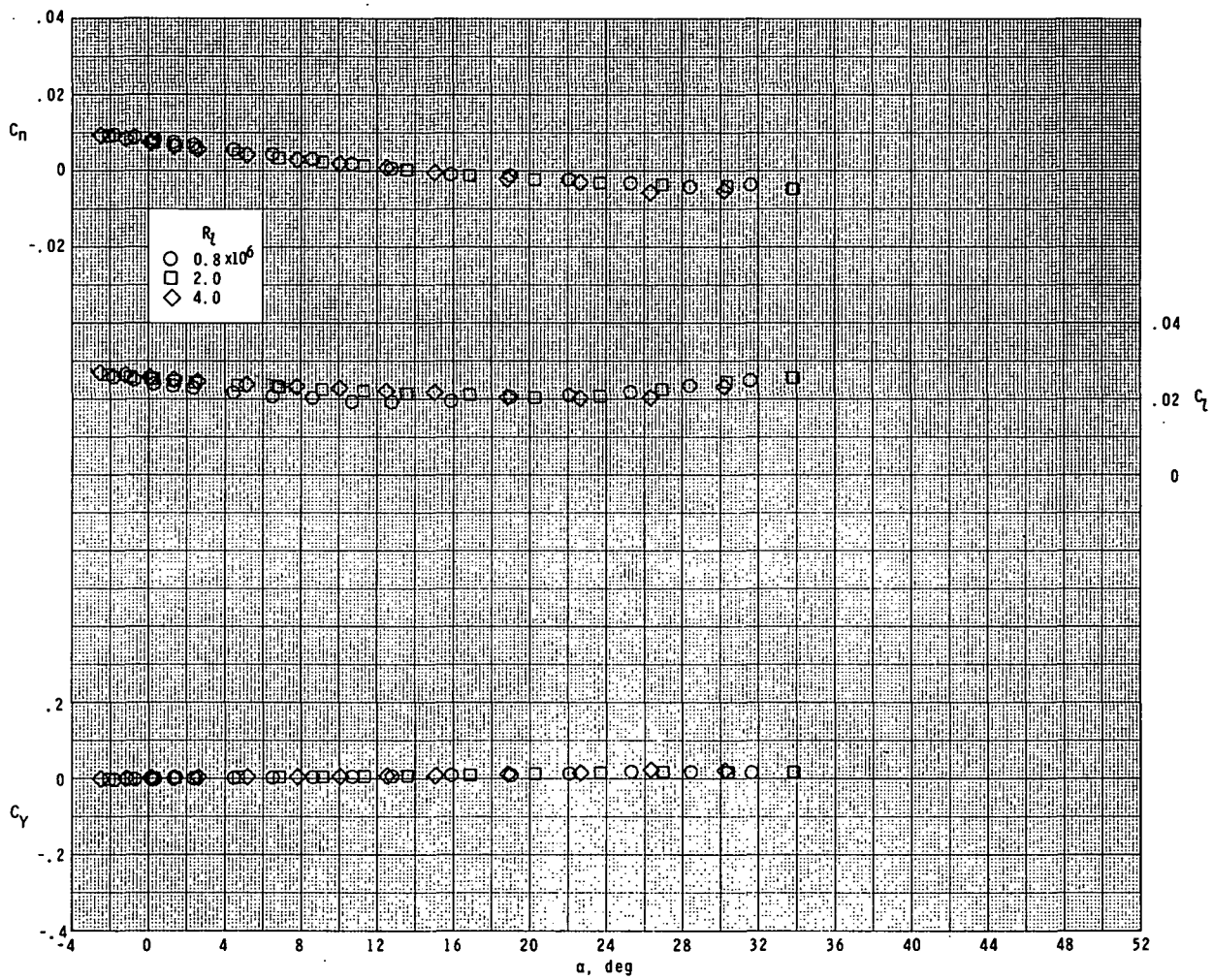

(a) M = 1.60.

Figure 18.- Effect of Reynolds number on lateral aerodynamic characteristics. Small model; $\delta_{e,L} = 0^o$ and $\delta_{e,R} = -30^o$.

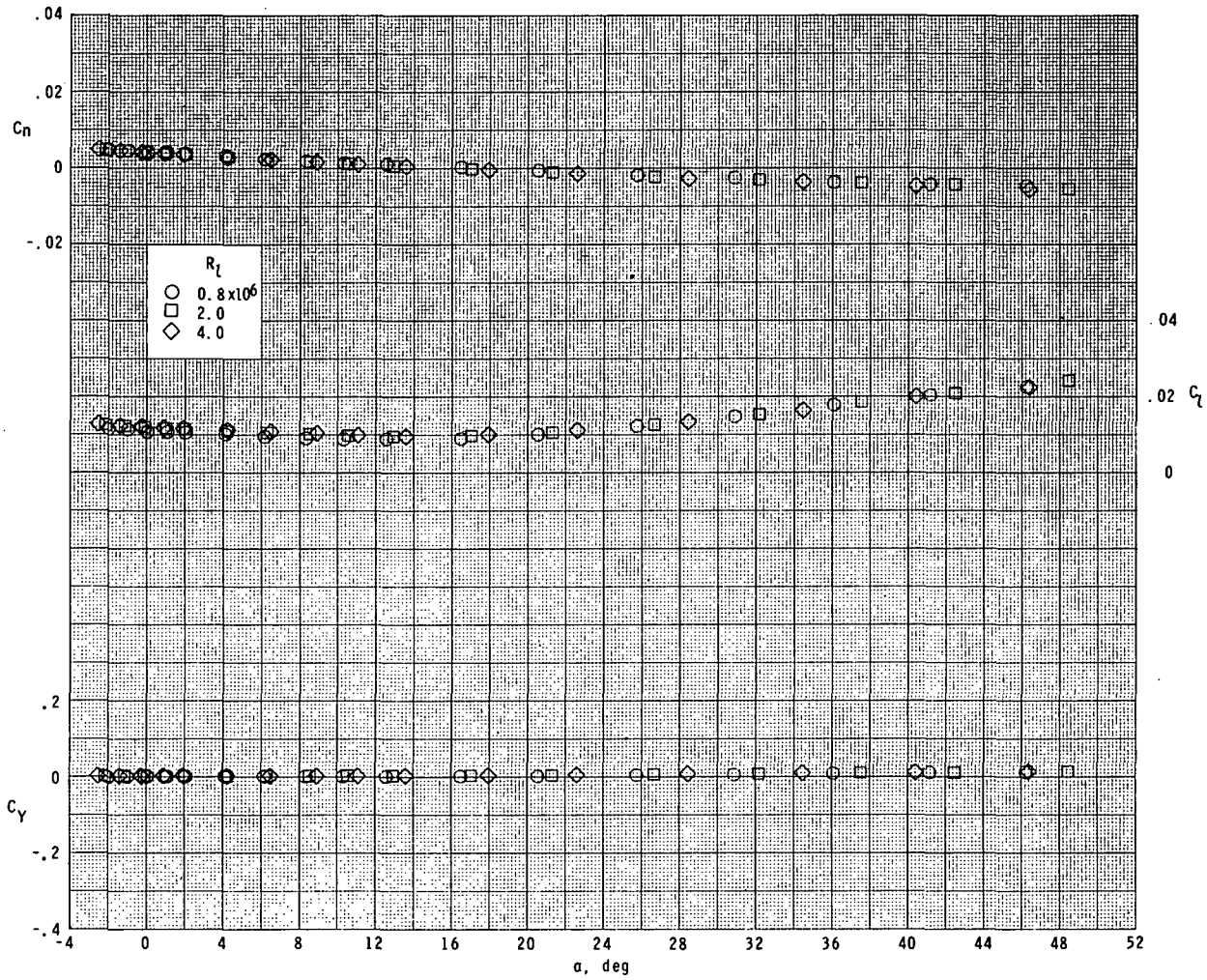

(b) M = 2.86.

Figure 18.- Continued.

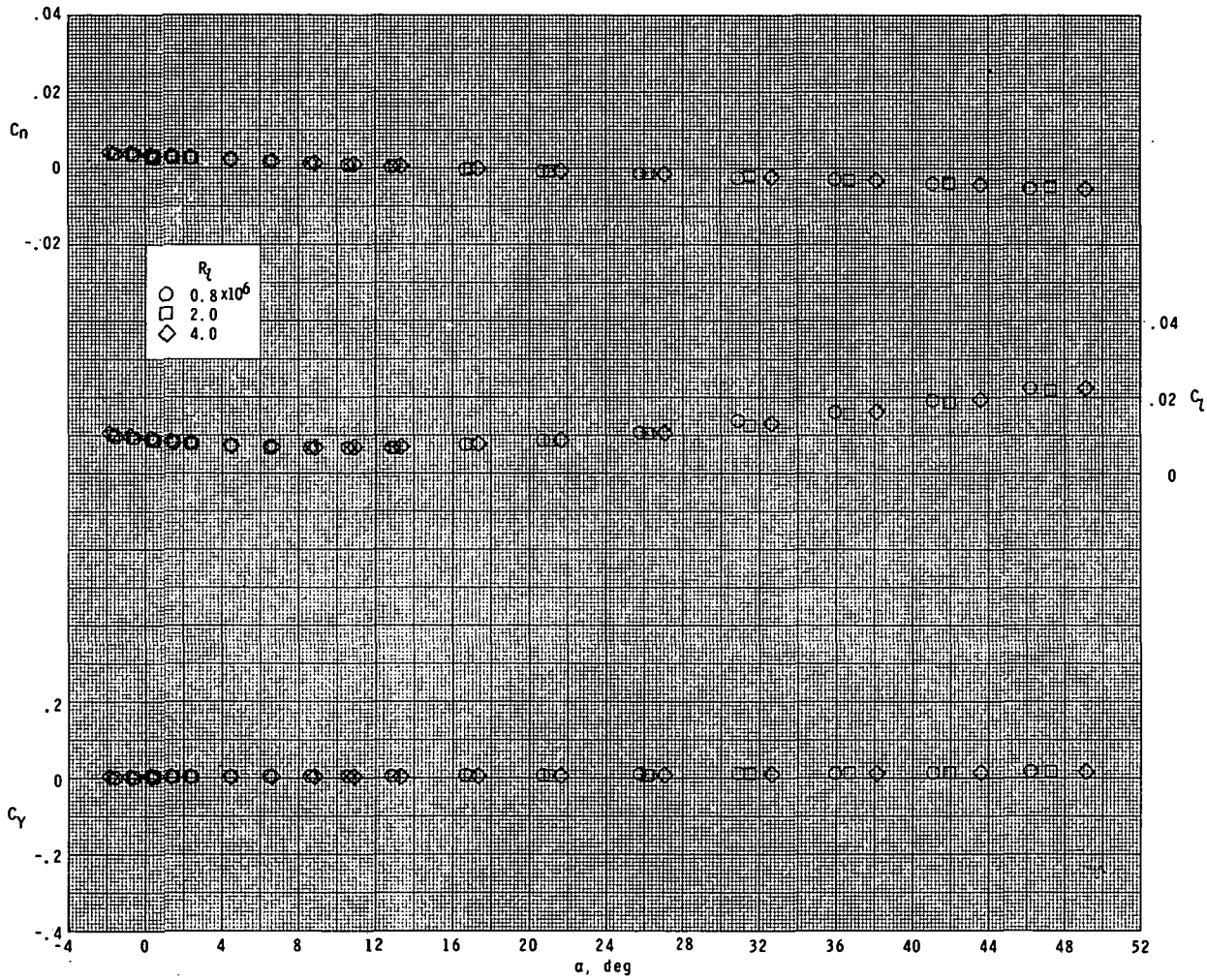

(c) M = 4.63.

Figure 18.- Concluded.

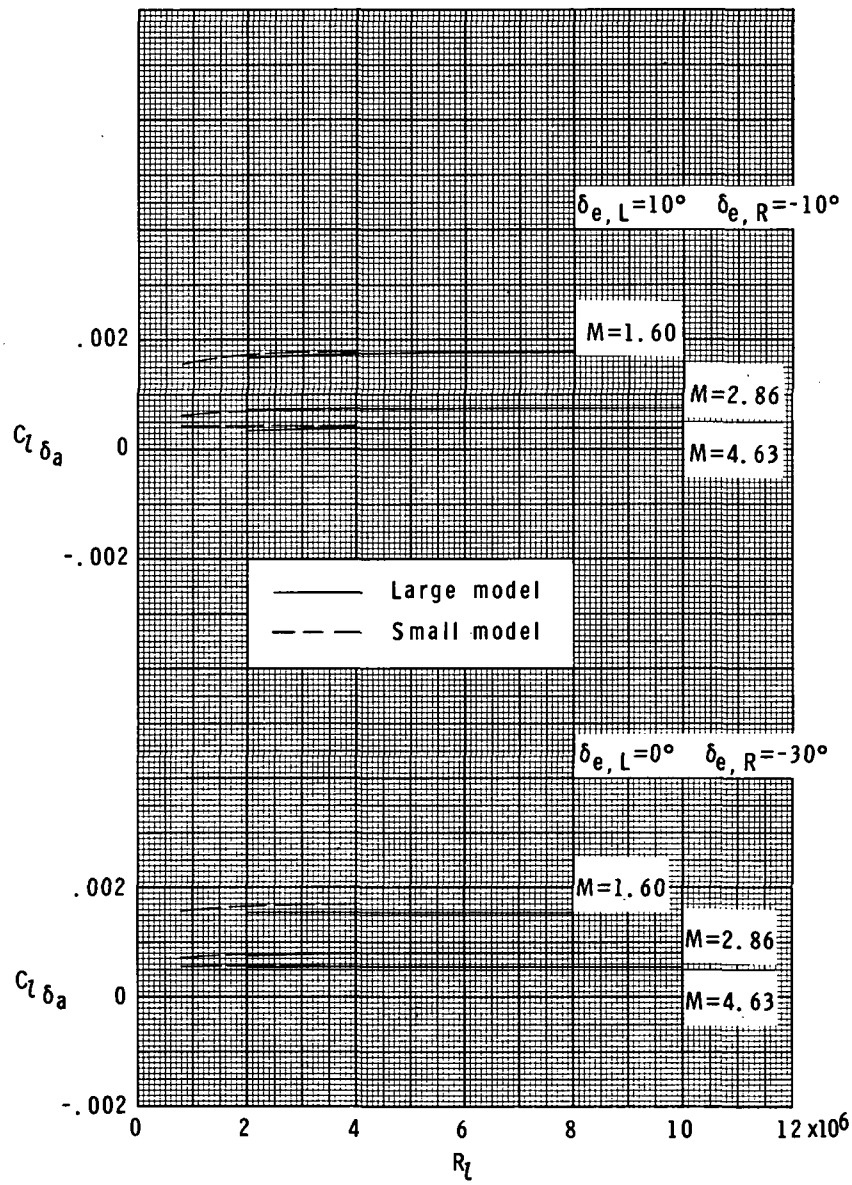

(a) $\alpha \approx 0^{o}$.

Figure 19.- Summary of roll-control characteristics.

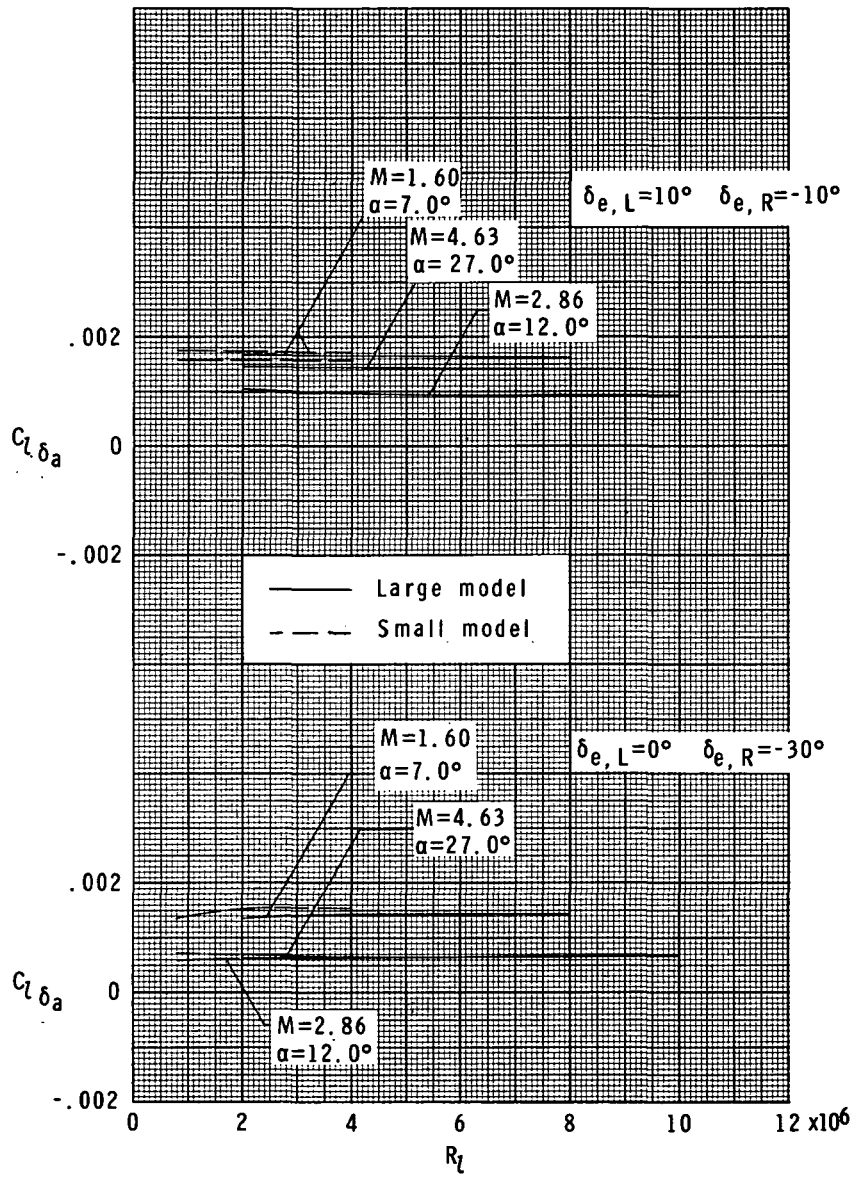

(b) Flight α-schedule for nominal operational high cross-range mission. (See ref. 1.)

Figure 19.- Concluded.

NATIONAL AERONAUTICS AND SPACE ADMINISTRATION
WASHINGTON, D.C. 20546

OFFICIAL BUSINESS
PENALTY FOR PRIVATE USE $300

SPECIAL FOURTH-CLASS RATE BOOK

POSTAGE AND FEES PAID
NATIONAL AERONAUTICS AND SPACE ADMINISTRATION
451

U.S.MAIL

POSTMASTER: If Undeliverable (Section 158 Postal Manual) Do Not Return

"The aeronautical and space activities of the United States shall be conducted so as to contribute . . . to the expansion of human knowledge of phenomena in the atmosphere and space. The Administration shall provide for the widest practicable and appropriate dissemination of information concerning its activities and the results thereof."

—NATIONAL AERONAUTICS AND SPACE ACT OF 1958

NASA SCIENTIFIC AND TECHNICAL PUBLICATIONS

TECHNICAL REPORTS: Scientific and technical information considered important, complete, and a lasting contribution to existing knowledge.

TECHNICAL NOTES: Information less broad in scope but nevertheless of importance as a contribution to existing knowledge.

TECHNICAL MEMORANDUMS: Information receiving limited distribution because of preliminary data, security classification, or other reasons. Also includes conference proceedings with either limited or unlimited distribution.

CONTRACTOR REPORTS: Scientific and technical information generated under a NASA contract or grant and considered an important contribution to existing knowledge.

TECHNICAL TRANSLATIONS: Information published in a foreign language considered to merit NASA distribution in English.

SPECIAL PUBLICATIONS: Information derived from or of value to NASA activities. Publications include final reports of major projects, monographs, data compilations, handbooks, sourcebooks, and special bibliographies.

TECHNOLOGY UTILIZATION PUBLICATIONS: Information on technology used by NASA that may be of particular interest in commercial and other non-aerospace applications. Publications include Tech Briefs, Technology Utilization Reports and Technology Surveys.

Details on the availability of these publications may be obtained from:

SCIENTIFIC AND TECHNICAL INFORMATION OFFICE

NATIONAL AERONAUTICS AND SPACE ADMINISTRATION

Washington, D.C. 20546